Student ID: 1821417

Doctoral Thesis

Analysis of nitrosative stress response mechanisms in the yeast *Saccharomyces cerevisiae* via protein tyrosine nitration and amino acid metabolism

Supapid Eknikom

Nara Institute of Science and Technology
Division of Biological Science
Laboratory of Applied Stress Microbiology
Prof. Hiroshi Takagi

Submitted on 2021/07/26

Table of contents

Page

ABSTRACT

Division of Biological Science Abstract of Doctoral Thesis

Laboratory (Supervisor)	Applied Stress Microbiology (Prof. Hiroshi Takagi)		
Name	Supapid Eknikom	Date	July, 26, 2021
Title	Analysis of nitrosative stress response mechanisms in the yeast *Saccharomyces cerevisiae* via protein tyrosine nitration and amino acid metabolism		

Nitric oxide (NO) is a signaling molecule involved in a wide range of physiological and pathological processes in various organisms. On the other hand, excess reactive nitrogen species (RNS), a class of NO-derived molecules, cause cellular dysfunction and/or cell death, called nitrosative stress. In mammals, NO has been reported to exert its function through the activation of soluble guanylyl cyclase by binding to its heme moiety and the post-translational modification of proteins. Protein tyrosine nitration (PTN), in which tyrosine residues on a protein molecule are converted into 3-nitrotyrosine (3NT), is one of the post-translational modifications mediated by RNS. Therefore, PTN has been thought to be only a marker for inflammation and nitrosative stress in cells. However, many recent studies have found that PTN contributes to a signaling system by altering proteins' local structures and/or functions. At the same time, organisms have several nitrosative stress response/tolerance systems, including NO dioxygenase. Previously, our laboratory reported the physiological functions and mechanisms of NO in the yeast *Saccharomyces cerevisiae*, which is an important microorganism not only as a model organism for higher eukaryotes and pathogenic yeasts/fungi but also for brewing or fine chemicals production. However, there are still many unclear points for the nitrosative stress response mechanisms in *S. cerevisiae*. Additionally, even though there have been a few reports on PTN, the physiological roles of PTN in *S. cerevisiae* have not been fully understood. This study aims to understand cellular responses to nitrosative stress in *S. cerevisiae* by analyzing PTN target proteins and amino acid metabolism in response to RNS.

First, I examined how nitrosative stress affects yeast cell growth and PTN levels in whole-cell lysates. Nitrite is protonated to HNO_2 at acidic pH, which can then be decomposed to RNS, resulting in nitrosative stress. Therefore, *S. cerevisiae* cells grown in the minimal medium at pH 4.0 were treated with 1 mM $NaNO_2$. Western blotting analysis with the anti-3NT antibody revealed that RNS treatment increased the PTN level in whole-cell lysate in a time-dependent manner. In order to identify PTN target proteins, the whole-cell lysate extracted from RNS-treated yeast cells was subjected to digestion with trypsin, followed by liquid chromatography coupled with tandem mass spectrometry. By searching mass shift corresponding to nitration and amination (reduced form of nitration), a wide range of proteins, including carbon metabolic enzymes, were identified as PTN-modified proteins.

In an earlier study, alcoholic fermentation was inhibited in the yeast *S. cerevisiae* caused by nitrite under an acidic condition, under which nitrite would lead to tyrosine

Laboratory (Supervisor)	Applied Stress Microbiology (Prof. Hiroshi Takagi)		
Name	Supapid Eknikom	Date	July, 26, 2021
Title	Analysis of nitrosative stress response mechanisms in the yeast *Saccharomyces cerevisiae* via protein tyrosine nitration and amino acid metabolism		

nitration results *via* the formation of RNS. My findings indicated that acidified nitrite reduces ethanol production in *S. cerevisiae,* which is consistent with previous research. On the other hand, pyruvate, a precursor of ethanol in the metabolic pathway, was highly accumulated in the cell. Subsequently, I measured the activities of enzymes involved in ethanol production, pyruvate decarboxylase (PDC), which produces acetaldehyde from pyruvate, and alcohol dehydrogenase (ADH), which reduces acetaldehyde to ethanol. RNS stimulus did not affect ADH activity but reduced PDC activity by about 50%. Among three isozymes of PDC in *S. cerevisiae* (Pdc1, Pdc5, and Pdc6), Pdc1 was further analyzed because it is a crucial isozyme responsible for PDC activity. Proteomic analysis with an LC-MS/MS confirmed the nitration of Pdc1 at positions Tyr38, Tyr157, and Tyr344. *In vitro* experiments using the site-specific 3NT-incorporated recombinant Pdc1 revealed that nitration of Tyr157 and Tyr344 significantly reduced Pdc1 activity by 64% and 87%, respectively. Interestingly, *S. cerevisiae* cells expressing the Tyr157Phe- or Tyr344Phe-Pdc1 variants produced higher ethanol than the wild-type cells under the RNS treatment conditions. These results indicate that tyrosine nitration at Tyr157 and Tyr344 in Pdc1 decreased ethanol production by reducing its enzymatic activity.

Moreover, I analyzed the intracellular amino acid profile in *S. cerevisiae* treated with nitrosative stress using HPLC. As a result, the intracellular content of γ-aminobutyric acid (GABA) highly increased under the nitrite treatment conditions at pH4.0 but did not at pH6.0. Therefore, I hypothesize that GABA might be involved in the nitrosative stress response. Previous work reported that the GABA degradation pathway or the GABA shunt, in which GABA is converted into succinate to generate NAD(P)H, was involved in oxidative and heat stress tolerance. To investigate the role of GABA and the GABA shunt in nitrosative stress, the GABA shunt-deficient strains, *gad1*Δ, which is unable to synthesize GABA, and *uga1*Δ, which does not degrade GABA, were constructed and analyzed. By treatment with acidified nitrite, *gad1*Δ cells exhibited higher sensitivity to nitrite than wild-type cells, but *uga1*Δ cells did not. Notably, the intracellular GABA levels in *gad1*Δ cells were not detectable regardless of nitrite treatment. Furthermore, supplementation of 0.1 mM GABA increased cell viability in all strains compared to non-supplemented GABA. These findings indicate that GABA is involved in nitrosative stress tolerance in *S. cerevisiae,* probably through a different pathway from the previously reported GABA shunt. For the future perspective, a comprehensive analysis of gene expression levels associated with nitrosative stress tolerance and GABA treatment to analyze the GABA-dependent NO tolerance mechanism is required to clarify the mechanism by which GABA protects yeast cells from nitrosative stress.

ABREVIATIONS

3NT	: 3-Nitrotyrosine
ATP	: Adenosine triphosphate
DNA	: Deoxyribonucleic acid
dNTP	: Deoxyribonucleotide triphosphate
EDTA	: Ethylenediamine tetraacetic acid
FAD	: Flavin adenine dinucleotide
FHb	: Flavohemoglobin
FMN	: Flavin mononucleotide
GABA	: γ-Aminobutyric acid
GSH	: Glutathione
GR	: Glutathione reductase
GSNO	: *S*-nitrosoglutathione
GSNOR	: *S*-nitrosoglutathione reductase
H_4B	: Tetrahydrobiopterin
IPTG	: Isopropyl β-D-1-thiogalactopyranoside
LC-MS/MS	: Liquid chromatography with tandem mass spectrometry
NaR	: Nitrate reductase
NAD^+	: Nicotinamide adenine dinucleotide
NADH	: Nicotinamide adenine dinucleotide, reduced form
$NADP^+$	: Nicotinamide adenine dinucleotide phosphate
NADPH	: Nicotinamide adenine dinucleotide phosphate, reduced form
NO	: Nitric oxide
NO_2^-	: Nitrite
NO_3^-	: Nitrate
NOD	: Nitric oxide dioxygenase
NOS	: Nitric oxide synthase
$O_2^{\cdot -}$	: Superoxide anion
OD	: Optical density

ONOO-	: Peroxynitrite
PCR	: Polymerase chain reaction
PTN	: Protein tyrosine nitration
PVDF	: Polyvinylidene fluoride or polyvinylidene difluoride
RNS	: Reactive nitrogen species
ROS	: Reactive oxygen species
SDS-PAGE	: Sodium dodecyl sulfate polyacrylamide gel electrophoresis
SILAC	: Stable isotope labeling by/with amino acids in cell culture
TBS-T	: Tris-buffered saline with tween 20
TCA	: Tricarboxylic acid
tRNA	: Transfer ribonucleic acid

1. INTRODUCTION

1.1 *Saccharomyces cerevisiae* as a model organism and industrial applications

The budding yeast *Saccharomyces cerevisiae* (*S. cerevisiae*) is a unicellular fungus containing a nuclear genomic DNA of 12 Mbp, organized in 16 chromosomes (Engel et al., 2014). Its genome has been completely sequenced and contained approximately 6,000 genes (Goffeau et al., 1996). As one of the simplest eukaryotes, *S. cerevisiae* is a classic model organism for studying common pathways in higher organisms, such as humans. The advantages of using yeast are its short life cycle, simple nutritional requirements, and similar genes implicated in human diseases (about 30%). Due to conserved biological functions between human and yeast, neurodegenerative disorders have been studied in yeast, such as Huntington's disease (HD) and Parkinson's disease (PD) (Miller-Fleming et al., 2008). Moreover, *S. cerevisiae* is well established for studies of aging (Jazwinski, 2002), signal transduction (Ždralević et al., 2012), apoptosis (Madeo et al., 2004), and many other biological processes.

As the pathogenic fungi, *Candida albicans* and *Candida glabrata* are the two most common pathogenic yeasts that inhabit the oral cavity and the gastrointestinal tract and skin, causing diseases in humans (Fidel Jr et al., 1999). *S. cerevisiae* is a closely related pathogenic *Candida* species classified in the Saccharomycotina (Roetzer et al., 2011). *S. cerevisiae* species also plays a role in probiotic yeasts, defined as live microorganisms with a positive effect on the host once ingested. Nowadays, major yeast species used as probiotics are *S. boulardii* and *S. cerevisiae*. Both strains share more than 99% genomic relatedness (Khatri et al., 2017). They are used as alternative treatments for gastrointestinal disorders or prevention, such as antibiotic-associated diarrhea (Czerucka et al., 2007). Recent research showed that *S. cerevisiae*, a commercially available product favoring animal digestion, can protect mice against intestinal pathogens (Martins et al., 2005).

Thus, *S. cerevisiae* is a good model organism and one of the most beneficial species for applications in food and beverage industries such as wine, beer, whisky, sake, and bread. Interestingly, yeast has also been used in the biofuel industry and for the production of heterologous compounds. Its unique biological characteristics are fermentation capacity and resilience to osmolality conditions, low pH, and high ethanol concentrations. Many yeast strains can function under both anaerobic as well as aerobic conditions of the environment, switching their metabolism types easily (Otterstedt et al., 2004). Altogether, using *S. cerevisiae*

as a model organism can provide higher insight into eukaryote, pathogenic fungi, probiotic approach, and industrial applications.

1.2 Nitric oxide

1.2.1 Biosynthesis and physiological functions of nitric oxide in eukaryote

Nitric oxide (NO), a highly diffusible free radical, regulates several significant physiological and pathological events. Generally, NO is generated within cells by the enzymatic activity of NO synthase (NOS). Characterization of NOS demonstrated three different isoforms in mammals; neuronal NOS (nNOS), inducible NOS (iNOS), and endothelial NOS (eNOS) (Lowry et al., 2013; Muntané & De la Mata, 2010). These isoforms utilize L-arginine as a substrate and molecular oxygen and NADPH as co-substrates. Flavin adenine dinucleotide (FAD), flavin mononucleotide (FMN), and tetrahydrobiopterin (H_4B) are cofactors of all isozymes. The nNOS, iNOS, and eNOS enzymes have similar structures and functions, but they are different in their activation mechanism. The isoenzymes eNOS and nNOS are regulated by the binding of calmodulin and calcium ion, whereas iNOS, involving in immune response, is not calcium-dependent but induced during infection (Knowles & Moncada, 1994).

NO is now known to be produced in various cells and tissues. When it presents at low concentrations, NO controls various regulatory functions in cells such as neurotransmission, gene transcription, and translation regulation, the apoptotic signaling cascade, and signal transduction (Brüne et al., 1995; O'Dell et al., 1991; Pozdnyakov et al., 1993; Schuman & Madison, 1991). However, NO is harmful to cellular systems at high concentrations, such as inactivating enzymes and the electron transport chain, leading to cellular dysfunction and/or cell death denoted as nitrosative stress (Brown, 1999). Furthermore, the post-translational modifications derived from NO or NO-related chemical species inhibit or induce various pathways involved in regulating cell growth and cell death (Radi, 2004).

1.2.2 Nitrosative stress

Oxygen plays an essential role in cell growth and cell death. It is known that mitochondria are the primary site of intracellular reactive oxygen species (ROS) production due to the mitochondria respiratory chain (Poyton et al., 2009). During respiration, most of the consumed oxygen is converted to water. On the other hand, 1-2% of the consumed oxygen is not completely reduced to water but forms superoxide anion ($O_2^{\cdot -}$), highly reactive (Ray et al.,

2012). Superoxide can also interact with NO to form peroxynitrite ($ONOO^-$) as a strong oxidant. NO-derived compounds and NO itself are referred to as reactive nitrogen species (RNS) (Dedon & Tannenbaum, 2004). A list of reactive nitrogen species is given in Table 1.

Table 1: Reactive nitrogen species (Dedon & Tannenbaum, 2004)

Radicals	**Nonradicals**
Nitric oxide ($NO^{\bullet}$)	Peroxynitrite ($ONOO^-$)
Nitrogen dioxide ($NO_2^{\bullet}$)	Peroxynitrous acid (ONOOH)
	Akyl peroxynitrite (ROONO)
	Nitrosyl cation (NO^+)
	Nitroxyl anion (NO^-)
	Nitronium anion (NO_2^+)
	Dinitrogen trioxide (N_2O_3)
	Dinitrogen tetraoxide (N_2O_4)
	Nitrous acid (HNO_2)
	Nitryl chloride (NO_2Cl)

1.2.3 Reactive nitrogen species generated by acidified nitrite

RNS is generated by chemical reactions as well. The gastrointestinal (GI) tract contains many sites of reactive nitrogen species generated by the host, the normal bacterial flora, and the chemical reaction of acidified nitrite in the stomach (Lundberg & Weitzberg, 2013). Nitrate (NO_3^-) and nitrite (NO_2^-) have been considered as sources of NO in the gastric environment. There are two primary sources of these compounds in the body: diet and the salivary gland. Dietary nitrate is mainly found in drinking water, green leafy vegetables, and processed meat. It is noteworthy that vegetables are a significant source of dietary nitrate in humans. The other sources are nitrate from salivary glands, which absorb from plasma. Both humans and rats show that 25% of the nitrate ingested is secreted from salivary glands. The salivary nitrate levels can reach 10 mM and nitrite levels 1-2 mM after a dietary nitrate load (Lundberg et al., 2004; Lundberg & Govoni, 2004).

As shown in Fig. 1-1, commensal facultative anaerobic bacteria effectively converts nitrate, which is derived from either the diet or swallowed saliva, to nitrite by nitrate reductase (NaR) as an alternative electron acceptor to oxygen during nitrate respiration (Lundberg et al.,

1994; Spiegelhalder et al., 1976). When saliva enters the acidic stomach (1.0 - 1.5 L per day), under the pH and temperature conditions of the gastric compartment, much of the nitrite is rapidly protonated to form nitrous acid (HNO_2; pK_a 3.4) (Pannala et al., 2006; Rocha et al., 2016). Due to its chemical instability, nitrous acid spontaneously decomposes into different RNS such as dinitrogen trioxide (N_2O_3), nitrogen dioxide (NO_2), and NO. This mechanism to generate RNS is vital as a defense against swallowed pathogenic microorganisms. The NO levels in the human stomach are about 10-100 ppm (Lundberg et al., 1994). This generation of NO in the gastric lumen plays a role in maintaining gastric integrity and participating in host defense mechanisms using the potent anti-microbial effects of RNS (Lundberg et al., 1994; Smith et al., 1994).

Acidified nitrite has been applied to skin treatment disease Buruli ulcer, a chronic debilitating disease caused by *Mycobacterium ulcerans* (Phillips, Adjei, et al., 2004; Phillips, Kuijper, et al., 2004). This treatment method is affordable price and thus applicable for long-term use. In addition, Anyim and co-workers demonstrated that acidified nitrite could be used as a potential antifungal agent for *C. albicans*, *C. glabrata*, *C. tropicalis*, *Cryptococcus neoformans*, *Aspergillus fumigatus*, and *Rhodotorula* (Anyim et al., 2005). However, the mechanism of tolerance or survival under this condition is still unclear. A study in the budding yeast *S. cerevisiae* could be a good model for understanding how nitrosative stress affects cell death/survival or adaptative mechanisms in pathogenic fungi and probiotic yeast (*S. boulardii*).

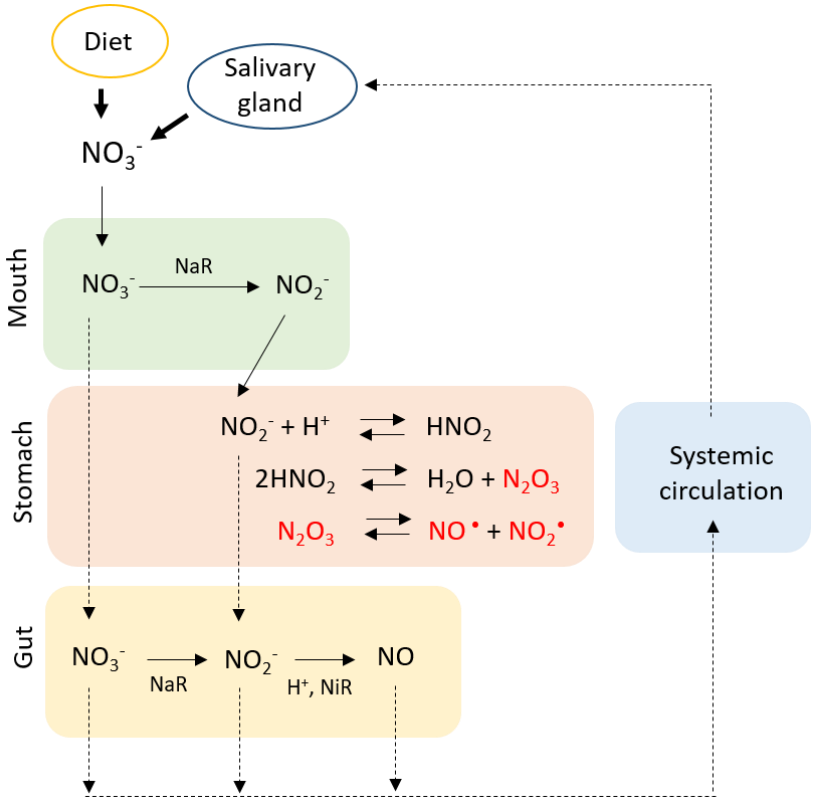

Fig. 1-1 NO cycle produced from nitrate and nitrite in the gastrointestinal tract (Lundberg & Weitzberg, 2013; Rocha et al., 2011). In the mouth, nitrate from diet and salivary glands is converted to nitrite by bacterial nitrate reductase (NaR). Nitrite is protonated to nitrous acid (HNO_2) and decomposed to RNS in the stomach leading to an anti-microbial effect. The remaining nitrate and nitrite in the gut are utilized by normal flora for respiration. Some of these compounds are absorbed into the circulation and accumulated in the salivary gland. NO_3^-, nitrate; NO_2^-, nitrite; NiR, nitrite reductase; NO, nitric oxide; NO_2, nitrogen dioxide; N_2O_3, dinitrogen trioxide.

1.3 Protein tyrosine nitration (PTN)

1.3.1 Formation and role of PTN

In addition to *S*-nitrosation, RNS induces another post-translational modification. Protein tyrosine nitration (PTN) is a chemical process that selectively introduces a nitro group (NO_2) to tyrosine residue at ortho carbons of the aromatic ring. These modifications are caused by several combinatorial reactions of RNS and ROS (Kanski & Schöneich, 2005). Excess ROS levels in the presence of NO or NO-derived metabolites lead to peroxynitrite ($ONOO^-$) production (Bottari, 2015). Because of the short biological half-life of $ONOO^-$ (5-20 ms), the target residues in the protein are generally in the vicinity of the ROS generation sites (Heijnen et al., 2006). Consequently, nitrated proteins (protein-containing PTN) are predominantly

found in the mitochondria, critical loci for the formation of $ONOO^-$. The amount of tyrosine residues in proteins is commonly 3-4 mol percentage on average. *In vivo* studies have shown the biological nitration yield as approximately 1-5 nitrated residues per 10,000 tyrosine residues (Kang et al., 2015; Radi, 2004). Current evidence indicates that the mechanism of PTN in biological systems is mediated by free radical reactions of tyrosyl radicals ($Tyr^{\bullet}$) and subsequent reactions with either NO or NO_2 (Fig. 1-2). Peroxynitrite does not react directly with tyrosine but instead reacts with peroxynitrite-derived radicals (Radi, 2004). Depending on the predominant nitrating species, mechanism, and relevant one-electron oxidants are carbonate radicals ($CO_3^{\bullet-}$) and oxo-metal complexes (e.g., myeloperoxidase (MPO) compound I, hemin), and even lipid peroxyl radicals ($LOO^{\bullet}$) (Alvarez et al., 1999).

Tyrosine nitration contributes to cellular signaling mechanisms by its properties of specificity, reversibility, and controlled rates of formation and modification of target proteins and cell functions (Gow et al., 1996; Kamisaki et al., 1998). PTN also has specific effects, such as affecting protein structure and function, leading to modulation of phosphorylation cascades, and occasionally an immune response induction (Hunter, 1995). Thus, it plays a role in various biological processes involved in the pathogenesis of inflammatory responses, cytoskeletal dysfunction, platelet activation, age-related diseases such as age-related macular degeneration (AMD), neurodegenerative disorders including Alzheimer's disease (AD), Parkinson's disease (PD), and amyotrophic lateral sclerosis (ALS), cardiovascular disease, and cancer (Beal, 2002; Ischiropoulos & Beckman, 2003; Kanski & Schöneich, 2005; Masri et al., 2005; Murdaugh et al., 2010; Sabetkar et al., 2008).

1.3.2 Selectivity of PTN

Tyrosine nitration is a selective process. Not all tyrosine residues are available for nitration. As *in vitro* study, the factors that may influence the biological selectivity of PTN depending on the protein structure, nitration mechanism, and environment of the protein (Bartesaghi et al., 2007). However, the factors of *in vitro* nitration are not always operative *in vivo*. In the aromatic rings positioned on the protein surface, PTN more easily occurs when they locate on loop structures (Souza et al., 1999). On the other hand, tyrosine residues that are not exposed to the solvent phase are not available for nitration. Different nitrating agents also affect the position of nitration and the target proteins. Moreover, as free radical reactions, abundant proteins sometimes are more readily nitrated due to better competition for the nitrating species (Radi, 2013).

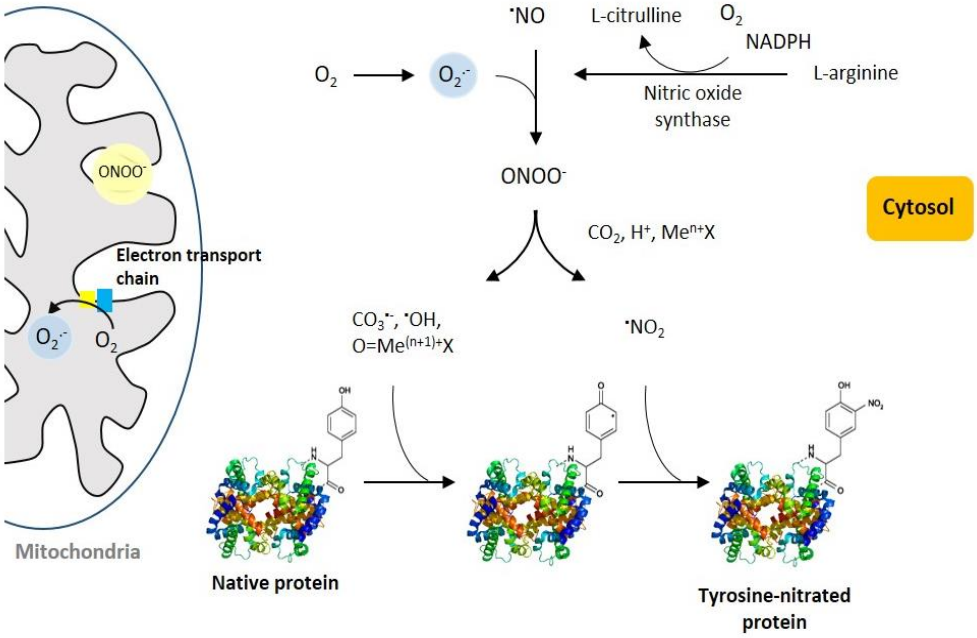

Fig. 1-2 Peroxynitrite-dependent tyrosine nitration of intracellular proteins (Ferrer-Sueta et al., 2018)**.** First, the combination of NO and $O_2^{\bullet-}$ forms in peroxynitrite in cells on mitochondria and cytosol. Then, once produced, peroxynitrite may decay through reaction with carbon dioxide, transition metal complexes (Me^{n+X}), or radical species, leading to tyrosine residues' oxidation to tyrosyl radical. Then, tyrosyl further interacts with NO_2 leading to the formation of NO_2Tyr in proteins**.**

1.4 Nitric oxide synthesis, detoxification, and PTN in yeast

1.4.1 Nitric oxide biosynthesis and its physiological role in yeast

NO has been found in various organisms, including animals, plants, bacteria, and yeasts. The NO sources in yeast cells remain unknown, owing to a lack of mammalian NOS orthologues in the yeast genome. (Astuti et al., 2016). However, discovering a 60-kDa protein with immunoreactivity against the anti-mammalian NOS antibody in the crude extracts of *S. cerevisiae* is reported to suggest the presence of yeast NOS (Kanadia et al., 1998; Kuo et al., 1996). On the other hand, yeast cells can produce NO in mitochondria under hypoxic conditions by nitrite-dependent cytochrome c oxidase (Castello et al., 2006). Menadione-treated in yeast led to NO production dependently on the intracellular L-arginine levels, suggesting the existence of an enzyme with NOS-like activity (Osório et al., 2007). Although data supporting NOS existence in yeast have emerged from both *in vitro* and *in vivo* analyses (Almeida et al., 2007; Kig & Temizkan, 2009; Yoshikawa et al., 2016), the gene or protein responsible for the yeast NOS-like activity has not yet been identified. NO is involved in fungal cellular

development in filamentous fungi, such as spore germination and asexual and sexual structures, and aspersorium (Zhao et al., 2020). Exogenous NO in the fission yeast *Schizosaccharomyces pombe* increases an oxidative stress response involving a negative feedback system to regulate intracellular ROS levels (Astuti et al., 2016). This result is consistent with Almeida and co-workers' study, indicating NO-induced cell death by *S*-nitrosation of GAPDH that possibly acted as an apoptotic trigger (Almeida et al., 2007). For industrial applications, enhancement of NO production improves stress tolerance and fermentation ability in baker's yeast (Sasano et al., 2012). It was previously shown that RNS enhances ethanol production, probably through the inactivation of tricarboxylic acid (TCA) cycle enzymes (Sengupta et al., 2020).

1.4.2 RNS detoxification in yeast

The exposure of either endogenous or exogenous RNS induces a stress response in cells. Yeast contains two central protective systems to confer resistance against nitrosative stress; flavohemoglobin (FHb) and *S*-nitrosoglutathione reductase (GSNOR). FHb harbors a hemoglobin-like domain and a reductase domain with the FAD and NAD(P)H binding sites (Zhao et al., 1996). The *YHB1* gene (known as nitric oxide oxidoreductase gene) is responsible for FHb in yeast (Yhb1) involved in both oxidative and nitrosative stresses (Liu et al., 2000). Yhb1 plays a role in the conversion of NO into nontoxic nitrate during aerobic conditions. The absence of Yhb1 shows more accumulation of NO and RNS (Bhattacharjee et al., 2009).

GSNOR also associates in RNS detoxification (Fig. 1-3). The major intracellular antioxidant glutathione (GSH) favorably reacts with RNS and is converted into *S*-nitrosoglutathione (GSNO). GSNO functions as a natural NO donor and transfers its NO moiety to other thiol compounds, including cysteine residues in protein, inducing the NO-mediated post-translational modification *S*-nitrosation to regulate NO homeostasis. (Barnett & Buxton, 2017). The role of GSNO for protein *S*-nitrosation implies that the metabolism of GSNO is a significant branch of NO metabolism that influences many regulatory processes. The produced GSNO can be turned over to ammonia and glutathione disulfide (GSSG) in the presence of GSNOR (Zhao et al., 2016). This process helps cells to handle nitrosative stress effectively. Furthermore, catalase has been reported to detoxify peroxynitrite in *S. cerevisiae* in the cell lacking Yhb1 and glutathione-dependent formaldehyde dehydrogenase Sfa1, which bifunctionally has the GSNOR activity (Sahoo et al., 2009). Recently, the gene encoding GTP cyclohydrolase II (GTPCH2) involved in riboflavin (RF) biosynthesis helps yeast cells from nitrosative stress by scavenged NO or its derivatives (Anam et al., 2020).

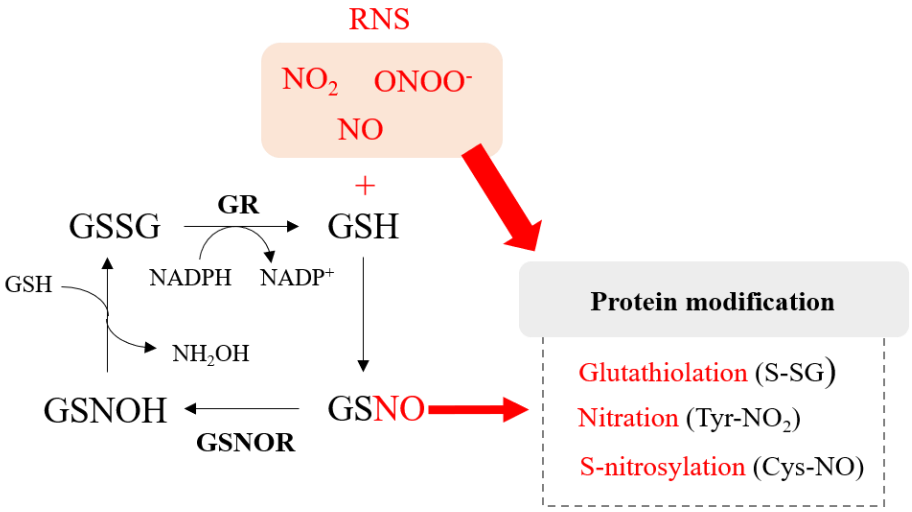

Fig. 1-3 Mechanisms of GSNOR in RNS detoxification. Reactive nitrogen species directly react with protein causing post-translational modification. Furthermore, the reduced form of glutathione (GSH) GSNO accumulations influences protein modification's cellular status. GSNO reduction by GSNOR is an irreversible reaction, and the products can no longer modify cellular proteins. Regeneration of GSH exists by glutathione reductase (GR) as an NADPH-dependent reduction of GSSG (Jahnová et al., 2019). GSH, glutathione; GSNO, S-nitrosoglutathione; GSNOR, S-nitrosoglutathione reductase; GSSG, glutathione disulfide; NO, nitric oxide; NO_2, nitrogen dioxide; NOS, nitric oxide synthases.

1.4.3 PTN in yeast

There are numerous researches about NO and its effect on protein post-translational modification in mammals and plants. However, the NO signaling pathway and its functional role in yeast have remained unclear and limited, including the molecular mechanism of PTN. Identification of yeast mitochondrial protein shows PTN profiles involving the TCA cycle (aconitase and isocitrate dehydrogenase) and respiratory system (Bhattacharjee et al., 2009). Furthermore, the 14-nitrated proteins in mating conditions have been identified by proteomic analysis using LC-MS/MS. These proteins are associated with transcription factors, actin cytoskeleton organization, cell wall organization, and spermidine transport relating to the signal transduction pathway (Kang et al., 2015). Altogether, the outcomes demonstrate the ability to generate NO and PTN in yeast. However, the effect of PTN on yeast proteins has not been investigated until now.

1.5 Ethanol fermentation in yeast

1.5.1 Role of the fermentative pathway in yeast

Alcoholic fermentation occurs when yeasts, bacteria, or a few other microorganisms convert sugars into pyruvate *via* the glycolysis pathway and produce ethanol and carbon dioxide (Malakar et al., 2020). The ethanol production is crucial for oxidizing the NADH to maintain and supply the NAD^+/NADH redox system for glycolysis. Maintaining aerobic cultivation conditions in *S. cerevisiae* is insufficient to achieve respiratory sugar metabolism. Even fully aerobic cultures exhibit mixed respiration-fermentation processes referred to as aerobic fermentation or Crabtree effect (Bakker et al., 2001). As Crabtree-positive yeast, *S. cerevisiae* prefers the fermentative pathway under aerobic conditions when the glucose concentration above 150 mg/L rather than respiration via the TCA cycle (De Deken, 1966; Verduyn et al., 1984). Therefore, pyruvate from glycolysis is mainly converted into acetaldehyde and ethanol by pyruvate decarboxylase (PDC) and alcohol dehydrogenase (ADH), respectively (Fig. 1-4). Only a relatively small amount of acetaldehyde is converted into acetate by acetaldehyde dehydrogenase (ALD) (Galdieri et al., 2014).

1.5.2 Nitrosative stress during ethanol production

As previously stated, the ability of yeast to ferment has been used in industrial applications. Bioethanol is produced through the fermentation of sugars derived from a variety of sources. The primary substrates for sugar fermentation are sucrose-rich plants from food crops such as sugarcane, sugar beet, a variety of fruits, and starch. As the most cost-effective way, molasses has been widely used to produce ethanol and other fermentative products in the industry. In complex worts such as beet molasses, some inhibitors caused by toxic amounts of organic or inorganic compounds limit the rate of alcohol production. Also, molasses contains varying amounts of nitrate, which can be converted into nitrite by bacteria. In fact, the nitrite concentration in undiluted beet molasses can reach 4,300 ppm and has been identified as a yeast fermentation inhibitor (Glacet et al., 1985). Nitrite concentrations above 30 ppm with pH below 5.0 dramatically increase nitrite accumulation in cells and cause dose-dependent growth inhibition and decreases in ATP and some enzyme activities such as glyceraldehyde-3-phosphate dehydrogenase and glutamate dehydrogenase (Hinze & Holzer, 1985a, 1985b; Jones & Gadd, 1990; Mortensen et al., 2008). Furthermore, the pH of the culture medium in glucose-fermenting yeast can fall below pH 2 (Jones & Gadd, 1990). The inhibitory effect of nitrite during ethanol production may be involved in the generation of RNS at acidic pH.

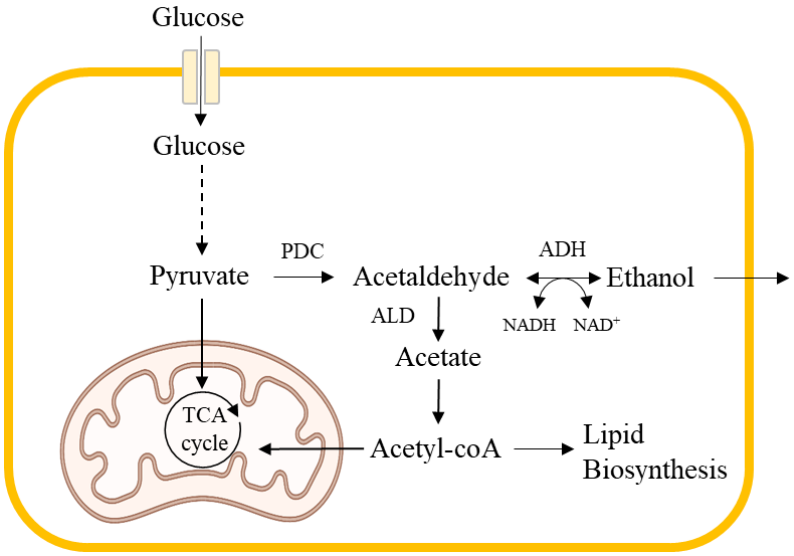

Fig. 1-4 Pyruvate metabolism and ethanol production pathway. Abbreviations: PDC, pyruvate decarboxylase; ADH, alcohol dehydrogenase; ALD, aldehyde dehydrogenase (Remize et al., 2000).

1.5.3 Pyruvate decarboxylase

Pyruvate decarboxylase (PDC) catalyzes the conversion of pyruvate into acetaldehyde and carbon dioxide. A significant cytosolic enzyme plays an essential role in diverting pyruvate flow towards fermentation and lipid synthesis in some bacteria, yeast, fungal species, and plants. The genome of *S.cerevisiae* contains three genes that encode the pyruvate decarboxylases (*PDC1*, *PDC5*, and *PDC6*). A major isozyme, Pdc1, is highly expressed under most physiological conditions (Romagnoli et al., 2012). Pdc5 shares 88% identical at the protein level with Pdc1, is highly expressed under nitrogen limitation (Boer et al., 2003, 2007), under thiamine limitation conditions (Muller et al., 1999), and in the *pdc1* deletion mutant, indicating the process of autoregulation between 2 genes (Hohmann & Cederberg, 1990). Interestingly, the autoregulation of PDC gene expression appears to be related to the protein's existence rather than its catalytic activity (Eberhardt et al., 1999). Pdc2 regulates both *PDC1* and *PDC5* as a transcription factor (Hohmann, 1993). The *PDC6* expression level is undetectable under normal conditions even in cells lacking both *PDC1* and *PDC5*; however, it was found to be highly expressed in sulfur-limited cultures (Fauchon et al., 2002). *S. cerevisiae* cells are lethal in the absence of PDC activity when grown on glucose as a carbon source (Flikweert et al., 1996).

PDCs catalyze the non-oxidative decarboxylation of pyruvate to acetaldehyde with thiamin diphosphate (TPP) and Mg(II) as cofactors. (Sergienko & Jordan, 2002). This enzyme

has been thoroughly studied in terms of protein structure and function (Fig. 1-5). The major structure gene *PDC1* encodes 563 amino acids with a typical molecular mass of 59-61 kDa per subunit. The catalytically active enzyme in yeast is composed of four identical subunits; however, the studies prove that the dimer is required as the smallest catalytically active unit (Killenberg-Jabs et al., 2001). PDC in brewer's yeast represents allosteric regulation of catalytic activity. Pyruvate, as its substrate, was discovered to be the effectors responsible for inducing conformational changes by binding at regulatory sites (Spinka et al., 2017).

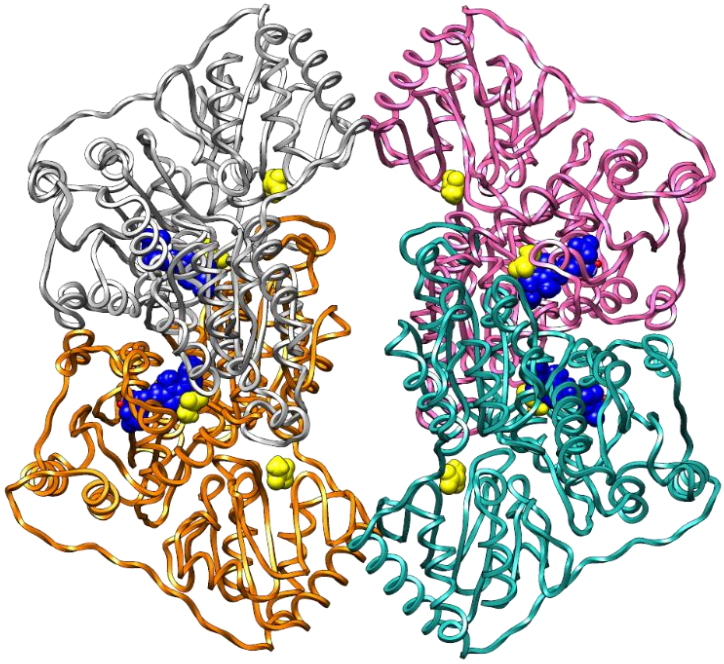

Fig. 1-5 Crystal structure of *S. cerevisiae* Pdc1 variant D28A (PDB ID: 2VK1) in tetramer with pyruvate bound at the regulatory and active sites (colored as yellow). The subunits are all represented in different colors, chains A, B, C, and D in gray, orange, pink, and cyan. In addition, the cofactors, thiamine diphosphate (dark blue) and magnesium ions (light green) are represented in space-filling mode.

1.6 GABA biosynthesis and its role in stress tolerance

γ-Aminobutyric acid (GABA) is a non-protein amino acid involving an intermediate bypassing steps of the TCA cycle, called GABA shunt. Glutamate decarboxylase (GAD) converts glutamate into GABA in the first step. 4-Aminobutyrate transaminase/GABA aminotransferase (GABA-T) then converts GABA into succinic semialdehyde (SSA), which is then irreversibly oxidized to succinate by succinic semialdehyde dehydrogenase (SSADH) (Bach et al., 2009). The GABA-shunt enzymes are found in a variety of organisms, with only minor differences in substrate and localization. GABA is catabolized to SSA in plants by a

pyruvate/glyoxylate-dependent GABA-T, whereas GABA-T in yeast is an α-ketoglutarate-dependent (Clark et al., 2009; Coleman et al., 2001). GAD is found in the plant cytosol, whereas GABA-T and SSADH are found in the mitochondria (Shelp et al., 2012). However, in yeast, all GABA-shunt enzymes are found in the cytosol (Cao et al., 2013b). In addition, GABA synthesis may occur via polyamine degradation (Shelp et al., 2012) and proline decarboxylation under oxidative stress conditions (Signorelli et al., 2015).

In the vertebrate brain, GABA is the primary inhibitory neurotransmitter. GABA catabolic pathway disorders cause neurological dysfunction. (Jakobs et al., 1993). GABA research in plants mainly focuses on its role in biotic and abiotic stresses. The GABA shunt is a critical signaling and metabolic pathway that allows *lentil cultivars* to adapt to salt, osmotic, and oxidative stresses during seeding. (Al-Quraan & Al-Omari, 2017). GABA-depleted gad1/2 mutant of *Arabidopsis thaliana* became a drought oversensitive phenotype (Mekonnen et al., 2016). During various stress conditions, the loss-of-function of the GABA transaminase gene, which is defective in GABA catabolism, causes early leaf senescence in *A. thaliana* (Jalil et al., 2017). Knockout mutants of SSADH produce more hydrogen peroxide and are more sensitive to UV and heat, developing necrosis when subjected to such stress. The GABA shunt appears to be essential for plant defense against environmental stresses because it prevents the accumulation of reactive oxygen intermediates and cell death (Bouché et al., 2003).

GABA accumulation in plant has been found in response to abiotic stresses, such as oxidative stress (Al-Quraan & Al-Omari, 2017), drought (Mekonnen et al., 2016), and heavy metals (Seifikalhor et al., 2020). Furthermore, GABA supplementation to the oxidative-stressed plants significantly increases chlorophyll content, osmolytes such as proline and trehalose, enzymatic antioxidants activity such as superoxide dismutase, catalase, ascorbate peroxidase, and glutathione reductase (Nayyar et al., 2014; Seifikalhor et al., 2020; Tang et al., 2020). These findings suggest that GABA influences defense mechanisms, leading to improved cell growth and survival.

The GABA shunt pathway in *S. cerevisiae* also includes three enzymes, glutamate decarboxylase, GABA aminotransferase, and succinic semialdehyde dehydrogenase, encoded by *GAD1*, *UGA1*, and *UGA2*, respectively. In contrast to plants, only GABA shunt is present in yeast for GABA synthesis. The GABA shunt is reported to play a role in forming succinate from α-ketoglutarate to the respiratory chain within mitochondria (Fig. 1-6). Three transport systems facilitate transporters of GABA in yeast: the general amino acid permease (Gap1), the proline permease (Put4), and a specific GABA permease (Uga4) (André et al., 1993). Gad1 has

been shown to bind calmodulin and is regulated by calcium levels in the same way in plants (Baum et al., 1993; Coleman et al., 2001). The induction of GABA regulates the expression of *UGA1*, *UGA2*, and *UGA4* via the transcriptional activator for GABA-dependent (encoded by *UGA3*) and the positive regulator of genes in nitrogen degradation pathways (encoded by *UGA35*/*DAL81*) (Vissers et al., 1989).

Previous research in yeast demonstrated that the GABA shunt is an important mechanism for oxidative stress tolerance and thermotolerance. Deletion of each gene in the GABA shunt, especially *uga1*, resulted in growth defects at high temperatures. The possible explanation for this is that carbon flux via the GABA shunt pathway reduces reactive oxygen intermediates accumulation, derived from mitochondrial electron transport chain, during heat stress (Cao et al., 2013a). On the other hand, *S. cerevisiae* exposed to oxidative stress requires *UGA2* for stress tolerance due to its ability to produce NADH or NADPH during the oxidation of succinate semialdehyde to succinate. (Coleman et al., 2001). Little is known about GABA accumulation and stress tolerance in yeast. Under hyperosmotic stress conditions, a non-conventional yeast, *Candida glycerinogenes*, accumulates intracellular GABA (Ji et al., 2018). The findings suggest that improving *C. glycerinogenes* intracellular GABA accumulation, either through an exogenous application or cellular synthesis, is a viable option for improving tolerance to hyperosmotic stress. However, the correlation between GABA and the nitrosative stress response in *S. cerevisiae* has yet to be determined.

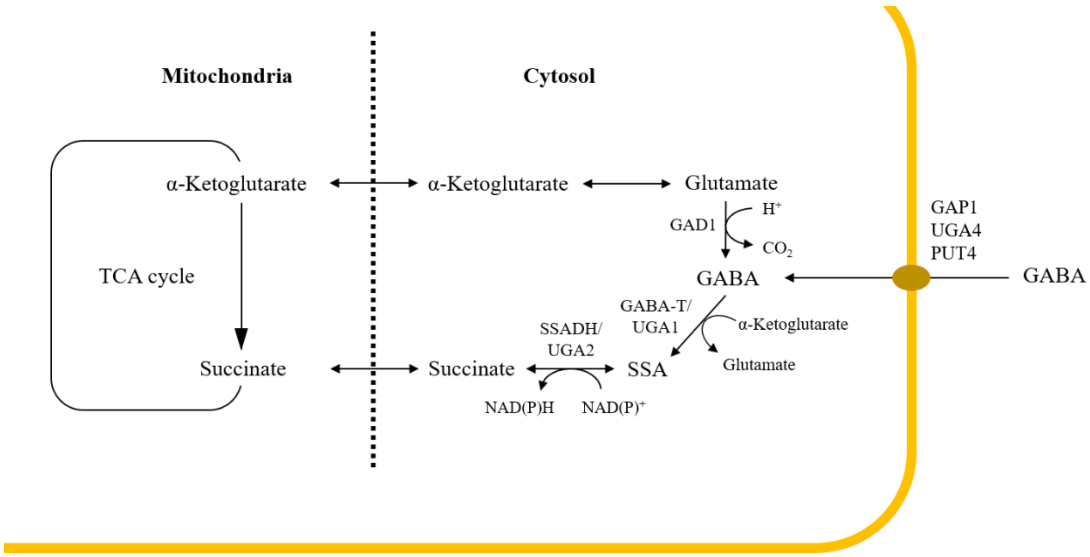

Fig. 1-6 GABA biosynthesis and metabolism pathway of *S. cerevisiae*. Abbreviations: GAD1, glutamate decarboxylase; GABA-T/UGA1, GABA aminotransferase; SSADH/UGA2,

succinate semialdehyde dehydrogenase; GAP1, general amino acid permease; UGA4, GABA permease; PUT4, proline-specific permease. (Bach et al., 2009)

1.7 Research objectives

In this study, exogenous reactive nitrogen species (RNS) generated by acidified nitrite are mainly focused in order to understand cellular responses to nitrosative stress in the budding yeast *S. cerevisiae*:

(1) Identification of tyrosine nitration under acidified nitrite conditions

(2) Impact of tyrosine nitration on pyruvate decarboxylase and ethanol production

(3) Physiological roles of GABA in nitrosative stress

2. MATERIALS AND METHODS

2.1 Materials

2.1.1 Strains

S. cerevisiae and *Escherichia coli* strains used in this study are shown in Table 2-1.

Table 2-1 Strains used in this study

Strains	Description	Sources
***Saccharomyces cerevisiae* X2180-1A (wild-type)**	*MAT*a *SUC2 mal mel gal2 CUP1*	Laboratory stock
***Saccharomyces cerevisiae* BY4741 (wild-type)**	*MATa his3Δ1 leu2Δ0 met15Δ0 ura3Δ0*	Laboratory stock
X2180-1A *arg1*Δ *lys*1Δ	X2180-1A *arg1Δ::natNT2 lys*1Δ*::hphNT1*	Laboratory stock
X2180-1A *ura3*Δ	X2180-1A *ura3Δ:: kanMX6*	Laboratory stock
X2180-1A *PDC1-1Myc7His*	X2180-1A *PDC1-1Myc7His::kanMX6*	This work
X2180-1A *PDC5-1Myc7His*	X2180-1A *PDC5-1Myc7His::kanMX6*	This work
X2180-1A *PDC6-1Myc7His*	X2180-1A *PDC6-1Myc7His::kanMX6*	This work
X2180-1A *ura3*Δ *pdc1*Δ	X2180-1A *ura3Δ::kanMX6 pdc1Δ::hphNT1*	This work
X2180-1A *ura3*Δ *pdc1*Δ [pRS416]	X2180-1A *ura*3Δ *pdc1*Δ harboring pRS416	This work
X2180-1A *ura3*Δ *pdc1*Δ [pRS416-*PDC1*-1Myc7His]	X2180-1A *ura*3Δ *pdc1*Δ harboring pRS416 with *PDC1*-1Myc7His	This work
X2180-1A *ura3*Δ *pdc1*Δ [pRS416-*PDC1*^{Y157F}-1Myc7His]	X2180-1A *ura*3Δ *pdc1*Δ harboring pRS416 with *PDC1*^{Y157F}-1Myc7His	This work
X2180-1A *ura3*Δ *pdc1*Δ [pRS416-*PDC1*^{Y344F}-1Myc7His]	X2180-1A *ura*3Δ *pdc1*Δ harboring pRS416 with *PDC1*^{Y344F}-1Myc7His	This work
BY4741 *gad1*Δ	BY4741 *gad1Δ::hphNT1*	This work
BY4741 *uga1*Δ	BY4741 *uga1Δ::hphNT1*	This work
BY4741[pRS416/pRS415-CgHIS3MET15]	BY4741 harboring pRS416 and pRS415-Cg*HIS3MET15*	This work
BY4741 *gad1*Δ [pRS416/pRS415-	BY4741 *gad1Δ::hphNT1* harboring pRS416 and pRS415-Cg*HIS3MET15*	This work

Strains	Description	Sources
CgHIS3MET15]		
BY4741 *uga1*Δ [pRS416/pRS415-CgHIS3MET15]	BY4741 *uga1*Δ*::hphNT1* harboring pRS416 and pRS415-Cg*HIS3MET15*	This work
***Escherichia coli* DH5α**	*F-, φ80dlacZΔM15, Δ(lacZYA-argF)U169, deoR, recA1, endA1, hdR17 (r_k^-, m_k^+), phoA, supE44, λ^-, thi-1, gyrA96, relA1*	Laboratory stock
***Escherichia coli* BL21 (DE3)**	B $F^–$ *ompT gal dcm lon hsdS*$_B$ ($r_B^–m_B^–$) λ(DE3 [*lacI lacUV5-T7p07 ind1 sam7 nin5*]) [$malB^+$]$_{K-12}$(λ^S)	Laboratory stock
***Escherichia coli* DH5α for plasmid multimerization**	*E. coli* DH5α harboring all constructed pRS416, pRS415, pDONR221 and pET-55-DEST plasmids	This work
***Escherichia coli* BL21 (DE3) for protein expression**	BL21(DE3) harboring all constructed pET-55-DEST plasmids	This work

2.1.2 Primers

The primers used in this study are shown in Table 2-2.

Table 2-2 Primers used in this study (restriction sites are underlined).

Primer	Sequences (5'-3')
F-*PDC1*_S1	5'-TTATTTTCTACTCATAACCTCACGCAAAATAACACAG TCAAATCAATCAA AATGCGTACGCTGCAGGTCGAC-3'
R-*PDC1*_S2	5'-GTTACATAAAAATGCTTATAAAACTTTAACTAATAAT TAGAGATTAAATCGCTTAATCGATGAATTCGAGCTCG-3'
F-*PDC1*_S3	5'-TCCACAAAACTTGGTTGAACAAGCTAAGTTGACTGC TGCTACCAACGCTAAGCAACGTACGCTGCAGGTCGAC-3'
F-attB1-*PDC1*	5'-GGGGACAAGTTTGTACAAAAAAGCAGGCTTCTCTGA AATTACTTTGGGTAAATATTTG -3'
R-attB2-*PDC1*	5'-GGGGACCACTTTGTACAAGAAAGCTGGGTTTTATTGC TTAGCGTTGGTAGCAGC -3'
F-attB1-*PDC1*-start codon	5'-GGGGACAAGTTTGTACAAAAAAGCAGGCTTCGAAGG AGATAGAACCATGTCTGAAAATTACTTTGGGTAAATAT-3'
R-attB2-*PDC1*_No stop	5'-GGGGACCACTTTGTACAAGAAAGCTGGGTGTTGCTTA GCGTTGGTAGCAGCAGT-3'
F-*PDC1*-Y38amber	5'-ATCTCATACCTTCAACTTCCTAGATCTTGTCCAACAAGG-3'
R-*PDC1*-Y38amber	5'-CCTTGTTGGACAAGATCTAGGAAGTTGAAGGTATGAGAT-3'
F-*PDC1*-Y157amber	5'-CTGGTCTTTGGGTGACCTAAGTGGTTCTGATACA-3'
R-*PDC1*-Y157amber	5'-TGTATCAGAACCACTTAGGTCACCCAAAGACCAG-3'

Primer	Sequences (5'-3')
F-*PDC1*-Y344amber	5'- AGCAACTGGCTTCTAACCCTTAGCGGCGTC -3'
R-*PDC1*-Y344amber	5'- GACGCCGCTAAGGGTTAGAAGCCAGTTGCT -3'
F-*PDC1*-Y157F	5'-GGTCTTTGGGTGACGAAAGTGGTTCTGATACAT-3'
R-*PDC1*-Y157F	5'-ATGTATCAGAACCACTTTCGTCACCCAAAGACC-3'
F-*PDC1*-Y344F	5'-AGCAACTGGCTTGAAACCCTTAGCGGC-3'
R-*PDC1*-Y344F	5'-GCCGCTAAGGGTTTCAAGCCAGTTGCT-3'
F-*PDC1*-239-Sq	5'-TGAACACGTCGGTGTTTTGC-3'
GAD1_FW	5'-AGTGGAATGCCGATTGGTT-3'
GAD1_RV	5'-AACGACTCTGGGTCAAGCAT-3'
UGA1_FW	5'-TTGCAGAAGAAATACCCTGAAAA-3'
UGA1_RV	5'-GCAAATCCCAGGCAATGA-3'
UGA2_FW	5'-CGTCGGTAAAATCTTGATGAAA-3'
UGA2_RV	5'-CCACCCAGCTCAAAAGACAG-3'
GAD1-S1	5'-CGTCGCTCTTAACAATCCAGGCTGAACAAAACAAGGAATA CGTACGCTGC AGGTCGAC-3'
GAD1-S2	5'-CATACATATAGGGGGCGGTATATTGGATGACCTTTTCAACA TCGATGAAT TCGAGCTCG-3'
UGA1-S1	5'-TACAGAAAGAACAGACAAGAAACCGTCAATAAGAAATAT AACTAAGAACAATGCGTACGCTGCAGGTCGAC-3'
UGA1-S2	5'-AGACCAAAAAAGGGAACGTGACACGGCCTCGCTAATATA CAATCAATCGATGAATTCGAGCTCG-3'
GAD1-dis1-F	5'TCTAGTTGGTTCTTGACATT-3'
UGA1_FWUP_741	5'TGGTGCGGTGATTGGATATG-3'

1

2

2.1.3 Plasmids

The plasmids used in this study are shown in Table 2-3.

Table 2-3 Plasmids used in this study

Plasmids	Description	Sources
pRS415-CgHIS3MET15	Yeast centromere vector pRS415-*LEU2HIS3MET15*	
pRS416	Yeast centromere vector pRS416-*URA3*	
pRS416-*PDC1*-1Myc7His	pRS416 harboring *PDC1-1Myc7His::kanMX6*	This work
pRS416-*PDC1*^{Y157F}-1Myc7His	pRS416 harboring *PDC1-1Myc7His::kanMX6* point mutation (Tyr38Phe)	This work
pRS416-*PDC1*^{Y344F}-1Myc7His	pRS416 harboring *PDC1-1Myc7His::kanMX6* point mutation (Tyr38Phe)	This work
pDONR221	Gateway® donor vector with attP1 and attP2 sites, *Kan*^{R}	Gateway®
pET-55-DEST	Gateway® bacterial destination vector for expressing proteins tagged at the N-terminus with Strep-Tag II and C-terminus with 6X-His affinity	Gateway®
pDule–nitroTyr–5B	Plasmid for incorporating the non-canonical amino acid 3-nitrotyrosine with the *Methanocaldococcus jannaschii* 3NY (5B) synthetase and cognate amber suppressing tRNA in *E.coli*	Addgene®
pDONR221-*PDC1*	pDONR221 harboring *PDC1* without a start codon and stop codon	This work
pDONR221-*PDC1* (Y38NT)	pDONR221 harboring mutated *PDC1* (Tyr38Amber stop codon)	This work
pDONR221-*PDC1* (Y157NT)	pDONR221 harboring mutated *PDC1* (Tyr157Amber stop codon)	This work
pDONR221-*PDC1* (Y344NT)	pDONR221 harboring mutated *PDC1* (Tyr344Amber stop codon)	This work
pET-55-DEST-*PDC1*	pET-55-DEST harboring *PDC1* without a start codon and stop codon	This work
pET-55-DEST-*PDC1*(Y38NT)	pET-55-DEST harboring mutated *PDC1* (Tyr38Amber stop codon)	This work
pET-55-DEST-*PDC1*(Y157NT)	pET-55-DEST harboring mutated *PDC1* (Tyr157Amber stop codon)	This work
pET-55-DEST-*PDC1*(Y344NT)	pET-55-DEST harboring mutated *PDC1* (Tyr344Amber stop codon)	This work

2.2 Methods

2.2.1 Strain and culture media

S. cerevisiae laboratory strain X2180-1A was used in this study. Cells were cultured in nutrient-rich yeast extract-peptone-dextrose medium (YPD) containing 1% yeast extract, 2% peptone, and 2% glucose) adjusted to pH 6.0 using 1 M HCl and a minimal synthetic medium (SD) containing 0.17% yeast nitrogen base without amino acids and ammonium sulfate, 0.5% ammonium sulfate, and 2% glucose. 1 M HCl was used to adjust the pH of the SD medium to 4.0. Cells were pre-cultured in 2 mL YPD or SD medium at 30˚C with shaking at 200 rpm overnight, then inoculated in 50 mL as the main cultures with the initial OD_{600} of 0.1 and incubated at 30˚C with shaking at 200 rpm until OD_{600} reached 0.8-1.0.

E. coli strains DH5α and *E. coli* BL21 (DE3) were grown at 37 ºC in LB medium (5 g/L yeast extract, 10 g/L tryptone (BD), and 10 g/L NaCl (Nacalai Tesque, Japan) or M9 medium by shaking at 250 rpm. Mediums containing antibiotics were used as a selective medium.

2.2.2 Cell viability

The stock solution of 1 M $NaNO_2$ was prepared immediately before use. Yeast cells were grown in SD medium pH 4.0 treated with 1 mM of $NaNO_2$, and incubated in shaking conditions. After the indicated time, 1 mL of culture was collected and serially diluted to a suitable concentration. Diluted cells were plated on a YPD agar medium and incubated at 30ºC for 2 days. The cell viability result was presented as percentages as a colony-forming unit, followed by this calculation: (The number of colonies with $NaNO_2$ treatment at indicated time / the number of colonies without $NaNO_2$ treatment at the indicated time) x 100.

2.2.3 Plasmids and DNA preparation

2.2.3.1 DNA and plasmid extraction

Yeast cells were grown in YPD medium, harvested, and resuspended in 300 µL of lysis buffer (100 mM Tris-HCl pH 8.0, 100 mM NaCl, and 10 mM EDTA), and then 250 µL of phenol/chloroform was added. An equal volume of 0.5 mm diameter glass beads was added to the mixture. Cells were disrupted by the multi-beads shocker (Multi-Beads Shocker, Yasui Kikai, Japan) under the following condition: 2,500 rpm, 60-sec on, and 30-sec off, 15 cycles. 400 mL TE Buffer was added and mixed by vortexing briefly. The mixture was centrifuged for

10 min at maximum speed at room temperature. The aqueous layer was transferred to a new tube. The supernatant was mixed with 1 mL ice-cold ethanol and centrifuged for 5 min at room temperature. The pellet was collected, washed with 70% ethanol, and dried at room temperature. Finally, the pellet was dissolved in 100 mL TE Buffer.

For plasmid extraction, *E.coli* cells harboring plasmid were grown in LB medium containing appropriated antibiotic, harvested, and resuspended in 250 µL of P1 buffer (50 mM Tris-HCl pH 8.0, 10 mM EDTA, and 100 µg/mL RNase A). 250 µL of P2 buffer (200 mM NaOH and 1% sodium dodecyl sulfate (SDS)) was added to the cell suspension and slightly mixed. Subsequently, 350 µL of N3 buffer (4.2 M guanidinium chloride and 0.9 M potassium acetate, pH 4.0) was added and centrifuged at a maximum speed for 10 min. The supernatant was transferred to a clean 1.5 mL tube where an equal volume of isopropanol was added, vortexed thoroughly, and centrifuged at a maximum speed for 5 min. The plasmid pellet was washed with 500 µL of 70% ethanol, centrifuged in the same manner, and dried up. An appropriate volume of milli-Q was used for resuspension. Finally, yeast genomic DNA and plasmid were quantified by Nanodrop (BioSpec-nano, Shimadzu Biotech, Japan).

2.2.3.2 Construction of protein expression vectors

Plasmid pDONR221 containing attP1 and attP2 was used as a donor vector in this system. PCR product of wild-type *PDC1* was tagged with attB1 and attB2, which react with attP1 and attP2 on pDONR221. PCR products were purified by mixing with 5 µL of 3 M sodium acetate, pH 5.0, and 125 µL of 100% cold ethanol. PCR mixture was incubated for 20 min at -20ºC and centrifuged at 13,000 x *g* for 10 min. The pellet was washed with 70% ethanol and dried up. 50 µL of milli-Q water was added. The DNA concentration was measured using Nanodrop.

Construction of pDONR221 harboring *PDC1* was carried out by mixing 75 ng/µL of pDONR221 and 75 ng/µL of PCR product within the total volume of 4 µL. Then, 1 µL of BP clonase™ II (Invitrogen, USA) was added and incubated at 25ºC overnight. Subsequently, 0.5 µL of proteinase K solution was added to the mixture and incubated at 37ºC for 10 min. BP clonase mixture was subsequently introduced to *E. coli* DH5α cells selected on LB medium containing 50 µg/mL of kanamycin. Desired transformants were subjected to plasmid DNA extraction. To construct the protein expression vectors, 75 ng/µL of pDONR221 harboring *PDC1* were incubated with 75 ng/µL of pET-53-DEST performed in the same manner as the

BP clonase reaction, but LR clonase™ II was used instead. Transformants were screened on LB containing 100 μg/mL of ampicillin. pET-53-DEST harboring Pdc1 was transformed to *E. coli* BL21 (DE3) as a protein expression host.

2.2.3.3 Site-directed mutagenesis

The modification of single nucleotide residues was performed as previously described (H. Liu & Naismith, 2008). Briefly, for mutation, a pair of oligonucleotides were synthesized, harboring the desired alterations. For amplification, 20 ng plasmid DNA was used in a total volume of 10 μl, including 1 μM each primer, 200 μM dNTPs, and 1 U of DNA polymerase. After denaturation (1 min at 98°C), 12 cycles were conducted, consisting of 10 sec at 98°C, 30 sec at 60°C, and 7 min at 68°C, followed by a final extension step at 68°C for 10min. Subsequently, the parental and semi-parental template DNA was digested with *Dpn*I, and the amplified plasmids were transformed into *E. coli* DH5α cells. The mutation was verified by sequencing.

2.2.3.4 DNA sequencing reaction

BigDye Terminator v3.1 Cycle Sequencing Kit (Applied Biosystems, USA) was used for the sequencing PCR reaction. DNA sequencing PCR was performed by preparing a reaction mixture consisting of 100 ng/μL of purified DNA, 3.5 μL of BigDye Terminator v3.1 Cycle 5x sequencing buffer, 1 μL of BigDye Terminator v3.1 Cycle sequencing reagent, 1.6 μL of 2 μM primer, and Milli-Q water in 20 μL solution. PCR products were subjected to ethanol precipitation and analyzed by a DNA sequencer (ABI3130xl/Genetic Analyzer, Applied Biosystem).

2.2.4 PCR-based tagging of yeast genes

The integration of epitope tagging on the yeast genome was performed as previously described (Janke et al., 2004). Briefly, primers F-*PDC1*_S3 and R-*PDC1*_S2 described in table 2-2 were used to amplify epitope tagging from pYM46 (1Myc7His tag). PCR product was purified and transformed into yeast. The integration of PCR product to yeast genome was illustrated in Fig. 2-1.

Yeast transformation was based on the lithium acetate (LiAc) method (Gietz & Schiestl, 2007) with several modifications. Briefly, cells were culture in YPD medium until OD_{600} = 0.6

and washed twice with 100 mM LiAc. Cells were added to the transformation mixture (240 µL of PEG 3350 (50%w/v), 36 µL of 1M LiAc, 25 µl of salmon sperm DNA solution, 0.1-1 µg of plasmid, and adjusted to final volume 351 µl by DI water). The mixture was incubated at 30ºC for 20-30 min and 42ºC for 20 min. Cells were added 1 mL of YPD medium and incubated on a shaker for at least 5–6 h at 30ºC, then collected the cells and spreaded onto the selection plates. The success of the integration was tested by colony PCR.

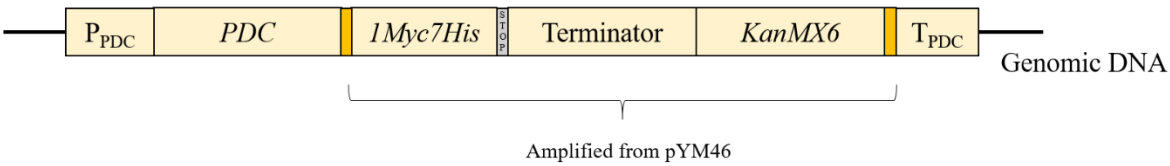

Fig. 2-1 Integration of 1Myc7His tagged to yeast genomic DNA. P_{PDC} : promoter of PDC, T_{PDC} : terminator of PDC

2.2.5 Yeast Pdc1 pull-down assay

Yeast cells (with genome integrated *PDC1*-1Myc7His) with OD_{600} = 0.8 were treated with 1 mM $NaNO_2$ in SD medium pH 4.0 for 3 h. Then, protein extraction was performed using RIPA buffer (50 mM Tris-HCl pH 7.2, 150 mM NaCl, 1% NP-40, 0.5% Sodium deoxycholate, 0.1% SDS) and bead beater. Add 800 µg of lysate to 40 µL of His Mag Sepharose™ Ni (Cytiva, Belgium), incubated sample, and beads at 4ºC on rotating mixer for 1.5 h. Beads were washed with a binding buffer 500 µL, 5 times (20 mM sodium phosphate, 20 mM imidazole, 500 mM NaCl, pH 7.4) and eluted by 20 µL of elution buffer (20 mM sodium phosphate, 500 mM imidazole, 500 mM NaCl, pH 7.4). Nitrated proteins were confirmed by western blotting.

2.2.6 Nitrated protein detection

Yeast cells OD_{600} = 0.8 were grown in SD medium pH 4.0 treated with 1 mM $NaNO_2$ and incubated in shaking condition at 30ºC. Cells were collected by centrifugation at 3,000 rpm, 4°C for 5 min, and washed twice with sterilized DI water. For whole-cell protein extraction, cells were suspended in iced 450 µL of 50 mM phosphate buffer saline. After that, and 50 µL of trichloroacetic acid was added to the samples and mixed. Cells were lysed with

glass beads. The samples were centrifuged at 15,000 rpm, 4ºC for 20 min, and discarded supernatants completely. The precipitates were re-suspended in 100 µL of 1x sample buffer (50 mM Tris-HCl (pH 6.8), 2% SDS, 2.25% glycerol, 5% 2-mercaptoethanol, and 0.0125% bromophenol blue). The samples were centrifuged at 15,000 rpm, 25ºC for 5 min. The supernatants were collected as whole-cell extracts. Cell lysate cells were suspended in iced lysis buffer (100 mM Tris-HCl (pH 7.5), 1 mM EDTA, 10 mM 2-mercaptoethanol, and protease inhibitors), and lysed with glass beads. The samples were then centrifuged and collected the supernatants.

Ten µg of each sample was subjected to SDS-PAGE by mixing sample with 5x SDS loading buffer (250 mM Tris-HCl, pH 6.8, 10% SDS, 30% (w/v) glycerol, 10 mM DTT, 0.05% (w/v) bromophenol blue). The sample mixture was heated at 95ºC for 10 min. Samples were loaded to the 10% SDS–PAGE, and electrophoresis was performed at 10 mA for 30 min for stacking gel and at 20 mA for 120 min for running gel, followed by the transfer of proteins to PVDF membranes. One membrane was subjected to chemical reduction of nitrotyrosine before western blotting, and the other membrane was used for western blotting without reduction. Reduction of nitrotyrosine to aminotyrosine was achieved by treating a membrane with 10 mM sodium dithionite in 50 mM pyridine-acetate buffer, pH 5.0, for 1 h at room temperature. After the reaction, the membrane was rinsed with distilled water. The reduced and non-reduced PVDF membranes were blocked for 1 h in 3% w/v skim milk in 1x TBS-T buffer (20 mM Tris-base, 150 mM NaCl, and 0.1% Tween-20). All washing steps were carried out using a 1x TBS-T buffer. The nitrated proteins and Pgk1 proteins were detected by the monoclonal anti-3-nitrotyrosine (3-NT) (Product No. sc-32757, Lot No. C1417, Santa Cruz Biotechnology, USA) at $1:2,000$ dilution and the monoclonal anti-phosphoglycerate kinase 1 (Pgk1) (Product No. 459250, Lot No. UA2696317, Invitrogen, USA) at 1:20,000 dilution, respectively. HRP-conjugated polyclonal anti-mouse IgG (Promega) was used at 1:2,000 dilution for secondary probing. Signals were produced by Amersham ECL prime reagents (GE healthcare) and captured by using ImageQuant^{TM} LAS4000 (GE healthcare).

2.2.7 Detection of nitrated protein by LC-MS/MS

Stable isotope-based methods were used to distinguish the status of protein/ peptide amount for relative quantitation and detect post-translational modifications more accurately. Yeast strain X2180-1A *arg1*Δ *lys*1Δ were cultured in SD medium at pH 4.0 containing 206.7 µM arginine and 205.2 µM lysine for control condition and isotopic labeled arginine and lysine

at the same concentration for treatment condition (Fig. 2-2). Cells were collected at 0, 1, 3, and 6 h and extracted protein. Proteins of both conditions were mixed with 1:1 ratio and subjected to SDS-PAGE. Gel samples were prepared and analyzed by the requested analysis in the division of biological sciences in NAIST using Ion Trap-Orbitrap Mass Spectrometer LTQ-Orbitrap XL (Thermo Fisher Scientific). A database search on NCBI (S_cerevisiae (baker's yeast)) was performed using Proteome Discoverer 1.4 (SequestHT node) (Thermo Fisher Scientific). Searches were done with tryptic specificity allowing maximum 4 missed cleavage sites and a precursor mass tolerance of 10 ppm and fragment mass tolerance of 0.8 Da. Searched modifications were detected as followed: Acetyl / +42.011 Da (Any N-Terminus), Oxidation / +15.995 Da (M), Carbamidomethyl / +57.021 Da (C), Nitro / +44.985 Da (Y), Amino / +15.011 Da (Y), Label:13C (1) / +1.003 Da (R), Label:2H(4) / +4.025 Da (K).

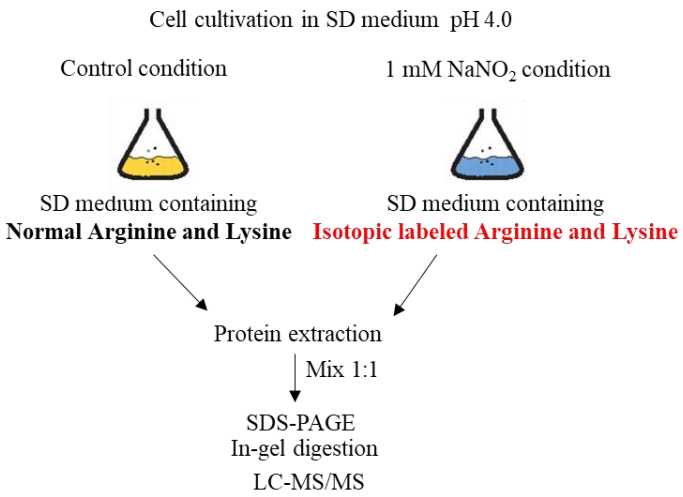

Fig. 2-2 Process of SILAC. Yeast strain X2180-1A *arg1*Δ::*nat*NT2 *lys*1Δ::*hph*NT1 were cultured in SD medium at pH 4.0 containing 206.7 µM arginine and 205.2 µM lysine for control condition and isotopic labeled Arginine and Lysine for 1 mM $NaNO_2$ treatment. Cells were collected at 0,1,3, and 6 h. Protein extracts of both conditions were mixed with a 1:1 ratio then performed LC-MS/MS analysis.

2.2.8 Recombinant Pdc1 expression

E. coli strain BL21(DE3) was transformed with pET-55-DEST-*PDC1*. Cells were pre-cultured at 37ºC overnight in a medium containing 100 µg/mL ampicillin. The culture was inoculated into a 300 mL flask at the initial OD_{600} of 0.05 and incubating at 37ºC with shaking at 250 rpm. When OD_{600} of the culture medium reached 0.6, cells were induced by 0.1 mM IPTG and continue cultured at 16°C overnight. Cells were harvested by centrifugation and resuspended in lysis buffer (50 mM Tris-HCl, 300 mM NaCl, 10 mM imidazole pH 7.4),

disrupted by sonication, and then centrifuged at 13,000 rpm at 4°C for 30 minutes. 200 µL of Ni-Sepharose 6 Fast Flow was applied to a column, washed, and equilibrated with binding buffer (20 mM sodium phosphate, 20 mM imidazole, 500 mM NaCl, pH 7.4). The protein solution was applied to the washed column and incubated for 1 h. The column was washed with binding buffer to remove the unbound proteins. Targeted-protein was eluted by elution buffer (20 mM sodium phosphate, 500 mM imidazole, 500 mM NaCl, pH 7.4). SDS-PAGE and western blotting were performed to check purified Pdc1.

2.2.9 PDC and ADH activity

The PDC assay was performed, as previously described (Flikweert et al., 1996). The assay mixture consisted of 40 mM imidazole-HCl buffers (pH 6.5), 0.2 mM thiamine pyrophosphate, 0.15 mM NADH, alcohol dehydrogenase 88 U/mL, 5 mM $MgCl_2$, and cell-free extract or purified Pdc1. The reaction was started by adding 50 mM pyruvate. The assay of ADH consisted of 100 mM phosphate buffer (pH 7.6), 8 mM acetaldehyde, and cell-free extract. Both enzymatic activities were measured spectrophotometrically by a decrease of NADH at an absorbance of 340 nm.

2.2.10 Nitrated Pdc1 expression

The plasmid containing PDC1 with an amber stop codon at tyrosine positions 38, 157, and 344 was constructed to direct nitrotyrosine incorporation. E.*coli* strain BL21(DE3) was co-transformed of pET-55-DEST-*PDC1*^{Y38NT}/pET-55-DEST-*PDC1*^{Y157NT}/pET-55-DEST-*PDC1*^{Y344NT} and pDule–nitroTyr–5B (Addgene). The orthogonal aminoacyl-tRNA synthetase and cognate amber suppressing tRNA to incorporate nitrotyrosine are expressed (Fig. 2-3). Transformant was cultured in M9 medium with 0.4% casamino acid containing 100 µg/mL ampicillin, 25 µg/mL tetracycline. When OD_{600} reached 0.6, 0.1 mM IPTG and 1 mM nitrotyrosine (3NT) were added and cultured for 16 h at 16ºC. Cells were harvested by centrifugation and purified by Ni-Sepharose 6 Fast Flow. Purified Pdc1 was checked by SDS-PAGE and western blotting.

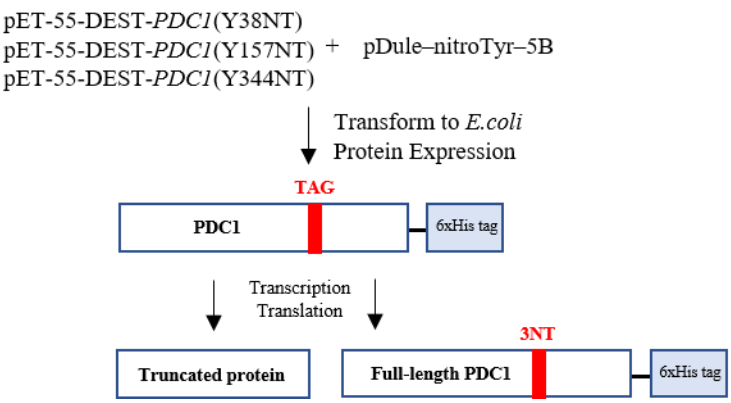

Fig. 2-3 Process of nitrotyrosine incorporation to Pdc1. Pdc1 recombinant protein with C-terminal 6xHis-tagged bearing amber stop codon at amino acid position 38, 157, or 344 was co-transformed with plasmid expressing a *Methanocaldococcus jannaschii* tyrosyl tRNA synthetase/$tRNA_{CUA}$ pair engineered to incorporate nitrotyrosine (pDule–nitroTyr–5B).

2.2.11 Ethanol quantification

Yeast cells were cultured in SD pH 4.0 with and without the addition of nitrite for 1 h. At the indicated time, 50 µL of supernatant were collected and stored at -20ºC until use. The ethanol concentration was determined using Ethanol Colorimetric/Fluorometric Assay Kit (Biovision, Switzerland)

2.2.12 Pyruvate quantification

Yeast cells were cultured in SD pH 4.0 with and without the addition of nitrite for 1 h. Cells were collected at the indicated time. Then, protein extraction was performed in 4 volumes of the pyruvate assay buffer, provided in Pyruvate Assay Kit (Sigma-Aldrich, Germany). Extracted sample was centrifuged at 13,000 rpm for 10 min to remove insoluble material. The supernatant was deproteinized with 10 kDa Amicon spin filters (Merck Millipore, USA) and measured pyruvate using Pyruvate Assay Kit.

2.2.13 Intracellular amino acid analysis

S. cerevisiae cells started OD_{600} = 0.8 – 1.0 were cultured in 50 mL of SD medium at 30 ºC. Cells were collected at the indicated time and washed three times with sterile distilled water. Cells were adjusted with a total OD_{600} = 40 and resuspended into 500 µL of sterile distilled water. Intracellular amino acids were extracted by boiling the cells suspension at 100ºC for 20 min and collected supernatant by centrifugation at 12,000 rpm for 1 min. The

sample was filtrated with a 0.2 µm syringe filter (medium, India) and analyzed by an amino acid analyzer (AminoTac^{TM} JL500/V, JEOL Ltd., Tokyo, Japan). Intracellular amino acid concentrations were calculated as nmol/g of dry weight.

2.2.14 Assay of glutathione reductase and catalase

Glutathione reductase (GR) and catalase activity were measured using crude cell-free extract. The GR activity was performed, as previously described (Carlberg & Mannervik, 1975). The assay mixture contained: 100 mM phosphate buffer (pH 7.6), 1 mM Oxidized Glutathione (GSSG), 0.15 mM NADPH, 0.5 mM EDTA and 20 µg of cell-free extract. A spectrophotometer measured the decrease of NADPH at an absorbance of 340 nm. The catalase activity was detected as previously described (Aebi, 1984). The assay mixture contained: 50 mM phosphate buffer (pH 7.0), 10 mM hydrogen peroxide, and 100 µg of cell-free extract. This activity was measured by the decrease in hydrogen peroxide at absorbance 240 nm.

2.2.15 Protein sequence alignment

The alignment of protein sequences was performed by using www.uniprot.org/align/. The protein sequence of pyruvate decarboxylase 1 from *Saccharomyces cerevisiae*, *Kluyveromyces marxianus*, *Schizosaccharomyces pombe*, *Candida albicans*, *Arabidopsis thaliana*, and *Oryza sativa*, obtained from the same website, was analyzed.

2.2.16 Protein visualization

Three-dimensional (3-D) protein models of yeast *Saccharomyces cerevisiae* Pdc1 (PDB ID: 2VK1) were obtained from https://swissmodel.expasy.org/. The 2-D model was visualized and manipulated with UCSF Chimera (Pettersen et al., 2004).

2.2.17 Statistical analysis

The student T-test, as implemented in Microsoft Office Excel, was used for statistical analysis with a significance level of *$\rho < 0.05$ and ** $\rho < 0.01$

3. RESULTS

3.1 Identification of PTN in yeast cells

3.1.1 Effect of acidified nitrite treatment on cell viability and PTN

To generate RNS in this study, I used the nitrite addition at an acidic pH of the medium (called acidified nitrite). First, I examined whether the acidified environment affects cell growth. Cell growth was monitored using the spectrophotometric method under various pH conditions ranging from 4 to 6 (Fig. 3-1A). As a result, there was no significant difference in cell growth between pH 4.0 and pH 6.0. This result suggests that the effect of acidic pH on cell growth is not critical, so SD medium with pH 4.0 was used to generate RNS in the following experiments. Subsequently, cells were cultured in SD medium pH 4.0 with 1 mM $NaNO_2$ for 6 h to monitor cell growth under acidified nitrite conditions. An acidified nitrite treatment completely inhibited cell growth (Fig. 3-1B). To determine whether an acidified nitrite treatment induces PTN, I tried to detect PTN in cell lysate extracted from yeast cells treated with acidified nitrite by western blotting with an anti-3-nitrotyrosine antibody (3NT). As shown in Fig. 3-1C, the signal from western blotting was shallow in the untreated samples throughout the 6 h culture. On the other hand, the PTN level clearly increased in a time-dependent manner in acidified nitrite-treated samples, particularly 3 h- and 6 h-treatment. Additionally, the PTN signal was not detected when the membrane was treated with dithionite, which reduces 3NT to 3-aminotyrosine (Fig. 3-1E), indicating that these signals were derived from PTN (Fig. 3-1D). These results showed that nitrite treatment in an acidic environment resulted in PTN in *S. cerevisiae* cells.

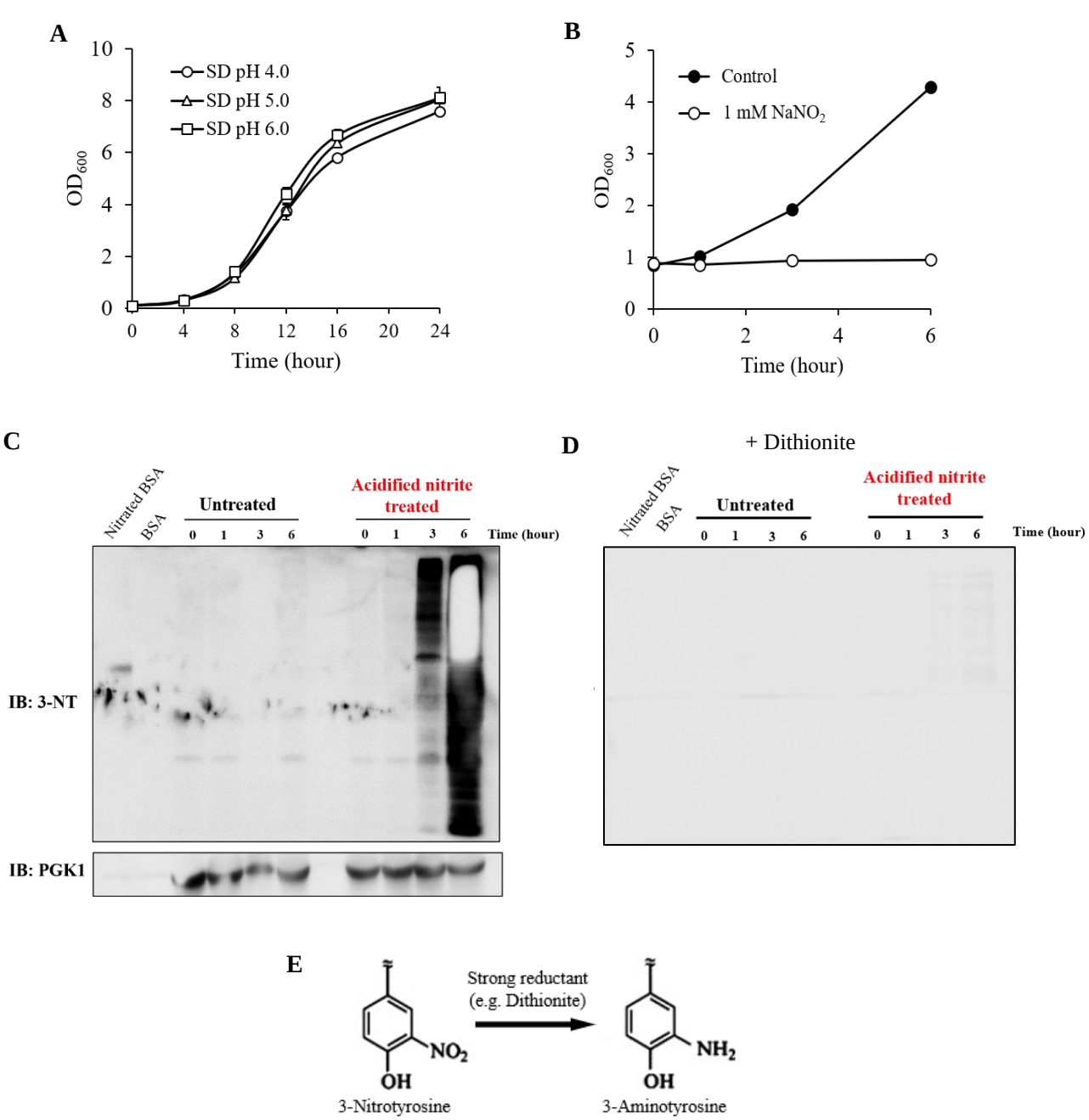

Fig. 3-1 Cell growth and PTN levels of *S. cerevisiae* under acidified nitrite conditions. (A) Yeast cells were grown in SD medium (pH 4.0-6.0) and measured growth at OD_{600}. (started OD_{600} = 0.1) (B) Growth curve of cells grown in SD medium pH 4.0 with and without 1 mM $NaNO_2$ for 6 h (started OD_{600} = 0.8) (C) Detection of nitrated proteins treated with 1 mM $NaNO_2$ at pH 4.0. Cell lysate (10 µg per lane) was subjected to Western blot analysis in duplicate to detect PTN. Immunoblot analysis was performed with anti-3NT antibody (1:2,000 dilution) and anti-PGK1 antibody (1:20,000 dilution) as the loading control. Bovine serum albumin (BSA) proteins and nitrated BSA proteins were used as negative and positive controls, respectively. (D) After transferring proteins to the PVDF membrane, the membrane was incubated with 10 mM sodium dithionite and performed immunoblotting. (E) Reduction of 3-nitrotyrosine to 3-aminotyrosine by dithionite.

3.1.2 Proteomic analysis of nitrated proteins

To identify and quantify the modified tyrosine (Y) residues in nitrite-treated yeast cells, stable isotope-labeled amino acids culture (SILAC) analysis using crude protein extracts treated with acidified nitrite was performed. Unfortunately, I was unable to obtain nitrated proteins quantification. Therefore, only identified PTN were displayed by searching for both tyrosine nitration and amination (reduced form of nitration). Table 3-1 summarizes the identified PTN involved in carbon metabolism, which was chosen due to their high detection rate. These findings suggested that under nitrosative stress, many enzymes involved in carbon metabolism are regulated by PTN. In addition, rather than carbon metabolism with PTN, the results of the proteomic analysis were shown in SUPPLEMENTARY INFORMATION (Table S1).

Table 3.1 List of nitrated/aminated proteins involved in glycolysis and ethanol production, which were identified by LC-MS/MS.

Protein name	Description	Nitration/amination site
Pfk1	Phosphofructokinase	Y^{740}
Fba1	Fructose 1,6-bisphosphate aldolase	Y^{230},Y^{310}
Tdh1	Glyceraldehyde-3-phosphate dehydrogenase	Y^{253}
Tdh2	Glyceraldehyde-3-phosphate dehydrogenase	Y^{138},Y^{312}
Tdh3	Glyceraldehyde-3-phosphate dehydrogenase	Y^{40}, Y^{43}, Y^{75}, Y^{138}, Y^{312}
Pgk1	Phosphoglycerate Kinase	Y^{381}
Pgm1	Phosphoglycerate Mutase	Y^{49}
Eno1	Enolase	Y^{145}
Eno2	Enolase	Y^{131}, Y^{145}
Pyk1	Pyruvate kinase	Y^{309}, Y^{368}
Pdc1	Pyruvate decarboxylase	Y^{38}, Y^{157}, Y^{344}
Pdc5	Pyruvate decarboxylase	Y^{243}
Adh1	Alcohol dehydrogenase	Y^{330}

3.2 Impact of PTN on pyruvate decarboxylase and ethanol production

3.2.1 Acidified nitrite led to pyruvate accumulation and decreased ethanol production

According to the results of proteomic analysis (Table 3-1), many enzymes involved in glycolysis and ethanol production were nitrated in response to nitrosative stress. Therefore, among the metabolites related to these pathways, pyruvate as an end product of glycolysis and its associated metabolites (ethanol and alanine) were analyzed under acidified nitrite conditions for 1 h (Fig. 3-2A). Interestingly, pyruvate was highly accumulated in cells about 10-folds by nitrite treatment (Fig. 3-2B). On the other hand, ethanol content in the medium was decreased by about 50% under acidified nitrite conditions (Fig. 3-2C), whereas nitrosative stress did not affect the intracellular alanine content (Fig. 3-2D).

3.2.2 Acidified nitrite decreased Pdc1 activity but not ADH activity

Due to a decrease in ethanol content under nitrosative stress conditions, I measured enzymatic activities of ethanol-related enzymes, pyruvate decarboxylase (PDC) and alcohol dehydrogenase (ADH), using cell lysate extracted from yeast cells treated with acidified nitrite. As shown in Fig. 3-3, acidified nitrite treatment reduced PDC activity by approximately 50% (Fig. 3-3A), whereas ADH was still fully active (Fig. 3-3B). These results suggest that PDC activity is affected by RNS. *S. cerevisiae* possesses three genes encoding pyruvate decarboxylase, *PDC1*, *PDC5*, and *PDC6*, in the genome. To examine the protein expression levels of these isozymes under control and acidified nitrite conditions, western blot analysis using yeast cells producing each PDC isozyme fused with c-Myc-tag was performed with anti c-Myc antibody (Fig. 3-4). The results showed that Pdc1 was a major isozyme in both conditions, whereas the expression of Pdc5 and Pdc6 was not detected. Therefore, Pdc1, as the main isozyme (Hohmann & Cederberg, 1990), was selected as a candidate protein for further analyzing the effect of PTN.

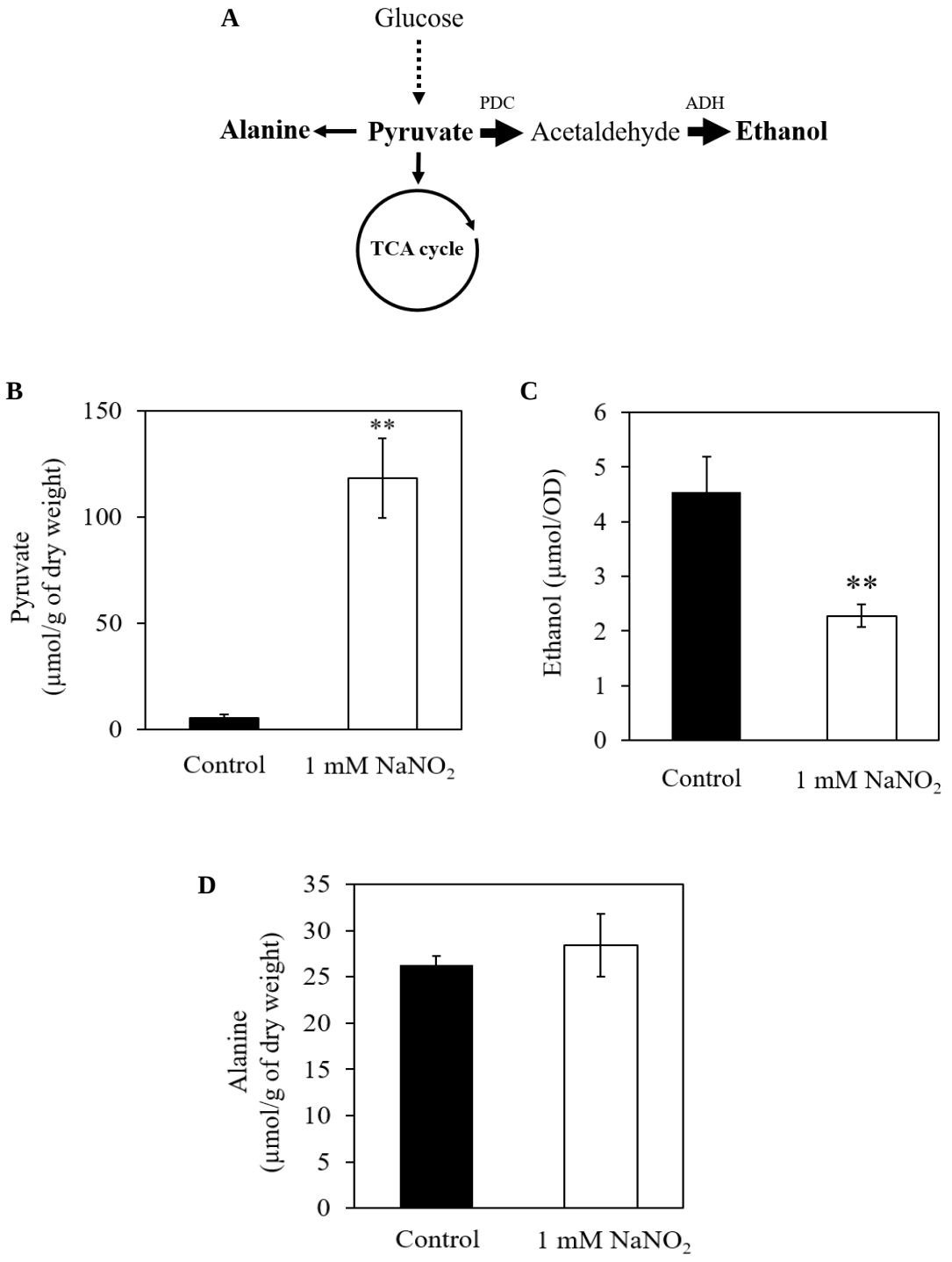

Fig. 3-2 The effect of acidified nitrite on pyruvate-related metabolites. (A) Pyruvate metabolic pathway, (B) intracellular pyruvate, (C) extracellular ethanol, and (D) intracellular alanine contents of *S. cerevisiae* under acidified nitrite treatment for 1 h. Data represent the averages of three independent experiments and standard deviations. Differences where $\rho < 0.01$ versus control (**) were significant when verified by the student's *t*-test.

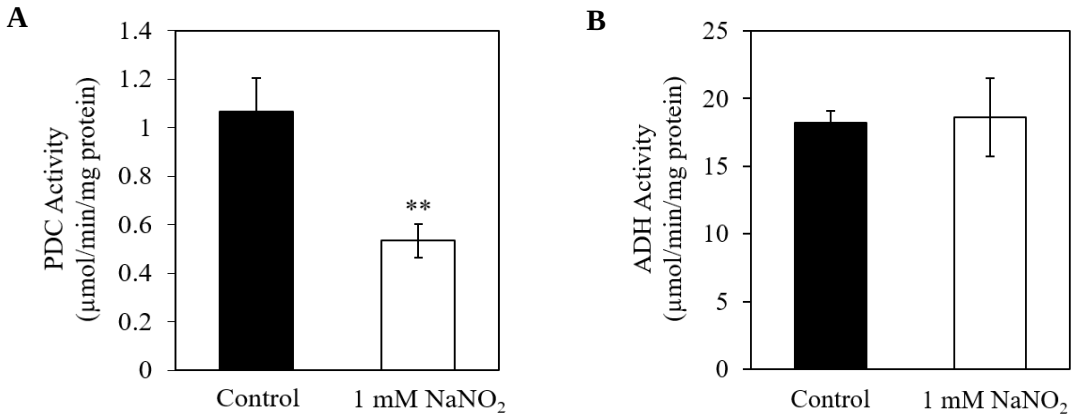

Fig. 3-3 The enzyme activity of PDC and ADH. Crude extract of yeast cells cultured in acidified nitrite condition was used for enzyme activity assay. Both enzyme activities were measured by detecting the decrease of NADH at A_{340}. (A) PDC activity using 5 μg protein. (B) ADH activity using 2 μg protein. Data represent the averages of three independent experiments and standard deviations. Differences where $\rho < 0.01$ versus control (**) were significant when verified by the student's *t*-test.

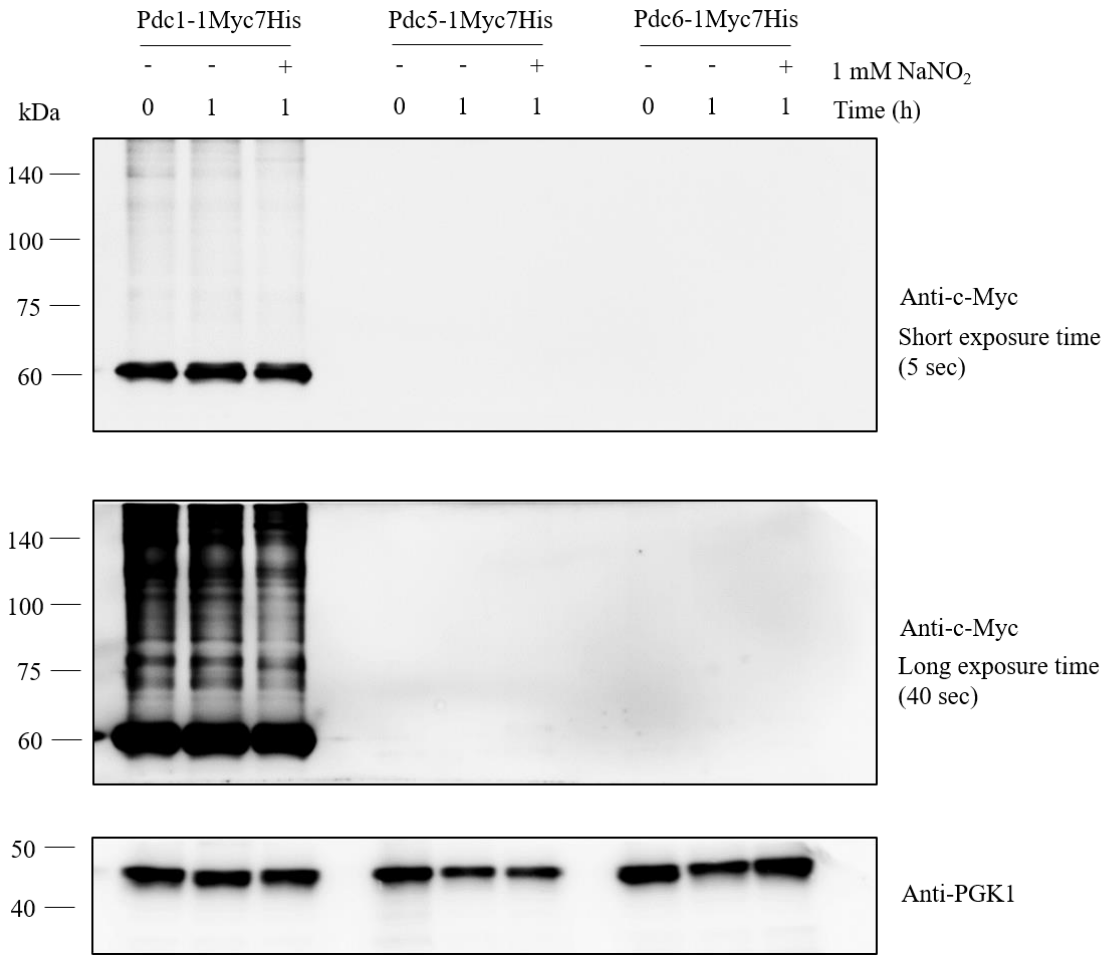

Fig. 3-4 Protein expression levels of Pdc1, Pdc5, and Pdc6. Yeast cells that express Pdc1, Pdc5, or Pdc6 fused with 1Myc7His were treated with 1 mM $NaNO_2$ in SD pH 4.0 for 1 h. Cell lysates were immunoblotted to analyze their protein expressions with anti-c-Myc (1:5,000 dilution) and anti-PGK1 (1:20,000 dilution) as the loading control.

3.2.3 Confirmation of nitrated Pdc1 *in vivo*

To confirm the PTN of Pdc1 with other analytical methods than mass spectrometry, the yeast strain producing Pdc1 fused with 1Myc7His-tagged at its C-terminus was used. The His-tagged Pdc1 was isolated by pull-down assay from the crude extract from yeast cells treated or untreated with acidified nitrite, and then the PTN level was analyzed by western blot with anti 3NT antibody. It was revealed that all samples contained comparable recombinant Pdc1 by western blot with anti c-Myc antibody (Fig. 3-5). Importantly, nitrite treatment increased the PTN level of Pdc1, which was abolished by dithionite reduction. This result indicated that Pdc1 was nitrated in response to acidified nitrite treatment *in vivo*.

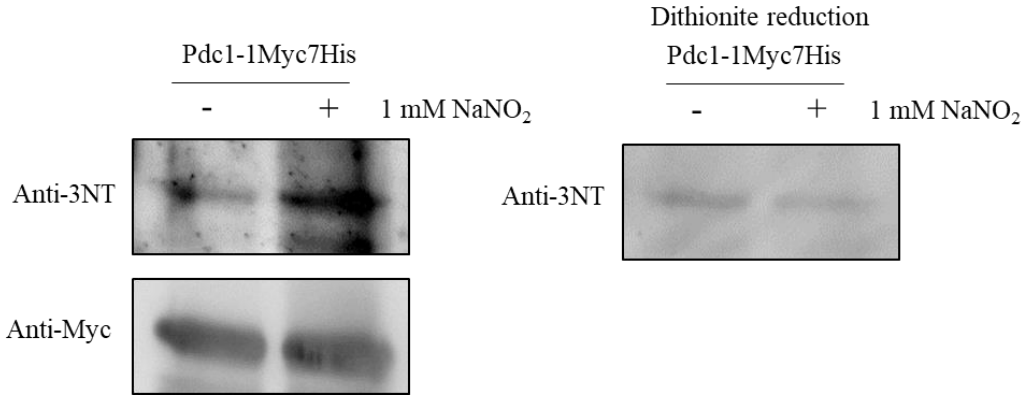

Fig. 3-5 Immunoblotting of nitrated Pdc1. Yeast cells that express Pdc1 fused with 1Myc7His were treated with 1 mM $NaNO_2$ for 1 h. The pull-down samples were subjected to Western blot analysis. The tyrosine nitration and protein level were detected by anti-nitrotyrosine (3NT) (1:2,500 dilution) and anti-c-Myc (1:5,000 dilution), respectively.

3.2.4 PTN altered Pdc1 activity

To investigate whether nitration caused by RNS affects Pdc1 activity, the recombinant Pdc1 was purified and analyzed. To prepare recombinant proteins, I used *E.coli* strain BL21(DE3) harboring pET-55-DEST-PDC1, in which Pdc1 fused with 6xHis-tagged at its C-terminus. SDS-PAGE analysis showed that Pdc1 was overexpressed in *E. coli* cells and that Pdc1 was successfully purified. Subsequently, purified Pdc1 was treated with 25-100 μM $ONOO^-$ and then the relative activity of Pdc1 was measured. Interestingly, Pdc1 activity was dramatically reduced when treated with $ONOO^-$ in the dose-dependent manner (Fig. 3-6B). Moreover, the PTN levels of $ONOO^-$ treated enzymes were analyzed by western blotting to examine whether PTN caused the inhibitory effect. Immunoreactivity to anti 3-NT antibody was found to increase as $ONOO^-$ concentrations increased (Fig. 3-6C). Taken together, these results suggest that RNS-dependent inactivation of Pdc1 is due to its PTN.

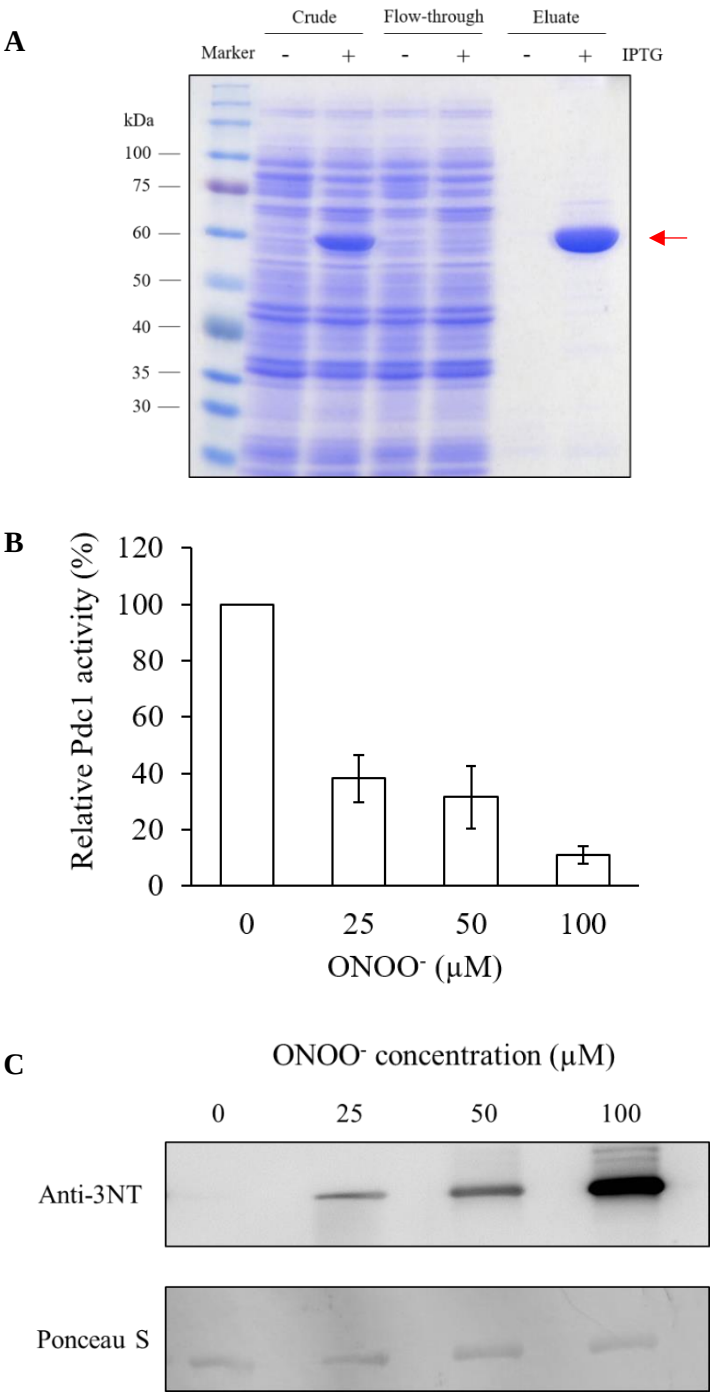

Fig. 3-6 Purification of recombinant Pdc1 and effect of $ONOO^-$ on Pdc1 activity. (A) *E.coli* strain BL21(DE3) harboring plasmid pET55-PDC1 was cultured in M9 medium with 0.4% casamino acid. After induction with 0.1 mM IPTG, proteins were extracted and purified by Ni-sepharose beads. Five μg of proteins were mixed with SDS sample buffer and heated at 95ºC for 10 min. Samples were loaded onto a 10% SDS-PAGE gel and stained with Coomassie Brilliant Blue. The red arrow indicates bacterial-expressed Pdc1 (approximately 61 kDa). (B) Relative Pdc1 activity of purified Pdc1 treated with 25, 50, and 100 μM of $ONOO^-$. Data represent the averages of three independent experiments and standard deviations. (C) Immunoblotting of Pdc1 treated with various concentrations of $ONOO^-$ using anti-nitrotyrosine

(3NT) (1:2,500 dilution) and protein loading was determined by membrane staining with Ponceau S.

3.2.5 Identification of PTN site in nitrated Pdc1

Subsequently, I analyzed the proteomic data shown in Table 3-1, in which Pdc1 was identified as a nitrated protein for more details. The protein sequence coverage was 76.02%, and the peptide fragments containing 14 tyrosine residues were identified among 17 tyrosine residues of Pdc1 (Fig. 3-7A). Table 3-2 summaries the peptides identified by LC-MS/MS. None of the identified peptides contained nitrated tyrosine; instead, those containing aminotyrosine, which is a reduced form of nitrotyrosine (Fig. 3-8A), were detected. The first peptide sequence, QVNVNTVFGLPGDFNLSLLDKIYEVEGMR, consisted of 29 amino acids and a mass of 3283.69 Da with aminotyrosine (+15.01090 Da) relating to aminated tyrosine at position 38 (Y38) (Fig. 3-8B). The second peptide sequence, TTYVTQRPVYLGLPANLVDLNVPAK, has a total of 25 amino acids and a mass of 2804.56 Da containing aminotyrosine (+15.01090 Da) at position 157 (Y157) (Fig. 3-8C). The third peptide sequence, GYKPVAVPAR, has a total of 10 amino acids and a mass of 1119.66 Da containing aminotyrosine (+15.01090 Da) at position 344 (Y344) (Fig. 3-8D). The position of tyrosine nitration on the 3D structure of Pdc1 was illustrated in Fig. 3-8B. The details of LC-MS/MS analysis of Pdc1 are shown in SUPPLEMENTARY INFORMATION (Table S2)

Table 3.2 Summary of the nitrated Pdc1 identified by LC-MS/MS

Peptide sequence	Nitration site	Charge(Z)	MH+	Retention Time (min)
QVNVNTVFGLPGDFNLSLLDKIY^{38}EVEGM**R**$^{\#}$	Tyr38	3	3283.69	73.38
T*TY^{157}VTQ**R**$^{\#}$PVYLGLPANLVDLNVPA**K**$^{\#}$	Tyr157	3	2804.57	56.48
G***Y**^{344}KPVAVPA**R**$^{\#}$	Tyr344	2	1119.66	16.73

Y = Aminated tyrosine (+15.011 Da), * = Acetylation (+42.01057 Da), # = SILAC labeling of K (+4.025 Da) and R (+1.003 Da), MH+ = mass values (Da)

A

```
1   MSEITLGKYL FERLKQVNVN TVFGLPGDFN LSLLDKIYEV EGMRWAGNAN
51  ELNAAYAADG YARIKGMSCI ITTFGVGELS ALNGIAGSYA EHVGVLHVVG
101 VPSISAQAKQ LLLHHTLGNG DFTVFHRMSA NISETTAMIT DIATAPAEID
151 RCIRTTYVTQ RPVYLGLPAN LVDLNVPAKL LQTPIDMSLK PNDAESEKEV
201 IDTILALVKD AKNPVILADA CCSRHDVKAE TKKLIDLTQF PAFVTPMGKG
251 SIDEQHPRYG GVYVGTLSKP EVKEAVESAD LILSVGALLS DFNTGSFSYS
301 YKTKNIVEFH SDHMKIRNAT FPGVQMKFVL QKLLTTIADA AKGYKPVAVP
351 ARTPANAAVP ASTPLKQEWM WNQLGNFLQE GDVVIAETGT SAFGINQTTF
401 PNNTYGISQV LWGSIGFTTG ATLGAAFAAE EIDPKKRVIL FIGDGSLQLT
451 VQEISTMIRW GLKPYLFVLN NDGYTIEKLI HGPKAQYNEI QGWDHLSLLP
501 TFGAKDYETH RVATTGEWDK LTQDKSFNDN SKIRMIEIML PVFDAPQNLV
551 EQAKLTAATN AKQ
```

38, 157, 344

B

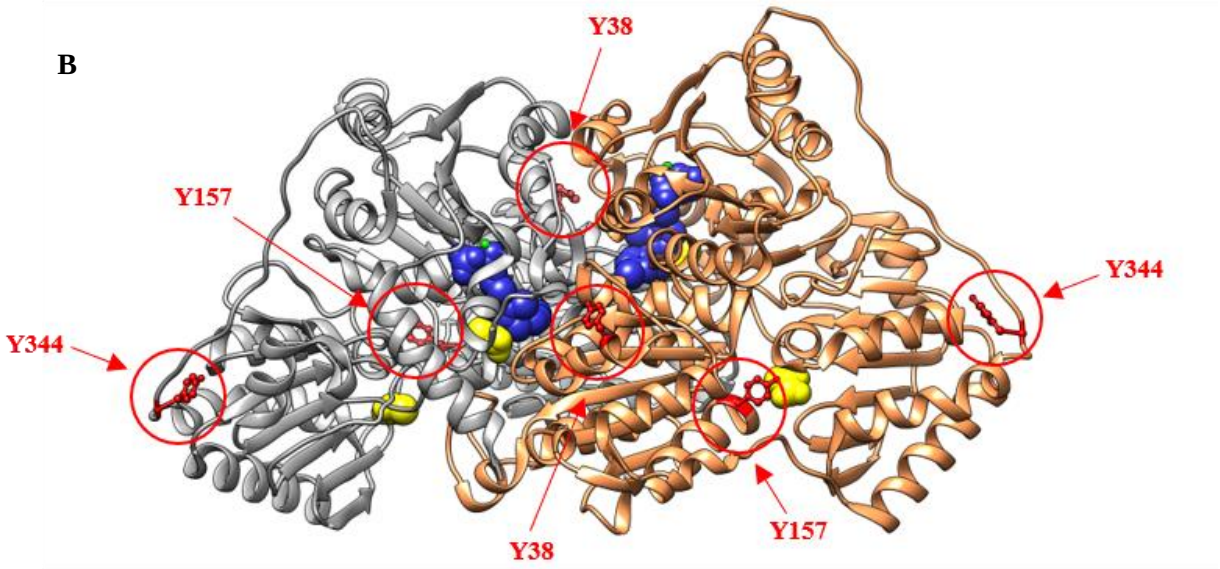

Fig. 3-7 Amino acid sequence and protein structure of Pdc1. (A) Peptide sequences identified by LC-MS/MS. Bold characters indicate tyrosine residues. Red characters show amino acid residues that were matched with Pdc1. Underline characters are peptide sequences with aminated tyrosine. The number represents the location of aminated tyrosine. (B) The structure of Pdc1 (PDB ID: 2VK1) is shown as a homodimer (Gray and orange) with tyrosine nitration positions (Red), Thiamine diphosphate (Blue), Pyruvate (Yellow), Magnesium ion (Light green).

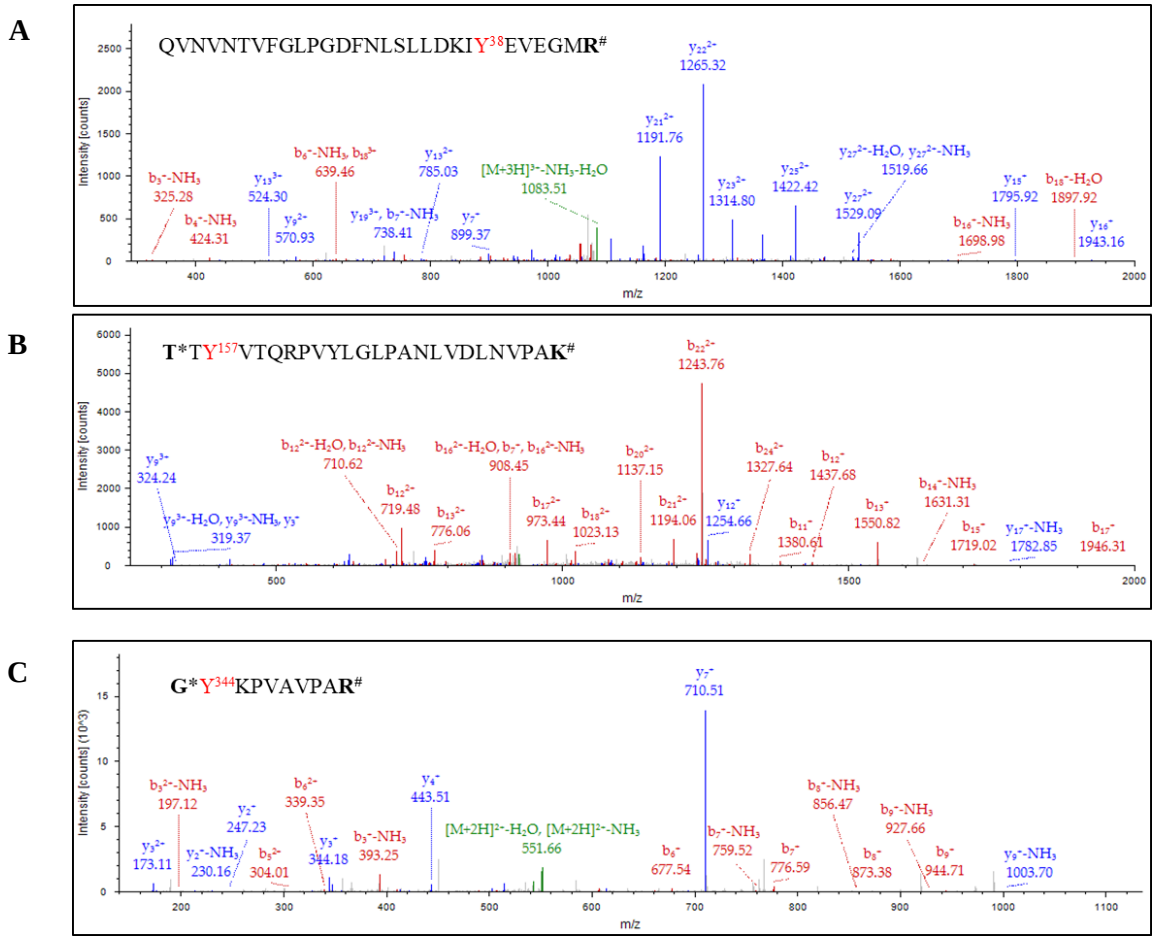

Fig. 3-8 MS/MS spectrum of aminated peptides from Pdc1. The MS/MS spectra for nitrated Y38 (A), Y157 (B), and Y344 (C), respectively.

3.2.6 Protein sequence alignment and structure of Pdc1

Proteomic analysis indicated tyrosine nitration in Pdc1 at positions 38, 157, and 344 (Y38, Y157, and Y344). An amino acid sequence of the *S. cerevisiae* Pdc1 was compared with the Pdc1 orthologues from other yeasts (*Kluyveromyces marxianus*, *Schizosaccharomyces pombe*, and *Candida albicans*) and plants (*Zea mays*, *Arabidopsis thaliana*, and *Oryza sativa*) (Fig. 3-9). It was shown that Y344 is highly conserved in both yeasts and plants. In contrast, Y38 and Y157 are conserved only in yeasts.

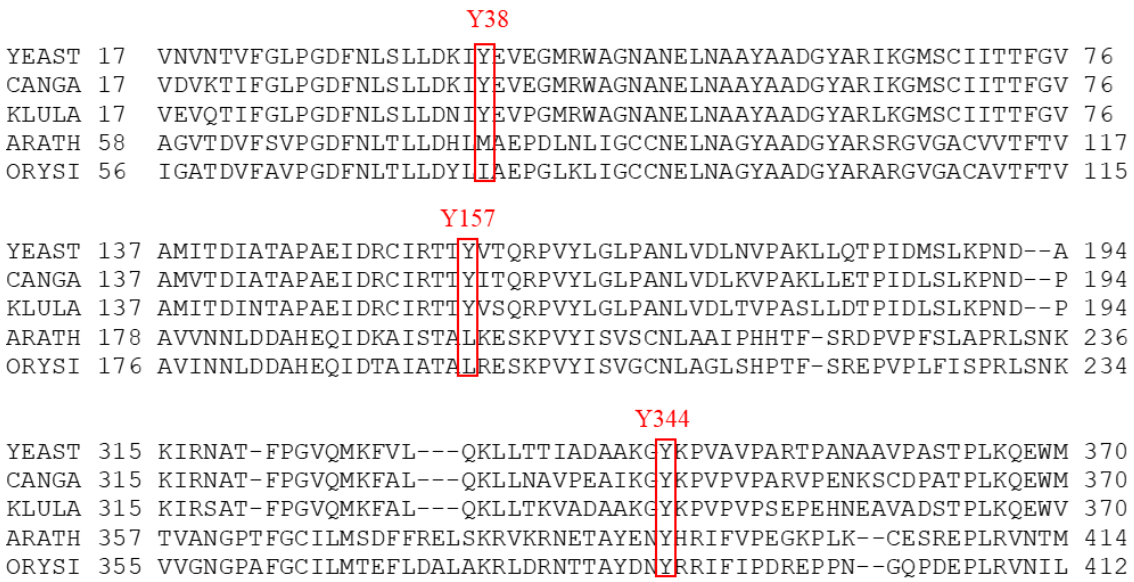

Fig. 3-9 Amino acid sequence alignment of various pyruvate decarboxylase enzymes. This alignment was performed using Uniprot (https://www.uniprot.org/align) (YEAST: *Saccharomyces cerevisiae*, CANGA: *Candida glabrata*, KLULA: *Kluyveromyces lactis*, ARATH: *Arabidopsis thaliana*, ORYSI: *Oryza sativa*).

3.2.7 Nitration at Y157 and Y344 altered Pdc1 activity

To identify the PTN position that affects Pdc1 activity, the site-specifically 3NT-incorporated Pdc1 at Y38, Y157, or Y344, which were named Y38NT-, Y157NT-, or Y344NT-Pdc1, respectively, was expressed and purified using *E. coli* cells as described in the MATERIALS AND METHODS section. SDS-PAGE followed by the immunoblotting with anti 3NT antibody and Ponceau S staining indicated that Y38NT-, Y157NT-, and Y344NT-Pdc1 were successfully purified (Fig. 3-10A). All nitrotyrosine-incorporated Pdc1 showed detectable signals from the 3NT antibody. Subsequently, I measured the enzymatic activity of the wild-type (WT) and the 3NT-incorporated Pdc1. It was found that the activity of Y157NT- or Y344NT-Pdc1 dropped about 60% or 90%, respectively. On the other hand, Y38NT-Pdc1 did not significantly alter its activity (Fig. 3-10B). These results suggest that nitration at Y157 and Y344 is important for the Pdc1 activity.

3.2.8 Substitution to phenylalanine at Y157 or Y344 recovered ethanol production

To analyze the effect of nitration *in vivo*, ethanol productivity of yeast cells expressing WT-, Y157F-, or Y344F-Pdc1 was measured under acidified nitrite conditions. The western blot analysis with anti c-Myc antibody showed that the protein level of each Pdc1 variant was almost the same (Fig. 3-11A). The measurement of ethanol content in medium indicated that RNS reduced ethanol productivity by about 40% compared to the control strain expressing WT-Pdc1. Interestingly, neither yeast cells producing Y157F-Pdc1 nor the Y344F-Pdc1 variants reduced ethanol production significantly by acidified nitrite treatment (Fig. 3-11B). This finding suggests that Y157 and Y344 are important PTN target residues for the regulation of Pdc1 activity.

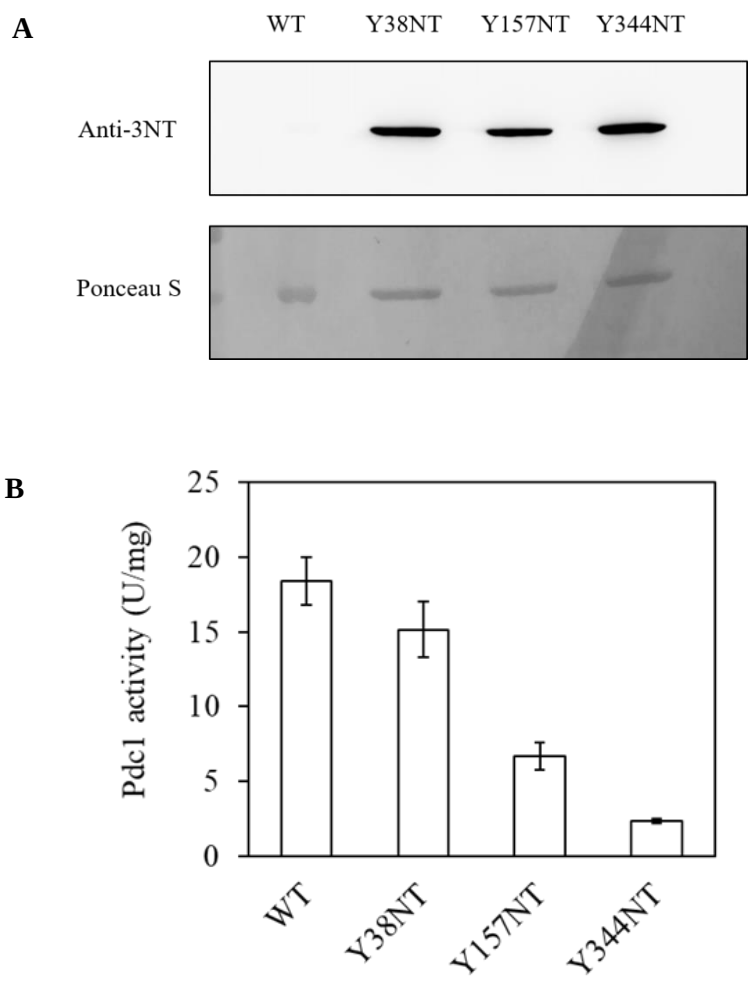

Fig. 3-10 Enzymatic activity of Pdc1with the incorporation of nitrotyrosine expressed in *E.coli*. (A) The wild-type (WT) Pdc1 and the 3-nitrotyrosine (NT)-incorporated Pdc1 at Y38, Y157, or Y344 (Y38NT, Y157NT, or Y344NT) were purified and detected by immunoblotting using a 3NT antibody. (B) Pdc1 activity of WT, Y38NT, Y157NT, or Y344NT. Data represent the averages of three independent experiments and standard deviations.

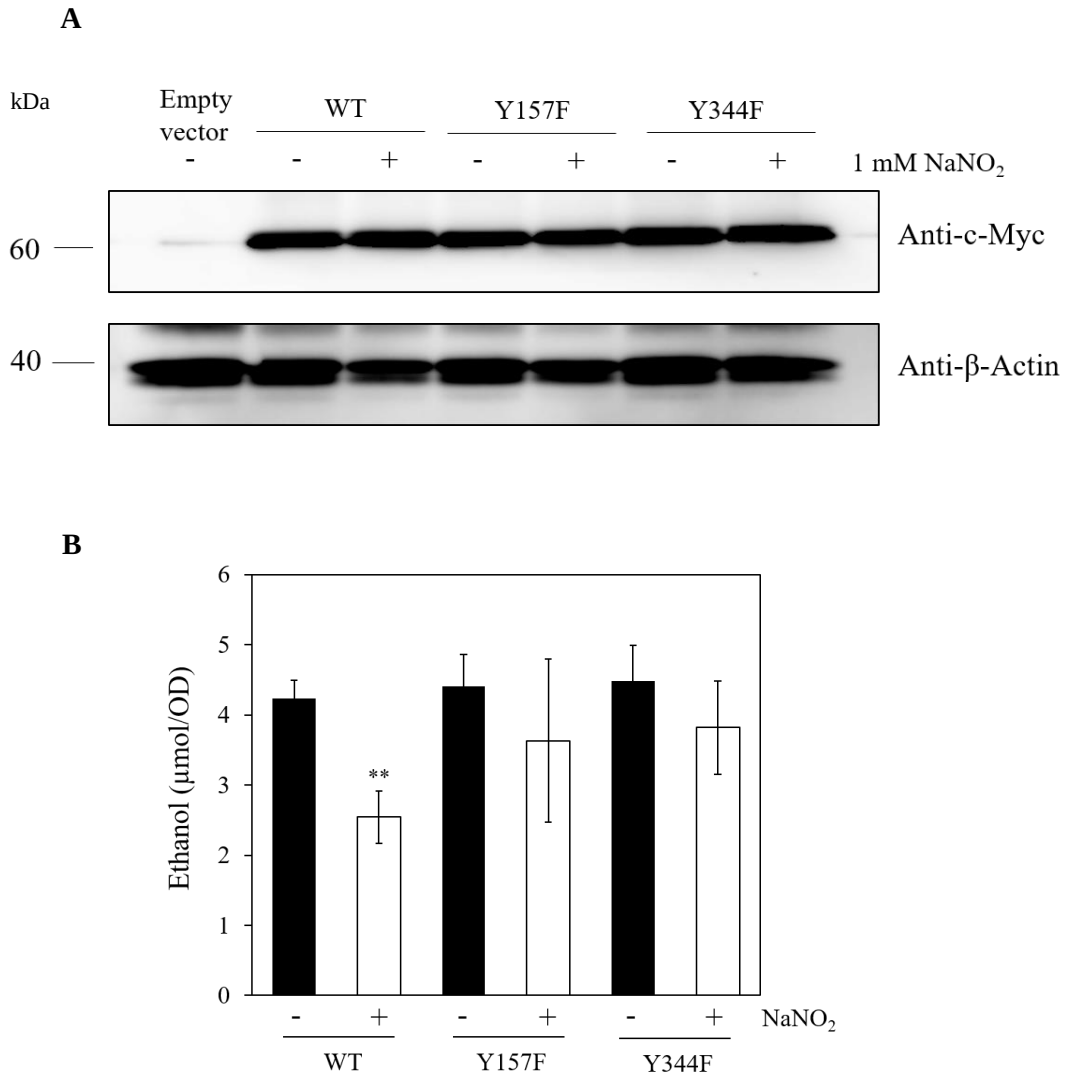

Fig. 3-11 Ethanol productivity of yeast cells expressing WT and phenylalanine variants of Pdc1. (A) Pdc1 expression in yeast strain X2180-1A *ura3*Δ *pdc1*Δ harboring pRS416-*PDC1*-1Myc7His and phenylalanine variants of Y157 (pRS416-*PDC1*^{Y157F}-1Myc7His) and Y344F (pRS416-*PDC1*^{Y344F}-1Myc7His) treated with 1 mM $NaNO_2$ for 1 h. (B) Extracellular ethanol contents of X2180-1A *ura3*Δ *pdc1*Δ cells harboring pRS416-*PDC1*-1Myc7His and phenylalanine variants treated with 1 mM $NaNO_2$ for 1 h. Data represent the averages of three independent experiments and standard deviations. Differences where $\rho < 0.01$ versus untreated of its strain (**) were significant when verified by the student's *t*-test.

3.3 Role of GABA under nitrosative stress

3.3.1 Nitrosative stress led to GABA accumulation

GABA accumulation has been reported in many organisms when cells were exposed to abiotic stress; however, there are no information available about the relationship between GABA and nitrosative stress in yeast. To further investigate GABA functions in yeast cells under nitrosative stress conditions, I measured cell viability and intracellular GABA content in *S. cerevisiae* strain treated with acidified nitrite. It was shown that nitrite treatment at pH 6.0 did not affect cell viability. On the other hand, the treatment at pH 4.0 dramatically decreased cell viability to 51% (Fig. 3-12A). Moreover, acidified nitrite treatment at pH 4.0 led to GABA accumulation up to 6.15 µmol/g of dry cell weight after 1 h-treatment; however, GABA was not detected in the medium with pH 6.0 regardless of nitrite (Fig. 3-12B). These results indicated that RNS produced from acidified nitrite decreased cell viability and resulted in GABA accumulation.

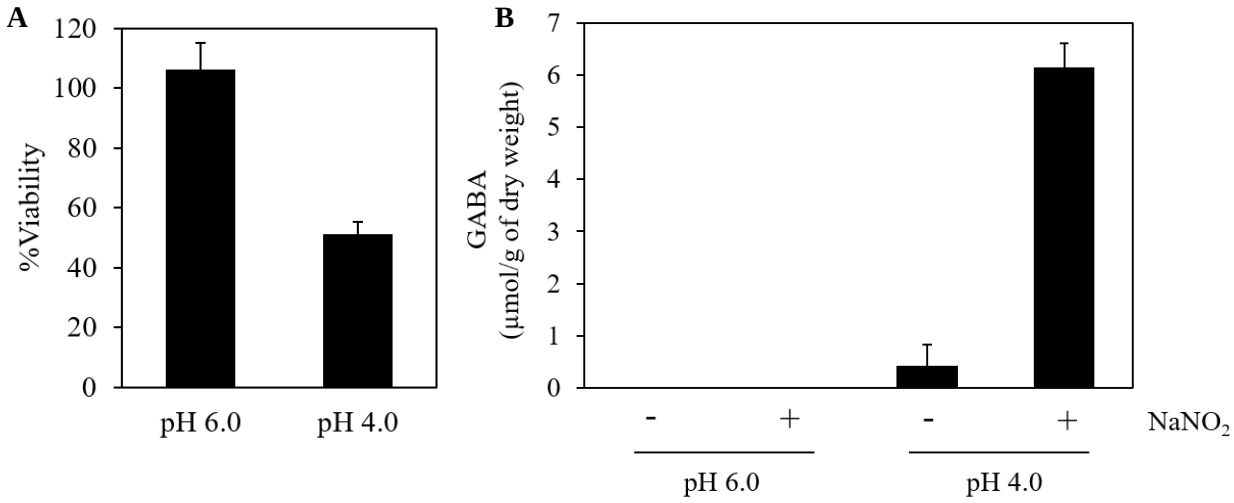

Fig. 3-12 Effects of acidified nitrite on cell viability and GABA content of strain BY4741. (A) Cell viability under nitrosative stress conditions. Yeast cells were cultured in SD medium pH 6.0 and pH 4.0 with and without 1 mM $NaNO_2$ and cultured for 1 h. Cultures were spread onto YPD agar plates and counting viable yeast colonies. (B) GABA content under nitrosative stress conditions. Yeast cells were cultured in SD medium pH 6.0 and pH 4.0 with and without 1 mM $NaNO_2$ and cultured for 1 h. Cells were extracted and intracellular GABA content was measured. Data represent the averages of three independent experiments and standard deviations.

3.3.2 GABA but not GABA shunt helps cells from nitrosative stress

The previous report (Cao et al., 2013a; Coleman et al., 2001) concluded that the GABA degradation pathway or GABA shunt is involved in the oxidative stress and heat stress tolerance mechanism. To investigate the role of the GABA shunt in nitrosative stress in yeast, cell viabilities of the *gad1*Δ (unable to synthesize GABA) and *uga1*Δ (unable to degrade GABA) strains were determined under acidified nitrite conditions for 1 h (Fig. 3-13A). Interestingly, cell viability of the *gad1*Δ strain after acidified nitrite treatment was significantly dropped to 33%, which was lower than the wild-type (WT) strain. In contrast, cell viability of the *uga1*Δ strain did not exhibit any difference from WT strain. Notably, the supplementation of 0.1 mM GABA increased the cell viability of all strains. Furthermore, cell viability of the *gad1*Δ strain was restored to the same level of WT strain when GABA was exogenously added. Based on these results, GABA may play a role in protecting yeast cells from nitrosative stress. Additionally, the analysis of intracellular GABA content demonstrated that *gad1*Δ cells did not produce GABA in both conditions, whereas the GABA content in *uga1*Δ cells was slightly lower than WT cells treated with acidified nitrite for 1 h (Fig. 3-13B). These findings suggest that GABA, but not the GABA shunt, play an important role in nitrosative stress tolerance. Furthermore, the intracellular GABA level of WT strain increased dramatically in a time-dependent manner, suggesting that the endogenous GABA is a key molecule in the nitrosative stress response/tolerance.

3.3.3 GABA did not regulate antioxidant enzyme activities

In plants, accumulation and supplementation of GABA increase activities of antioxidant-related enzymes, such as catalase, glutathione reductase, peroxidase, leading to oxidative stress tolerance (Nayyar et al., 2014; Seifikalhor et al., 2020; Tang et al., 2020). The enzymatic activities of catalase and glutathione reductase, which have been implicated in nitrosative stress, were measured to investigate the role of GABA in regulating antioxidant enzymes in yeast. Cells were cultured in nitrosative stress conditions with or without supplementation of GABA, and the enzyme activity of crude protein extract was measured. As a result, catalase activity was reduced after acidified nitrite treatment, and the GABA supplementation did not restore it (Fig. 3-14A). In contrast, nitrosative stress and GABA supplementation did not affect glutathione reductase activity (Fig. 3-14B). These findings indicated that GABA did not participate in the regulation of antioxidant-related enzyme activity during nitrosative stress.

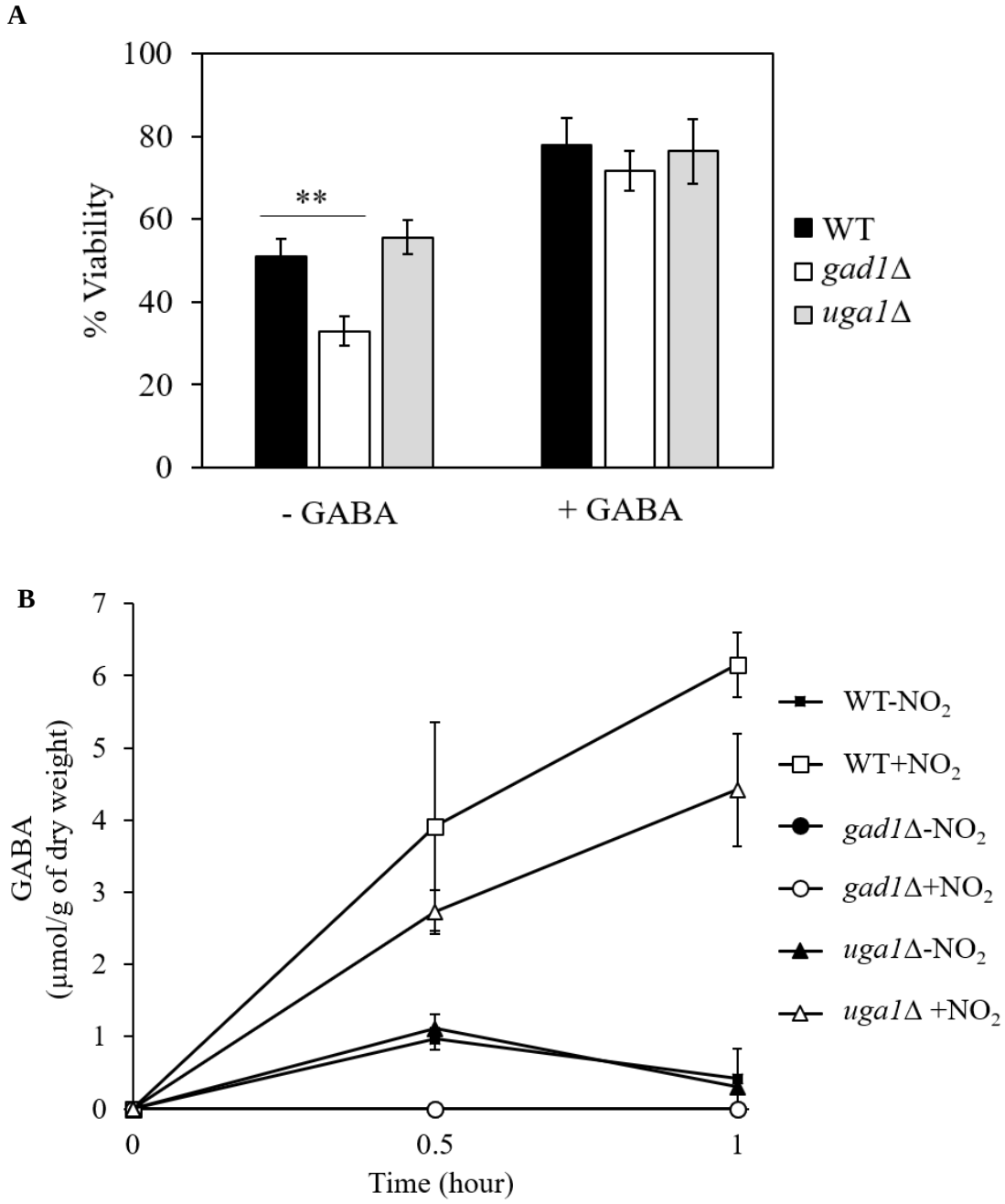

Fig. 3-13 Cell viability and GABA content of yeast strains BY4741 WT, *gad1*Δ, and *uga1*Δ. (A) Cell viability of the WT, *gad1*Δ, and *uga1*Δ strains with and without 0.1 mM GABA addition were treated with 1 mM $NaNO_2$ and cultured for 1 h. Cultures were spread onto YPD agar plates and counting viable yeast colonies. (B) GABA content of the WT, *gad1*Δ, and *uga1*Δ strains. Cells were cultured in control ($-NO_2$) and nitrite treatment ($+NO_2$) for 1 h. The intracellular GABA content of the WT, *gad1*Δ, and *uga1*Δ strains under control and treatment conditions was verified by an amino acid analyzer. Data represent the averages of three independent experiments and standard deviations. Differences where $\rho < 0.01$ versus WT (**) were significant when verified by the student's *t*-test.

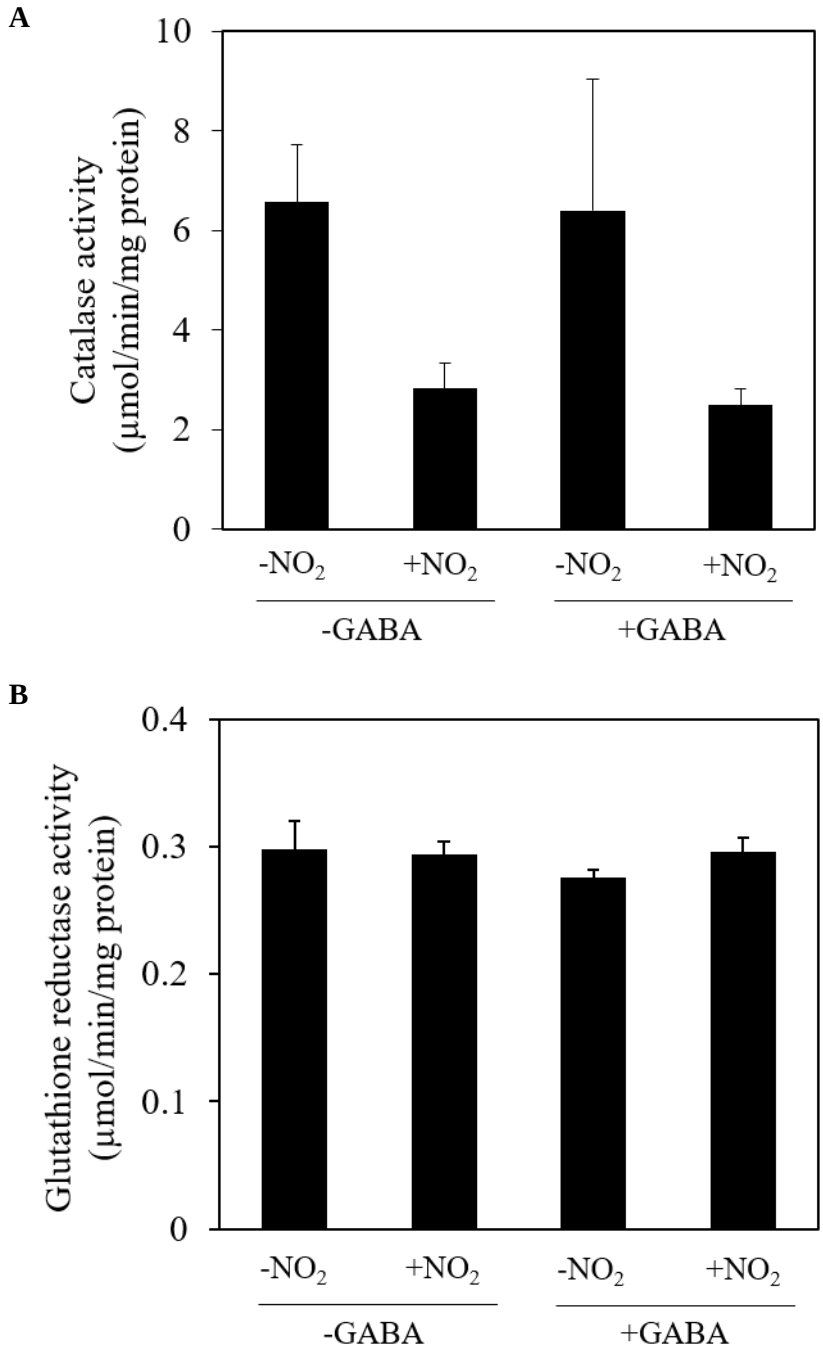

Fig. 3-14 Catalase and glutathione reductase activities under nitrosative stress conditions. Yeast cells were cultured in control (-NO_2) and nitrite treatment (+NO_2) with and without 0.1 mM GABA. (A) Catalase and (B) glutathione reductase activities were measured using crude extract 20 μg and 100 μg, respectively. Data represent the averages of three independent experiments and standard deviations.

4. DISCUSSION

This study demonstrated that nitrosative stress inhibits yeast cell growth and increases PTN levels in a time-dependent manner. My proteomic analysis also identified many metabolic enzymes involved in carbon metabolism as proteins with PTN modifications. Furthermore, it was indicated that nitrosative stress reduces ethanol production by decreasing the Pdc1 activity *via* PTN at Y157 and/or Y344. On the other hand, accumulation of GABA in response to nitrosative stress is likely to be important for nitrosative stress tolerance, although its detailed mechanisms are still unknown. I will discuss these findings in this section.

4.1 RNS generated by acidified nitrite induce PTN in yeast

The acidification of nitrite produces a complex mixture of RNS, which mimics RNS production in the gastrointestinal tract. Acidic pH alone (from pH 4-6) did not affect yeast cell growth (Fig. 3-1A), but acidified nitrite led to growth inhibition (Fig. 3-1B), coinciding with the formation of NO/RNS. This finding is consistent with previous research that acidic pH is insufficient to eliminate gut pathogens and that acidified nitrite may provide protection against gut pathogens in humans (Dykhuizen et al., 1996). Furthermore, RNS can inhibit mitochondrial respiration and affect ATP content in cells (Brown, 1999), potentially inhibiting yeast cell growth. RNS produced by acidified nitrite resulted in PTN *in vivo* (Fig. 3-1C).

Given the abundance of carbon metabolic enzymes in cells (Table 3-1), it stands to reason that they would be easily detected as modified proteins by proteomic analysis of whole-cell lysate extracted. Previous literatures also showed that carbon metabolic enzymes are the target of post-translational modifications, such as tyrosine nitration, *S*-nitrosylation, oxidation, and carbonylation in various organisms (Bolaños et al., 2008; Cabiscol & Ros, 2006; Tripodi et al., 2015). To overcome the limitation of PTN identification, a specific immunoprecipitation assay using anti-3NT antibody would be a better strategy to identify more PTN by enrichment of proteins containing PTN before being subjected to LC-MS/MS analysis. The list of nitrated proteins shown in Table 3-1 indicated that exogenous RNS highly affect various enzymes involving glycolytic and ethanol synthetic pathways that are important for yeast cells to generate energy and metabolites.

4.2 Pdc1 inactivation triggered by PTN inhibits ethanol production

When *S. cerevisiae* cells grow exponentially in the presence of high concentrations of fermentable carbon source with air, glucose degradation is primarily accomplished through aerobic fermentation of ethanol rather than respiration in mitochondria called the Crabtree effect (Vemuri et al., 2007). Ethanol biosynthesis is an essential process for yeast cells because NAD^+ regeneration is crucial for many cellular mechanisms (Förster et al., 2003). Previous research about nitrite in molasses suggests that nitrite affects ethanol production, which may be due to the acidified nitrite effect under the lower pH conditions following longer culture. Molasses has been used as an inexpensive sugar source in industrial fermentation. However, it contains various inorganic and organic substrates, including nitrite, which may interfere with ethanol production (Jones & Gadd, 1990). Therefore, the acidified nitrite treatment as a condition to generate RNS in this study can mimic yeast cultivation using molasses containing nitrite as a physiological condition.

Based on the results of the proteomic analysis, I am primarily interested in both glycolytic and ethanol synthetic pathways by checking metabolites involved in ethanol production and pyruvate related-metabolite. This study found that when nitrite was present in acid, ethanol production was decreased while pyruvate was accumulated (Fig. 3-2B, C). The accumulation of pyruvate may imply that glucose degradation *via* the glycolytic pathway can still function at this time point, even though enzymes in this pathway are nitrated (Table 3-1). It would imply that PTN does not significantly impact protein function because PTN can cause protein function to be lost, be improved, or have no effect (Radi, 2013). There are two possible explanations for pyruvate accumulation. First, nitrosative stress can inhibit the mitochondrial respiratory chain, leading to ATP depletion. A higher AMP:ATP ratio can stimulate glycolysis *via* 5' AMP-activated protein kinase to produce ATP, resulting in pyruvate accumulation (Bolaños et al., 2008). Second, pyruvate accumulation could be caused by a problem with pyruvate degradation pathways. Pyruvate can be degraded by alanine biosynthesis, the TCA cycle in mitochondria, and ethanol biosynthesis. Alanine, which is a pyruvate-related metabolite and an essential protein component synthesized by alanine transaminase, did not change in its concentration (Fig. 3-3D). I did not measure this metabolite in the TCA cycle in this study; however, it has been reported that the activities of some TCA cycle enzymes, including α-ketoglutarate dehydrogenase and pyruvate dehydrogenase, are inhibited by nitric oxide in *Salmonella enterica* (Richardson et al., 2011). Moreover, the yeast aconitase and NAD^+-dependent isocitrate dehydrogenase were found to be nitrated *in vivo*; the nitration

consequence has yet to be elucidated (Bhattacharjee et al., 2009). These findings suggest that the TCA cycle enzymes are the targets of RNS-mediated post-translational modification, which is likely to be one of the causes of pyruvate accumulation.

The pyruvate degradation pathway may encounter difficulties, resulting in pyruvate accumulation. Pyruvate decarboxylase activity was shown to decrease without changing expression levels (Fig. 3-3A, 3-4). I assume that the decrease in ethanol production may result from decreased PDCs activity because ADH activity did not change during nitrite treatment (Fig. 3-3B). However, the amounts of pyruvate and ethanol cannot be directly compared in this experiment because pyruvate is measured from intracellular content, whereas ethanol is measured from extracellular content. PDC activity decreases during nitrosative stress, most likely due to Pdc1. Only Pdc1 protein was detected in this study, while Pdc5 and Pdc6 were not detected (Fig. 3-4), indicating that Pdc1 is likely to be the main isozyme during nitroative stress which was coincided with the previous report that *PDC1* gene is highly expressed in most conditions (Hohmann & Cederberg, 1990) and is induced by the presence of glucose (van den Berg et al., 1998). On the other hand, using 1Myc7His tagging with c-Myc antibody may cause sensitivity issues. To address this issue, protein tagging with a 9Myc tag or another tag may be used to increase sensitivity. Aside from transcriptional control of *PDC1*, post-translational modification of the protein is proposed to be another way to modulate its function. Dephosphorylation of Pdc1 in *S. cerevisiae* cells, mediated by serine/threonine-protein phosphatase, increases ethanol fermentation and Pdc1 activity by altering the apparent affinity for TPP and pyruvate (de Assis et al., 2013). Here, I hypothesized that Pdc1 is a new candidate for NO-dependent post-translational regulation via PTN and investigated this hypothesis using both *in vitro* and *in vivo* approaches.

Pdc1 is critical for directing the glucose flux to ethanol production illustrated to be nitrated by acidified nitrite (Fig. 3-5) and inactivated by nitrating agent $ONOO^-$ (Fig. 3-6B). Peroxynitrite ($ONOO^-$) is probably the primary nitrating agent *in vivo* (Abello et al., 2009). On the other hand, $ONOO^-$ is a fast-acting reactive oxidant that can promote modification of amino acids besides PTN, such as oxidation and *S*-nitrosylation. Therefore, incorporation of 3NT at a specific position is suitable for identification of nitration sites that affect enzyme activity. Proteomic analysis from yeast whole-cell lysate revealed that Pdc1 was aminated at Y38, Y157, and Y344 with the score of protein sequence coverage 76.02% (Table 3-2). PTN is hypothesized to be a selective mechanism that is nitrated preferentially depending on structure and environment. (Radi, 2013). In the LC-MS/MS analysis (Fig. 3-8), three positions of

tyrosine amination were detected instead of tyrosine nitration. The lack of PTN in Pdc1 can be explained by treatments performed during sample preparation prior to mass spectrometry analysis or during protein ionization leading to reduced form of nitration. (Söderling et al., 2007). To elucidate the functional roles of Y38, Y157, and Y344, I performed an *in vitro* assay with the incorporation of 3NT to these tyrosine residues. Site-specific 3NT incorporation on the Pdc1 experiment revealed that nitration at positions Y157 and Y344 affects Pdc1 activity (Fig. 3-10C). To our knowledge, this is the first study to identify the tyrosine nitration site in Pdc1 and to analyze their functions in *S. cerevisiae*.

Nitration of Pdc1 at Y157 and Y344 was responsible for a decrease in enzyme activity, as inferred by the finding of NT incorporation in the recombinant Pdc1. Since it has been reported that incorporation of a nitro group into a tyrosine residue can result in profound structural and functional changes (Radi, 2013), tyrosine nitration in Pdc1 is likely to contribute to alteration of the Pdc1 structure and activity. Both Y157 and Y344 are directly involved in neither the substrate-binding nor regulatory sites. It is difficult to understand how nitration at these positions affects enzyme activity. The structure of the *S. cerevisiae* Pdc1 (Fig. 4-1) implies that nitration sites determined in this study may affect to the thiamine diphosphate (TPP) binding site and the regulatory site. Nitration at Y157 is likely to disrupt the residue Lys65 and Gly66 in the loop structure of Asn50-Gly66 that contains the TPP binding site at Glu51 (Fig. 4-1A). Glu51 interacts with the N1‘-atom of the cofactor TPP, which strongly influences the catalytic activity, and the E51Q and E51A variants resulted in a loss of catalytic activity. (Margrit Killee nberg-Jabs et al., 1997). Therefore, nitration at Y157 may indirectly interfere with Glu51, resulting in a decrease in activity. Nitration at Y344 could trigger a conformational change in the regulatory site and decreases Pdc1 activity. According to the previous report (Kutter et al., 2009), PDCs are regulated by binding an effector molecule (pyruvate) at the regulatory site, inducing the conformational changes of the active site. The nitration at Y344 may result in unfavorable interactions with Ala211, Lys212, Asn213, and Pro214, interfering with the folding of loop structure that contained Cys221 and His 225, the core of the regulatory site (Fig. 4-1B). Site-directed mutagenesis revealed that C221A and H225F, which are involved in the substrate binding sites, showed a weaker binding affinity for the substrate at the regulatory site and decreased its enzyme activity (Spinka et al., 2017). Furthermore, PTN at both 157 and 344 positions at the same time may amplify the effect of PTN alteration to both the TPP binding site and the regulatory site. This extraordinary phenomenon may result in lower enzymatic activity than PTN at only one position. Moreover,

replacement of tyrosine with phenylalanine, which cannot be nitrated, showed an increase in ethanol production in *S. cerevisiae* cells treated with acidified nitrite (Fig. 3-11B). These results confirmed the positions of nitration *in vivo*, which is resistant to nitration-dependent inhibition. The limitation of this study is the quantification of nitrated Pdc1 *in vivo*. First, I intended to obtain this result using the SILAC method by relatively comparing PTN and non-PTN peptides of Pdc1; however, it failed to quantify nitrated protein. To address this issue, the SILAC method combined with immunoprecipitation/pull-down assays of the Pdc1 in both control and nitrosative stress conditions may be used. Previously, I used the SILAC method to extract whole cells, which may have caused sensitivity issues and resulted in the inability to quantify PTN of Pdc1. The other method is to quantify PTN protein by ELISA. An in vitro nitrated Pdc1 is used to create the standard curve. Pdc1 nitration values are presented as arbitrary units in relation to the relative amount quantified by densitometry.

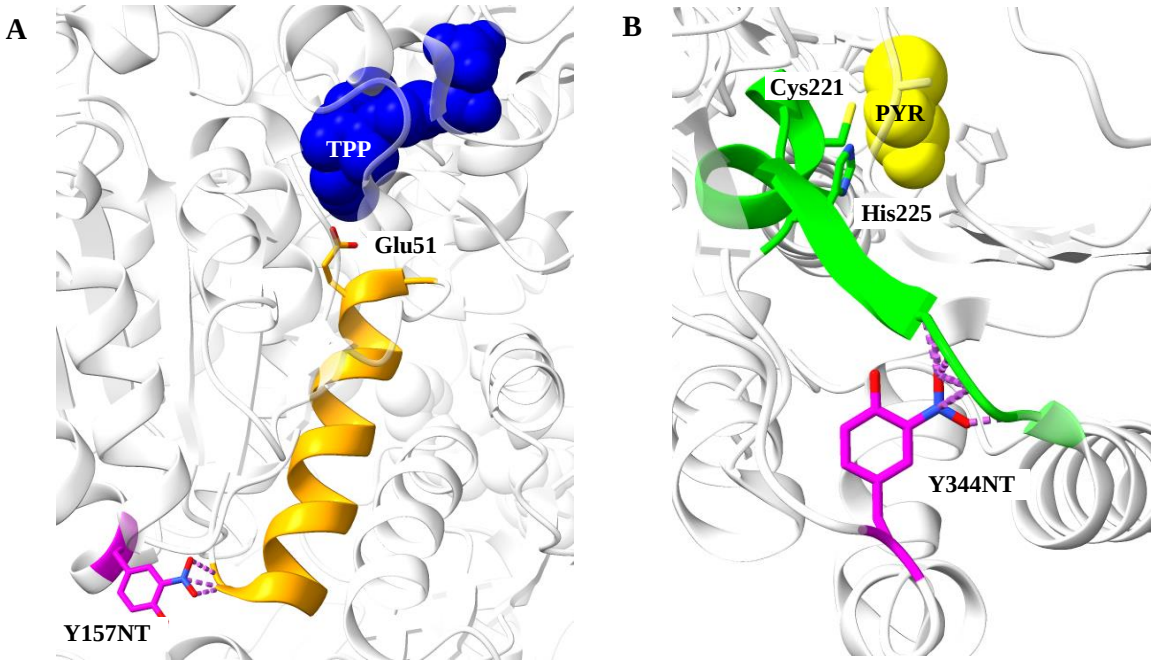

Fig. 4-1 Structure illustration of Pdc1 nitration. Part of the structure model of the *S. cerevisiae* Pdc1 (PDB ID: 2VK1) showing (A) the TPP binding site with nitration at Tyr157 (Y157NT) and (B) the regulatory site with nitration at Tyr344 (Y344NT). Tyrosine nitration residues are shown in purple, thiamine pyrophosphate (TPP) and pyruvate (PYR) are shown in blue and yellow, respectively. Glu51 is the residue binding to TPP. Cys221 and His 225 are the residues binding to PYR. Purple dashed lines exhibit the clash contact of tyrosine nitration and protein structure (orange and green).

In contrast to my findings, a previous study reported that yeast cells exposed to nitrosative stress were capable of producing more ethanol in a rich medium by increasing alcohol dehydrogenase activity under stress conditions by using 0.5 mM $NaNO_2$ for acidified nitrite (Sengupta et al., 2020). It is possible that lower concentrations of acidified nitrite produce lower RNS, which may be insufficient to cause Pdc1 nitration. On the other hand, low concentrations of RNS may inhibit the mitochondrial electron transport chain and activate glycolysis to produce ATP (Brown, 1999). This may result in an increase in ethanol production. Compared to this study, the use of rich medium versus minimal medium in the experiment may cause different metabolic processes inside cells, leading to different mechanisms to produce ethanol during nitrosative stress.

Nitration-induced post-translational modification of Pdc1 may serve as a regulatory mechanism to control ethanol production in response to nitrosative stress. The decrease in ethanol production may impair NAD^+ regeneration, leading to an increase in NADH. I hypothesize that NADH could be channeled into other metabolic processes, such as the NO detoxification system. NO dioxygenase (NOD), encoded by the *YHB1* gene, is the main enzyme in the detoxification of NO to nitrate (Liu et al., 2000) (Fig. 4-2). A previous work found that nitrite ions are completely converted into nitrate ions during the fermentation latency in molasses containing nitrite (Glacet et al., 1985). This phenomenon may imply that the conversion of nitrite into nitrate results from acidified nitrite chemically converting nitrite into NO and then nitrate via NOD.

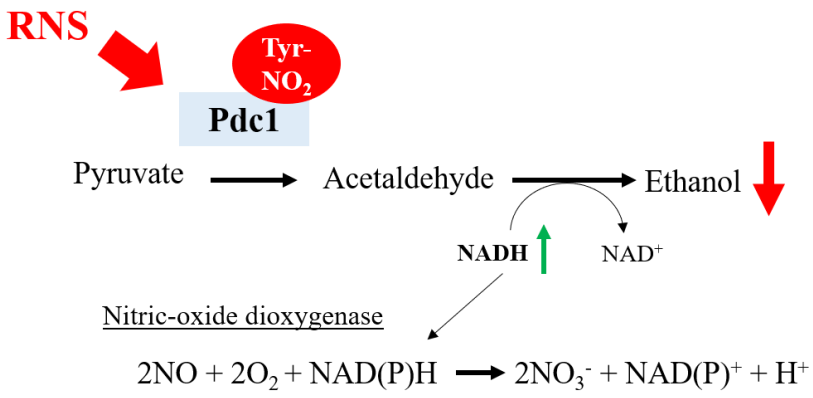

Fig. 4-2 A proposed model to the biological event of reducing ethanol production via Pdc1 nitration. Under nitrosative stress conditions, Pdc1 is modified by RNS and decrease in its activity via PTN. Consequently, ethanol production is dropped, and the NADH redox system

via fermentation may be dropped. Then, NADH could be used via NO dioxygenase (NOD) to detoxify NO, which is converted into its unharmful form (nitrate).

4.3 GABA and nitrosative stress tolerance

The GABA shunt, a closed-loop process of producing and conserving GABA supply, has been shown to protect yeast cells against oxidative stress and heat stress (Cao et al., 2013a; Coleman et al., 2001). Until now, it is unclear about the GABA shunt and the role of GABA in yeast under nitrosative stress conditions. In this study, *S. cerevisiae* cells were shown to respond to nitrosative stress by accumulating GABA (Fig. 3-12B). The accumulation of GABA has been extensively studied in plants as a model organism that is constantly exposed to environmental stresses, and most of the time, this accumulation is associated with a stress response in plant cells (Al-Quraan & Al-Omari, 2017; Mekonnen et al., 2016; Seifikalhor et al., 2020). On the other hand, the earlier yeast study indicated that GABA accumulation is unlikely to positively affect stress tolerance during heat stress (Cao et al., 2013a). Therefore, it is an interesting finding that GABA accumulation positively helps yeast cells from nitrosative stress by measuring cell viability and a cell's ability to proliferate (Carmona-Gutierrez et al., 2018). In my study, the *gad1*Δ mutant, which cannot produce GABA (Fig. 3-13B), exhibited lower viability than the WT and *uga1*Δ strains when cells are facing nitrosative stress (Fig 3-13A). A previous research indicated that both *gad1*Δ and *uga1*Δ mutants showed reduced tolerance to heat stress; in contrast with my study, *uga1*Δ cells could be tolerant to nitrosative stress at the same level as WT cells. In this study, *uga1*Δ cells had a slightly lower GABA content than WT cells by unknown reasons; however, GABA accumulation in the *uga1*Δ mutant is sufficient to protect cells from nitrosative stress. These findings strongly suggest that GABA itself, rather than the GABA shunt, plays an important role in nitrosative stress response. A previous study on the GABA shunt in yeast suggests that NADPH production via the SSADH enzyme, which catalyzes the last step of the GABA shunt encoded by the *UGA2* gene, is most likely the critical component in reducing ROS generation during heat stress, resulting in heat-stress tolerance of yeast cells. NADPH is required for regeneration of reduced glutathione and thioredoxin by GR and thioredoxin reductase, respectively, leading to maintenance of the normal redox balance. (Jamieson, 1998). However, it does not appear that nitrosative stress associates to NADPH production via the GABA shunt because the *uga1* mutant did not affect cell viability. Based on these results, I propose that GABA itself could act as a protective and/or signaling molecule against nitrosative stress in *S. cerevisiae*.

In plants, GABA supplementation can support cells from many kinds of stresses. The addition of GABA is associated with significantly increased antioxidant enzyme activities, such as superoxide dismutase, catalase, and glutathione reductase (Tang et al., 2020). In order to investigate the role of GABA on nitrosative stress in yeast. I measured enzymatic activities of catalase and GR, which has been reported as an RNS antioxidative enzyme (Jamieson, 1998; Sahoo et al., 2009). As a result, GABA did not affect enzyme activities related to nitrosative stress response (Fig. 3-14A, B), suggesting that GABA would help yeast cells through an unknown mechanism different from that regulating enzyme activity. Interestingly, catalase activity was decreased after acidified nitrite treatment which would be a result from NO-related post-translational modification (Purwar et al., 2011). At the same time, nitrosative stress did not affect GR activity. A recent plant research shows that RNS does not affect GR, implying that GR is required for the antioxidant system to function (Begara-Morales et al., 2015).

According to plant research, environmental stress induces GABA accumulation via two distinct mechanisms, (1) decreases cytosolic pH leading to pH-dependent activation of GAD expression, leading to GABA synthesis, and (2) increases cytosolic Ca^{2+}, which stimulates Ca^{2+}/calmodulin-dependent Gad activity, leading to GABA synthesis (Fig. 4-3) (Mei et al., 2016). A recent work in *Arabidopsis thaliana* suggests that hypoxia-induced GABA accumulation restores membrane potential, prevents ROS-induced disruption to ion homeostasis, and functions as a ligand directly controlling ion channels (Wu et al., 2021). The phenomenon by which GABA is essential for hypoxia stress may be adapted to nitrosative stress because both situations result in ATP depletion and membrane depolarization (Ghasemi et al., 2018). On the other hand, the phenomenon of elevated GABA content in yeast cells during nitrosative stress and its physiological role in stress tolerance are important points to further investigate and comprehend in-depth. A comprehensive analysis of gene expression levels associated with nitrosative stress and GABA supplementation is required to clarify how GABA protects yeast cells from nitrosative stress in the future.

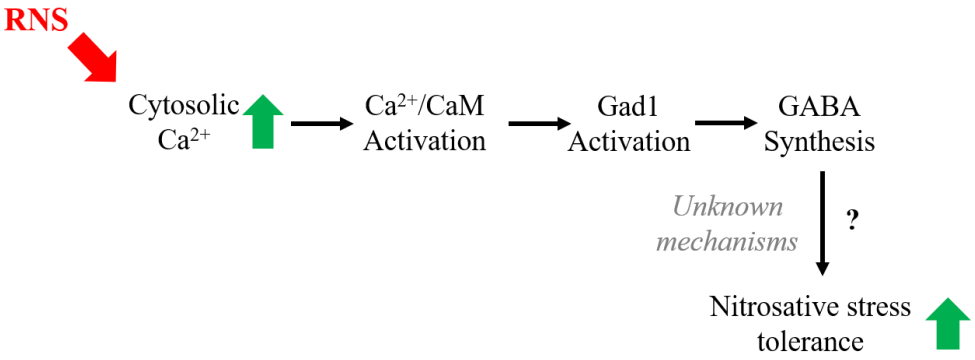

Fig. 4-3 A Proposed model for GABA accumulation and its role in nitrosative stress tolerance. When yeast cells are exposed to RNS, RNS causes membrane depolarization and increases in Ca^{2+} level, activating GABA synthesis. GABA involves in nitrosative stress tolerance through unknown mechanisms.

5. CONCLUSIONS

According to the findings of this research, acidified nitrite inhibits cell growth of the yeast *S. cerevisiae* while increasing PTN levels. Proteomic analysis revealed that many enzymes involved in carbon metabolism are targets for PTN modification. Based on these results, the investigation into PTN and ethanol production was carried out. The current study indicates that when cells were exposed to nitrosative stress, ethanol production by *S. cerevisiae* decreased, associating with a decrease in Pdc1 activity via PTN at Y157 and/or Y344. Reduced ethanol production is hypothesized to be a stress response designed to supply NADH to the NO detoxification system. Taken together, these findings provide new insights into the molecular mechanism underlying the negative regulation of Pdc1 via RNS-mediated PTN during nitrosative stress.

This study also found a novel role for GABA in *S. cerevisiae*. against nitrosative stress. GABA accumulation is likely to play a role in nitrosative stress tolerance, most probably through mechanisms other than the previously reported GABA shunt. To my knowledge, this is the first study to show that GABA protects *S. cerevisiae* cells from nitrosative stress. This information opens the door to new insights into the functional aspects of GABA. However, the precise mechanisms are still unknown. More research is needed to understand the role of GABA-mediated regulation in stress tolerance in precise mechanisms at the molecular and genetic levels. Future research may extend this work by conducting a comprehensive analysis of gene expression levels associated with nitrosative stress and GABA supplementation in order to elucidate these protective mechanisms.

ACKNOWLEDGEMENTS

Firstly, I would like to express my sincere appreciation to Prof. Hiroshi Takagi. As a Principal Investigator of the laboratory of Applied Stress Microbiology and supervisor in my Ph.D. study, Takagi-sensei is always willing to instruct and support me. I am grateful for his hard work, insightful advice, and concern for my studies and daily life. In addition, this doctoral thesis would not have been completed without assistance from Assist. Prof. Ryo Nasuno for kindly supporting my experiments and thesis writing.

I would like to give a special thanks to my advisors Prof. Tomoya Tsukazaki, Prof. Kazuhiro Shiozaki and Assoc. Prof. Yukio Kimata for providing me a great advice and valuable comments in my thesis. I would also thank all former and present members of Applied stress microbiology who kindly helped me in both experiments and daily life. I would like to thank the Konosuke Matsushita Memorial Foundation Scholarship and the Japanese Government Scholarship (Monbukagakusho) for financial assistance in making my life and studies in Japan go smoothly.

My doctoral study could not be finished without the help and support from my friends, Umaporn Towijit, Jirasin Koonthongkaew, Natthaporn Takpho, Fauzee Yasmin, Mai Chi Thanh, Nguyen Thi Mai Phuong, and Huong Thi Phuong. I am grateful for their physical and mental assistance throughout my studies here. They always cheer me up when I am having a poor day and celebrate with me when I am having a good day.

Finally, I would like to express my highest gratitude to my family for their understanding, unconditional love, and support in whatever situation I encountered.

Supapid Eknikom

REFERENCES

Abello, N., Kerstjens, H. A. M., Postma, D. S., & Bischoff, R. (2009). Protein tyrosine nitration: selectivity, physicochemical and biological consequences, denitration, and proteomics methods for the identification of tyrosine-nitrated proteins. *Journal of Proteome Research*, *8*(7), 3222–3238. https://doi.org/10.1021/pr900039c

Aebi, H. (1984). Catalase *in vitro*. *Methods in Enzymology*, *105*, 121–126. https://doi.org/10.1016/s0076-6879(84)05016-3

Al-Quraan, N. A., & Al-Omari, H. A. (2017). Gaba accumulation and oxidative damage responses to salt, osmotic and H_2O_2 treatments in two lentil (*Lens culinaris* medik) accessions. *Plant Biosystems*, *151*(1), 148–157. https://doi.org/10.1080/11263504.2015.1115440

Almeida, B., Buttner, S., Ohlmeier, S., Silva, A., Mesquita, A., Sampaio-Marques, B., Osório, N. S., Kollau, A., Mayer, B., Leão, C., Laranjinha, J., Rodrigues, F., Madeo, F., & Ludovico, P. (2007). NO-mediated apoptosis in yeast. *Journal of Cell Science*, *120*(Pt 18), 3279–3288. https://doi.org/10.1242/jcs.010926

Alvarez, B., Ferrer-Sueta, G., Freeman, B. A., & Radi, R. (1999). Kinetics of peroxynitrite reaction with amino acids and human serum albumin. *The Journal of Biological Chemistry*, *274*(2), 842–848. https://doi.org/10.1074/jbc.274.2.842

Anam, K., Nasuno, R., & Takagi, H. (2020). A novel mechanism for nitrosative stress tolerance dependent on GTP cyclohydrolase II activity involved in riboflavin synthesis of yeast. *Scientific Reports*, *10*(1), 1–10. https://doi.org/10.1038/s41598-020-62890-3

André, B., Hein, C., Grenson, M., & Jauniaux, J.-C. (1993). Cloning and expression of the *UGA4* gene coding for the inducible GABA-specific transport protein of *Saccharomyces cerevisiae*. *Molecular and General Genetics MGG*, *237*(1), 17–25. https://doi.org/10.1007/BF00282779

Anyim, M., Benjamin, N., & Wilks, M. (2005). Acidified nitrite as a potential antifungal agent. *International Journal of Antimicrobial Agents*, *26*(1), 85–87. https://doi.org/10.1016/j.ijantimicag.2005.03.011

Astuti, R. I., Watanabe, D., & Takagi, H. (2016). Nitric oxide signaling and its role in oxidative

stress response in *Schizosaccharomyces pombe*. *Nitric Oxide*, *52*, 29–40. https://doi.org/10.1016/j.niox.2015.11.001

Bach, B., Meudec, E., Lepoutre, J. P., Rossignol, T., Blondin, B., Dequin, S., & Camarasa, C. (2009). New insights into γ-aminobutyric acid catabolism: Evidence for γ-hydroxybutyric acid and polyhydroxybutyrate synthesis in *Saccharomyces cerevisiae*. *Applied and Environmental Microbiology*, *75*(13), 4231–4239. https://doi.org/10.1128/AEM.00051-09

Bakker, B. M., Overkamp, K. M., AJ, van M., Kötter, P., Luttik, M. A., JP, van D., & Pronk, J. T. (2001). Stoichiometry and compartmentation of NADH metabolism in *Saccharomyces cerevisiae*. *FEMS Microbiology Reviews*, *25*(1), 15–37. https://doi.org/10.1111/j.1574-6976.2001.tb00570.x

Barnett, S. D., & Buxton, I. L. O. (2017). The role of *S*-nitrosoglutathione reductase (GSNOR) in human disease and therapy. *Critical Reviews in Biochemistry and Molecular Biology*, *52*(3), 340–354. https://doi.org/10.1080/10409238.2017.1304353

Bartesaghi, S., Ferrer-Sueta, G., Peluffo, G., Valez, V., Zhang, H., Kalyanaraman, B., & Radi, R. (2007). Protein tyrosine nitration in hydrophilic and hydrophobic environments. *Amino Acids*, *32*(4), 501–515. https://doi.org/10.1007/s00726-006-0425-8

Baum, G., Chen, Y., Arazi, T., Takatsuji, H., & Fromm, H. (1993). A plant glutamate decarboxylase containing a calmodulin binding domain. Cloning, sequence, and functional analysis. *Journal of Biological Chemistry*, *268*(26), 19610–19617. https://doi.org/10.1016/S0021-9258(19)36560-3

Beal, M. F. (2002). Oxidatively modified proteins in aging and disease. *Free Radical Biology & Medicine*, *32*(9), 797–803. https://doi.org/10.1016/s0891-5849(02)00780-3

Begara-Morales, J. C., Sánchez-Calvo, B., Chaki, M., Mata-Pérez, C., Valderrama, R., Padilla, M. N., López-Jaramillo, J., Luque, F., Corpas, F. J., & Barroso, J. B. (2015). Differential molecular response of monodehydroascorbate reductase and glutathione reductase by nitration and *S*-nitrosylation. *Journal of Experimental Botany*, *66*(19), 5983–5996. https://doi.org/10.1093/jxb/erv306

Bhattacharjee, A., Majumdar, U., Maity, D., Sarkar, T. S., Goswami, A. M., Sahoo, R., & Ghosh, S. (2009). *In vivo* protein tyrosine nitration in *S. cerevisiae*: identification of

tyrosine-nitrated proteins in mitochondria. *Biochemical and Biophysical Research Communications*, *388*(3), 612–617. https://doi.org/10.1016/j.bbrc.2009.08.077

Boer, V. M., De Winde, J. H., Pronk, J. T., & Piper, M. D. W. (2003). The genome-wide transcriptional responses of *Saccharomyces cerevisiae* grown on glucose in aerobic chemostat cultures limited for carbon, nitrogen, phosphorus, or sulfur. *Journal of Biological Chemistry*, *278*(5), 3265–3274. https://doi.org/10.1074/jbc.M209759200

Boer, V. M., Tai, S. L., Vuralhan, Z., Arifin, Y., Walsh, M. C., Piper, M. D. W., De Winde, J. H., Pronk, J. T., & Daran, J.-M. (2007). Transcriptional responses of *Saccharomyces cerevisiae* to preferred and nonpreferred nitrogen sources in glucose-limited chemostat cultures. *FEMS Yeast Research*, *7*(4), 604–620. https://doi.org/10.1111/j.1567-1364.2007.00220.x

Bolaños, J. P., Delgado-Esteban, M., Herrero-Mendez, A., Fernandez-Fernandez, S., & Almeida, A. (2008). Regulation of glycolysis and pentose-phosphate pathway by nitric oxide: impact on neuronal survival. *Biochimica et Biophysica Acta*, *1777*(7–8), 789–793. https://doi.org/10.1016/j.bbabio.2008.04.011

Bottari, S. P. (2015). Protein tyrosine nitration: A signaling mechanism conserved from yeast to man. *PROTEOMICS*, *15*(2–3), 185–187. https://doi.org/10.1002/pmic.201400592

Bouché, N., Fait, A., Bouchez, D., Møller, S. G., & Fromm, H. (2003). Mitochondrial succinic-semialdehyde dehydrogenase of the γ-aminobutyrate shunt is required to restrict levels of reactive oxygen intermediates in plants. *Proceedings of the National Academy of Sciences of the United States of America*, *100*(11), 6843–6848. https://doi.org/10.1073/pnas.1037532100

Brown, G. C. (1999). Nitric oxide and mitochondrial respiration. *Biochimica et Biophysica Acta (BBA) - Bioenergetics*, *1411*(2), 351–369. https://doi.org/10.1016/S0005-2728(99)00025-0

Brüne, B., Meβmer, U. k., & Sandau, K. (1995). The role of nitric oxide in cell injury. *Toxicology Letters*, *82–83*, 233–237. https://doi.org/10.1016/0378-4274(95)03481-1

Cabiscol, E., & Ros, J. (2006). Oxidative damage to proteins: structural modifications and consequences in cell function. *Redox Proteomics: From Protein Modification to Cellular Dysfunction and Disease*, 399–471. https://doi.org/10.1002/0471973122.ch14

Cao, J., Barbosa, J. M., Singh, N. K., & Locy, R. D. (2013a). GABA shunt mediates thermotolerance in *Saccharomyces cerevisiae* by reducing reactive oxygen production. *Yeast*, *30*(4), 129–144. https://doi.org/10.1002/yea.2948

Cao, J., Barbosa, J. M., Singh, N., & Locy, R. D. (2013b). GABA transaminases from *Saccharomyces cerevisiae* and *Arabidopsis thaliana* complement function in cytosol and mitochondria. *Yeast*, *30*(7), 279–289. https://doi.org/10.1002/yea.2962

Carlberg, I., & Mannervik, B. (1975). Purification and characterization of the flavoenzyme glutathione reductase from rat liver. *Journal of Biological Chemistry*, *250*(14), 5475–5480. https://doi.org/10.1016/S0021-9258(19)41206-4

Carmona-Gutierrez, D., Bauer, M. A., Zimmermann, A., Aguilera, A., Austriaco, N., Ayscough, K., Balzan, R., Bar-Nun, S., Barrientos, A., & Belenky, P. (2018). Guidelines and recommendations on yeast cell death nomenclature. *Microbial Cell*, *5*(1), 4. https://doi.org/10.15698/mic2018.01.607

Castello, P. R., David, P. S., McClure, T., Crook, Z., & Poyton, R. O. (2006). Mitochondrial cytochrome oxidase produces nitric oxide under hypoxic conditions: implications for oxygen sensing and hypoxic signaling in eukaryotes. *Cell Metabolism*, *3*(4), 277–287. https://doi.org/10.1016/j.cmet.2006.02.011

Clark, S. M., Di Leo, R., Van Cauwenberghe, O. R., Mullen, R. T., & Shelp, B. J. (2009). Subcellular localization and expression of multiple tomato γ-aminobutyrate transaminases that utilize both pyruvate and glyoxylate. *Journal of Experimental Botany*, *60*(11), 3255–3267. https://doi.org/10.1093/jxb/erp161

Coleman, S. T., Fang, T. K., Rovinsky, S. A., Turano, F. J., & Moye-Rowley, W. S. (2001). Expression of a glutamate decarboxylase homologue is required for normal oxidative stress tolerance in *Saccharomyces cerevisiae*. *Journal of Biological Chemistry*, *276*(1), 244–250. https://doi.org/10.1074/jbc.M007103200

Czerucka, D., Piche, T., & Rampal, P. (2007). Review article: yeast as probiotics -- *Saccharomyces boulardii*. *Alimentary Pharmacology & Therapeutics*, *26*(6), 767–778. https://doi.org/10.1111/j.1365-2036.2007.03442.x

de Assis, L. J., Zingali, R. B., Masuda, C. A., Rodrigues, S. P., & Montero-Lomelí, M. (2013). Pyruvate decarboxylase activity is regulated by the Ser/Thr protein phosphatase Sit4p in

the yeast *Saccharomyces cerevisiae*. *FEMS Yeast Research*, *13*(6), 518–528. https://doi.org/10.1111/1567-1364.12052

De Deken, R. H. (1966). The crabtree effect: a regulatory system in yeast. *Microbiology*, *44*(2), 149–156. https://doi.org/10.1099/00221287-44-2-149

Dedon, P. C., & Tannenbaum, S. R. (2004). Reactive nitrogen species in the chemical biology of inflammation. *Archives of Biochemistry and Biophysics*, *423*(1), 12–22. https://doi.org/10.1016/j.abb.2003.12.017

Dykhuizen, R. S., Frazer, R., Duncan, C., Smith, C. C., Golden, M., Benjamin, N., & Leifert, C. (1996). Antimicrobial effect of acidified nitrite on gut pathogens: importance of dietary nitrate in host defense. *Antimicrobial Agents and Chemotherapy*, *40*(6), 1422 LP – 1425. https://doi.org/10.1128/AAC.40.6.1422

Eberhardt, I., Cederberg, H., Li, H., König, S., Jordan, F., & Hohmann, S. (1999). Autoregulation of yeast pyruvate decarboxylase gene expression requires the enzyme but not its catalytic activity. *European Journal of Biochemistry*, *262*(1), 191–201. https://doi.org/10.1046/j.1432-1327.1999.00370.x

Engel, S. R., Dietrich, F. S., Fisk, D. G., Binkley, G., Balakrishnan, R., Costanzo, M. C., Dwight, S. S., Hitz, B. C., Karra, K., Nash, R. S., Weng, S., Wong, E. D., Lloyd, P., Skrzypek, M. S., Miyasato, S. R., Simison, M., & Cherry, J. M. (2014). The reference genome sequence of *Saccharomyces cerevisiae*: then and now. *G3 (Bethesda, Md.)*, *4*(3), 389–398. https://doi.org/10.1534/g3.113.008995

Fauchon, M., Lagniel, G., Aude, J.-C., Lombardia, L., Soularue, P., Petat, C., Marguerie, G., Sentenac, A., Werner, M., & Labarre, J. (2002). Sulfur sparing in the yeast proteome in response to sulfur demand. *Molecular Cell*, *9*(4), 713–723. https://doi.org/10.1016/S1097-2765(02)00500-2

Ferrer-Sueta, G., Campolo, N., Trujillo, M., Bartesaghi, S., Carballal, S., Romero, N., Alvarez, B., & Radi, R. (2018). Biochemistry of peroxynitrite and protein tyrosine nitration. *Chemical Reviews*, *118*(3), 1338–1408. https://doi.org/10.1021/acs.chemrev.7b00568

Fidel Jr, P. L., Vazquez, J. A., & Sobel, J. D. (1999). *Candida glabrata*: review of epidemiology, pathogenesis, and clinical disease with comparison to *C. albicans*. *Clinical Microbiology Reviews*, *12*(1), 80–96. https://doi.org/10.1128/cmr.12.1.80

Flikweert, M. T., van der Zanden, L., Janssen, W. M. T. M., Yde Steensma, H., van Dijken, J. P., & Pronk, J. T. (1996). Pyruvate decarboxylase: An indispensable enzyme for growth of *Saccharomyces cerevisiae* on glucose. *Yeast*, *12*(3), 247–257. https://doi.org/10.1002/(SICI)1097-0061(19960315)12:3<247::AID-YEA911>3.0.CO;2 -I

Förster, J., Famili, I., Fu, P., Palsson, B. Ø., & Nielsen, J. (2003). Genome-scale reconstruction of the *Saccharomyces cerevisiae* metabolic network. *Genome Research*, *13*(2), 244–253. https://doi.org/10.1101/gr.234503

Galdieri, L., Zhang, T., Rogerson, D., Lleshi, R., & Vancura, A. (2014). Protein acetylation and acetyl coenzyme a metabolism in budding yeast. *Eukaryotic Cell*, *13*(12), 1472–1483. https://doi.org/10.1128/EC.00189-14

Ghasemi, M., Mayasi, Y., Hannoun, A., Eslami, S. M., & Carandang, R. (2018). Nitric oxide and mitochondrial function in neurological diseases. *Neuroscience*, *376*, 48–71. https://doi.org/10.1016/j.neuroscience.2018.02.017

Gietz, R. D., & Schiestl, R. H. (2007). High-efficiency yeast transformation using the LiAc/SS carrier DNA/PEG method. *Nature Protocols*, *2*(1), 31–34. https://doi.org/10.1038/nprot.2007.13

Glacet, A., Letourneau, F., Leveque, P., & Villa, P. (1985). Kinetic study of nitrite inhibition during alcoholic fermentation of beet molasses. *Biotechnology Letters*, *7*(1), 47–52. https://doi.org/10.1007/BF01032419

Goffeau, A., Barrell, B. G., Bussey, H., Davis, R. W., Dujon, B., Feldmann, H., Galibert, F., Hoheisel, J. D., Jacq, C., Johnston, M., Louis, E. J., Mewes, H. W., Murakami, Y., Philippsen, P., Tettelin, H., & Oliver, S. G. (1996). Life with 6000 genes. *Science (New York, N.Y.)*, *274*(5287), 546,563-567. https://doi.org/10.1126/science.274.5287.546

Gow, A. J., Duran, D., Malcolm, S., & Ischiropoulos, H. (1996). Effects of peroxynitrite-induced protein modifications on tyrosine phosphorylation and degradation. *FEBS Letters*, *385*(1–2), 63–66. https://doi.org/10.1016/0014-5793(96)00347-x

Heijnen, H. F. G., van Donselaar, E., Slot, J. W., Fries, D. M., Blachard-Fillion, B., Hodara, R., Lightfoot, R., Polydoro, M., Spielberg, D., Thomson, L., Regan, E. A., Crapo, J., & Ischiropoulos, H. (2006). Subcellular localization of tyrosine-nitrated proteins is dictated by reactive oxygen species generating enzymes and by proximity to nitric oxide synthase.

Free Radical Biology & Medicine, *40*(11), 1903–1913. https://doi.org/10.1016/j.freeradbiomed.2005.09.006

Hinze, H., & Holzer, H. (1985a). Accumulation of nitrite and sulfite in yeast cells and synergistic depletion of the intracellular ATP content. *Zeitschrift Für Lebensmittel-Untersuchung Und Forschung*, *180*(2), 117–120. https://doi.org/10.1007/BF01042634

Hinze, H., & Holzer, H. (1985b). Effect of sulfite or nitrite on the ATP content and the carbohydrate metabolism in yeast. *Zeitschrift Für Lebensmittel-Untersuchung Und Forschung*, *181*(2), 87–91. https://doi.org/10.1007/BF01042566

Hohmann, S. (1993). Characterisation of *PDC2*, a gene necessary for high level expression of pyruvate decarboxylase structural genes in *Saccharomyces cerevisiae*. *Molecular & General Genetics : MGG*, *241*(5–6), 657–666. https://doi.org/10.1007/BF00279908

Hohmann, S., & Cederberg, H. (1990). Autoregulation may control the expression of yeast pyruvate decarboxylase structural genes *PDC1* and *PDC5*. *European Journal of Biochemistry*, *188*(3), 615–621. https://doi.org/10.1111/j.1432-1033.1990.tb15442.x

Hunter, T. (1995). Protein kinases and phosphatases: the yin and yang of protein phosphorylation and signaling. *Cell*, *80*(2), 225–236. https://doi.org/10.1016/0092-8674(95)90405-0

Ischiropoulos, H., & Beckman, J. S. (2003). Oxidative stress and nitration in neurodegeneration: cause, effect, or association? *The Journal of Clinical Investigation*, *111*(2), 163–169. https://doi.org/10.1172/JCI17638

Jahnová, J., Luhová, L., & Petřivalský, M. (2019). *S*-Nitrosoglutathione reductase-the master regulator of protein *S*-nitrosation in plant NO signaling. *Plants (Basel, Switzerland)*, *8*(2), 48. https://doi.org/10.3390/plants8020048

Jakobs, C., Jaeken, J., & Gibson, K. M. (1993). Inherited disorders of GABA metabolism. *Journal of Inherited Metabolic Disease*, *16*(4), 704–715. https://doi.org/10.1007/bf00711902

Jalil, S. U., Ahmad, I., & Ansari, M. I. (2017). Functional loss of GABA transaminase (GABA-T) expressed early leaf senescence under various stress conditions in *Arabidopsis thaliana*. *Current Plant Biology*, *9–10*, 11–22. https://doi.org/https://doi.org/10.1016/j.cpb. 2017.02.001

Jamieson, D. J. (1998). Oxidative stress responses of the yeast *Saccharomyces cerevisiae*. *Yeast (Chichester, England)*, *14*(16), 1511–1527. https://doi.org/10.1002/(SICI)1097-0061(199812)14:16<1511::AID-YEA356>3.0.CO;2-S

Janke, C., Magiera, M. M., Rathfelder, N., Taxis, C., Reber, S., Maekawa, H., Moreno-Borchart, A., Doenges, G., Schwob, E., Schiebel, E., & Knop, M. (2004). A versatile toolbox for PCR-based tagging of yeast genes: New fluorescent proteins, more markers and promoter substitution cassettes. *Yeast*, *21*(11), 947–962. https://doi.org/10.1002/yea.1142

Jazwinski, S. M. (2002). Growing old: metabolic control and yeast aging. *Annual Reviews in Microbiology*, *56*(1), 769–792. https://doi.org/10.1146/annurev.micro.56.012302.160830

Ji, H., Lu, X., Zong, H., & Zhuge, B. (2018). γ-aminobutyric acid accumulation enhances the cell growth of *Candida glycerinogenes* under hyperosmotic conditions. *Journal of General and Applied Microbiology*, *64*(2), 84–89. https://doi.org/10.2323/jgam.2017.08.002

Jones, R. P., & Gadd, G. M. (1990). Ionic nutrition of yeast—physiological mechanisms involved and implications for biotechnology. *Enzyme and Microbial Technology*, *12*(6), 402–418. https://doi.org/10.1016/0141-0229(90)90051-Q

Kamisaki, Y., Wada, K., Bian, K., Balabanli, B., Davis, K., Martin, E., Behbod, F., Lee, Y. C., & Murad, F. (1998). An activity in rat tissues that modifies nitrotyrosine-containing proteins. *Proceedings of the National Academy of Sciences of the United States of America*, *95*(20), 11584–11589. https://doi.org/10.1073/pnas.95.20.11584

Kanadia, R. N., Kuo, W. N., Mcnabb, M., & Botchway, A. (1998). Constitutive nitric oxide synthase in *Saccharomyces cerevisiae*. *Biochemistry and Molecular Biology International*, *45*(6), 1081—1087. https://doi.org/10.1080/15216549800203302

Kang, J. W., Lee, N. Y., Cho, K.-C., Lee, M. Y., Choi, D.-Y., Park, S.-H., & Kim, K. P. (2015). Analysis of nitrated proteins in *Saccharomyces cerevisiae* involved in mating signal transduction. *Proteomics*, *15*(2–3), 580–590. https://doi.org/10.1002/pmic.201400172

Kanski, J., & Schöneich, C. B. T.-M. in E. (2005). Protein nitration in biological aging: proteomic and tandem mass spectrometric characterization of nitrated sites. In *Nitric Oxide, Part E* (Vol. 396, pp. 160–171). Academic Press. https://doi.org/10.1016/S0076-

6879(05)96016-3

Khatri, I., Tomar, R., Ganesan, K., Prasad, G. S., & Subramanian, S. (2017). Complete genome sequence and comparative genomics of the probiotic yeast *Saccharomyces boulardii*. *Scientific Reports*, *7*(1), 371. https://doi.org/10.1038/s41598-017-00414-2

Kig, C., & Temizkan, G. (2009). Nitric oxide as a signaling molecule in the fission yeast *Schizosaccharomyces pombe*. *Protoplasma*, *238*(1–4), 59–66. https://doi.org/10.1007/s00709-009-0074-3

Killenberg-Jabs, M, Jabs, A., Lilie, H., Golbik, R., & Hübner, G. (2001). Active oligomeric states of pyruvate decarboxylase and their functional characterization. *European Journal of Biochemistry*, *268*(6), 1698–1704. https://doi.org/10.1046/j.1432-1327.2001.02044.x

Killenberg-Jabs, Margrit, König, S., Eberhardt, I., Hohmann, S., & Hübner, G. (1997). Role of Glu51 for cofactor binding and catalytic activity in pyruvate decarboxylase from yeast studied by site-directed mutagenesis. *Biochemistry*, *36*(7), 1900–1905. https://doi.org/10.1021/bi961341l

Knowles, R. G., & Moncada, S. (1994). Nitric oxide synthases in mammals. *Biochemical Journal*, *298*(2), 249–258. https://doi.org/10.1042/bj2980249

Kuo, W. N., Jn-Baptiste, J. B., Kanadia, R. N., McNabb, L. D., Zhai, L., Weeks, K., Dopson, N., & Chambers, M. C. (1996). Immunoreactivities of m-calpain, calpastatin, nitric oxide synthase, myelin basic protein and dynamin II in baker's yeast, wheat germ and lobster tail muscle. *Cytobios*, *87*(351), 251–263.

Kutter, S., Weiss, M. S., Wille, G., Golbik, R., Spinka, M., & König, S. (2009). Covalently bound substrate at the regulatory site of yeast pyruvate decarboxylases triggers allosteric enzyme activation. *The Journal of Biological Chemistry*, *284*(18), 12136–12144. https://doi.org/10.1074/jbc.M806228200

Liu, H., & Naismith, J. H. (2008). An efficient one-step site-directed deletion, insertion, single and multiple-site plasmid mutagenesis protocol. *BMC Biotechnology*, *8*, 91. https://doi.org/10.1186/1472-6750-8-91

Liu, L., Zeng, M., Hausladen, A., Heitman, J., & Stamler, J. S. (2000). Protection from nitrosative stress by yeast flavohemoglobin. *Proceedings of the National Academy of Sciences*, *97*(9), 4672 LP – 4676. https://doi.org/10.1073/pnas.090083597

Lowry, J. L., Brovkovych, V., Zhang, Y., & Skidgel, R. A. (2013). Endothelial nitric-oxide synthase activation generates an inducible nitric-oxide synthase-like output of nitric oxide in inflamed endothelium. *Journal of Biological Chemistry*, *288*(6), 4174–4193. https://doi.org/10.1074/jbc.M112.436022

Lundberg, J. O., Weitzberg, E., Lundberg, J. M., & Alving, K. (1994). Intragastric nitric oxide production in humans: measurements in expelled air. *Gut*, *35*(11), 1543 LP – 1546. https://doi.org/10.1136/gut.35.11.1543

Lundberg, J. O., & Govoni, M. (2004). Inorganic nitrate is a possible source for systemic generation of nitric oxide. *Free Radical Biology and Medicine*, *37*(3), 395–400. https://doi.org/10.1016/j.freeradbiomed.2004.04.027

Lundberg, J. O., & Weitzberg, E. (2013). Biology of nitrogen oxides in the gastrointestinal tract. *Gut*, *62*(4), 616–629. https://doi.org/10.1136/gutjnl-2011-301649

Lundberg, J. O., Weitzberg, E., Cole, J. A., & Benjamin, N. (2004). Nitrate, bacteria and human health. *Nature Reviews Microbiology*, *2*(7), 593–602. https://doi.org/10.1038/nrmicro929

Madeo, F., Herker, E., Wissing, S., Jungwirth, H., Eisenberg, T., & Fröhlich, K.-U. (2004). Apoptosis in yeast. *Current Opinion in Microbiology*, *7*(6), 655–660. https://doi.org/10.1016/j.mib.2004.10.012

Malakar, S., Paul, S. K., & Pou, K. R. J. (2020). Biotechnological interventions in beverage production. In *Biotechnological Progress and Beverage Consumption* (pp. 1–37). https://doi.org/10.1016/B978-0-12-816678-9.00001-1

Martins, F. S., Nardi, R. M. D., Arantes, R. M. E., Rosa, C. A., Neves, M. J., & Nicoli, J. R. (2005). Screening of yeasts as probiotic based on capacities to colonize the gastrointestinal tract and to protect against enteropathogen challenge in mice. *The Journal of General and Applied Microbiology*, *51*(2), 83–92. https://doi.org/10.2323/jgam.51.83

Masri, F. A., Comhair, S. A. A., Koeck, T., Xu, W., Janocha, A., Ghosh, S., Dweik, R. A., Golish, J., Kinter, M., Stuehr, D. J., Erzurum, S. C., & Aulak, K. S. (2005). Abnormalities in nitric oxide and its derivatives in lung cancer. *American Journal of Respiratory and Critical Care Medicine*, *172*(5), 597–605. https://doi.org/10.1164/rccm.200411-1523OC

Mei, X., Chen, Y., Zhang, L., Fu, X., Wei, Q., Grierson, D., Zhou, Y., Huang, Y., Dong, F., & Yang, Z. (2016). Dual mechanisms regulating glutamate decarboxylases and

accumulation of gamma-aminobutyric acid in tea (*Camellia sinensis*) leaves exposed to multiple stresses. *Scientific Reports*, *6*(1), 1–11. https://doi.org/10.1038/srep23685

Mekonnen, D. W., Flügge, U. I., & Ludewig, F. (2016). Gamma-aminobutyric acid depletion affects stomata closure and drought tolerance of *Arabidopsis thaliana*. *Plant Science*, *245*, 25–34. https://doi.org/10.1016/j.plantsci.2016.01.005

Miller-Fleming, L., Giorgini, F., & Outeiro, T. F. (2008). Yeast as a model for studying human neurodegenerative disorders. *Biotechnology Journal*, *3*(3), 325–338. https://doi.org/10.1002/biot.200700217

Mortensen, H. D., Jacobsen, T., Koch, A. G., & Arneborg, N. (2008). Intracellular pH homeostasis plays a role in the tolerance of *Debaryomyces hansenii* and *Candida zeylanoides* to acidified nitrite. *Applied and Environmental Microbiology*, *74*(15), 4835 LP – 4840. https://doi.org/10.1128/AEM.00571-08

Muller, E. H., Richards, E. J., Norbeck, J., Byrne, K. L., Karlsson, K.-A., Pretorius, G. H. J., Meacock, P. A., Blomberg, A., & Hohmann, S. (1999). Thiamine repression and pyruvate decarboxylase autoregulation independently control the expression of the *Saccharomyces cerevisiae PDC5* gene. *FEBS Letters*, *449*(2–3), 245–250. https://doi.org/10.1016/s0014-5793(99)00449-4

Muntané, J., & De la Mata, M. (2010). Nitric oxide and cancer. *World Journal of Hepatology*, *2*(9), 337–344. https://doi.org/10.4254/wjh.v2.i9.337

Murdaugh, L. S., Wang, Z., Del Priore, L. V, Dillon, J., & Gaillard, E. R. (2010). Age-related accumulation of 3-nitrotyrosine and nitro-A2E in human Bruch's membrane. *Experimental Eye Research*, *90*(5), 564–571. https://doi.org/10.1016/j.exer.2010.01.014

Nayyar, H., Kaur, R., Kaur, S., & Singh, R. (2014). γ-Aminobutyric acid (GABA) imparts partial protection from heat stress injury to rice seedlings by improving leaf turgor and upregulating osmoprotectants and antioxidants. *Journal of Plant Growth Regulation*, *33*(2), 408–419. https://doi.org/10.1007/s00344-013-9389-6

O'Dell, T. J., Hawkins, R. D., Kandel, E. R., & Arancio, O. (1991). Tests of the roles of two diffusible substances in long-term potentiation: evidence for nitric oxide as a possible early retrograde messenger. *Proceedings of the National Academy of Sciences of the United States of America*, *88*(24), 11285–11289. https://dx.doi.org/10.1073%2F

pnas.88.24.11285

Osório, N. S., Carvalho, A., Almeida, A. J., Padilla-Lopez, S., Leão, C., Laranjinha, J., Ludovico, P., Pearce, D. A., & Rodrigues, F. (2007). Nitric oxide signaling is disrupted in the yeast model for Batten disease. *Molecular Biology of the Cell*, *18*(7), 2755–2767. https://doi.org/10.1091/mbc.e06-11-1053

Otterstedt, K., Larsson, C., Bill, R. M., Ståhlberg, A., Boles, E., Hohmann, S., & Gustafsson, L. (2004). Switching the mode of metabolism in the yeast *Saccharomyces cerevisiae*. *EMBO Reports*, *5*(5), 532–537. https://doi.org/10.1038/sj.embor.7400132

Pannala, A. S., Mani, A. R., Rice-Evans, C. A., & Moore, K. P. (2006). pH-dependent nitration of para-hydroxyphenylacetic acid in the stomach. *Free Radical Biology and Medicine*, *41*(6), 896–901. https://doi.org/https://doi.org/10.1016/j.freeradbiomed.2006.05.010

Pettersen, E. F., Goddard, T. D., Huang, C. C., Couch, G. S., Greenblatt, D. M., Meng, E. C., & Ferrin, T. E. (2004). UCSF Chimera—a visualization system for exploratory research and analysis. *Journal of Computational Chemistry*, *25*(13), 1605–1612. https://doi.org/10.1002/jcc.20084

Phillips, R., Adjei, O., Lucas, S., Benjamin, N., & Wansbrough-Jones, M. (2004). Pilot randomized double-blind trial of treatment of *Mycobacterium ulcerans* disease (Buruli ulcer) with topical nitrogen oxides. *Antimicrobial Agents and Chemotherapy*, *48*(8), 2866–2870. https://doi.org/10.1128/AAC.48.8.2866-2870.2004

Phillips, R., Kuijper, S., Benjamin, N., Wansbrough-Jones, M., Wilks, M., & Kolk, A. H. J. (2004). *In vitro* killing of *Mycobacterium ulcerans* by acidified nitrite. *Antimicrobial Agents and Chemotherapy*, *48*(8), 3130–3132. https://doi.org/10.1128/AAC.48.8.3130-3132.2004

Poyton, R. O., Ball, K. A., & Castello, P. R. (2009). Mitochondrial generation of free radicals and hypoxic signaling. *Trends in Endocrinology & Metabolism*, *20*(7), 332–340. https://doi.org/10.1016/j.tem.2009.04.001

Pozdnyakov, N., Lloyd, A., Reddy, V. N., & Sitaramayya, A. (1993). Nitric oxide-regulated endogenous ADP-ribosylation of rod outer segment proteins. *Biochemical and Biophysical Research Communications*, *192*(2), 610–615. https://doi.org/10.1006/bbrc.1993.1459

Purwar, N., McGarry, J. M., Kostera, J., Pacheco, A. A., & Schmidt, M. (2011). Interaction of nitric oxide with catalase: structural and kinetic analysis. *Biochemistry*, *50*(21), 4491–4503. https://doi.org/10.1021/bi200130r

Radi, R. (2004). Nitric oxide, oxidants, and protein tyrosine nitration. *Proceedings of the National Academy of Sciences*, *101*(12), 4003 LP – 4008. https://doi.org/10.1073/pnas.0307446101

Radi, R. (2013). Protein tyrosine nitration: biochemical mechanisms and structural basis of functional effects. *Accounts of Chemical Research*, *46*(2), 550–559. https://doi.org/10.1021/ar300234c

Ray, P. D., Huang, B.-W., & Tsuji, Y. (2012). Reactive oxygen species (ROS) homeostasis and redox regulation in cellular signaling. *Cellular Signalling*, *24*(5), 981–990. https://doi.org/10.1016/j.cellsig.2012.01.008

Remize, F., Andrieu, E., & Dequin, S. (2000). Engineering of the pyruvate dehydrogenase bypass in *Saccharomyces cerevisiae*: role of the cytosolic Mg^{2+} and mitochondrial K^{+} acetaldehyde dehydrogenases Ald6p and Ald4p in acetate formation. *Applied and Environmental Microbiology*, *66*(8), 3151 LP – 3159. https://doi.org/10.1128/AEM.66.8.3151-3159.2000

Richardson, A. R., Payne, E. C., Younger, N., Karlinsey, J. E., Thomas, V. C., Becker, L. A., Navarre, W. W., Castor, M. E., Libby, S. J., & Fang, F. C. (2011). Multiple targets of nitric oxide in the tricarboxylic acid cycle of *Salmonella enterica* serovar typhimurium. *Cell Host & Microbe*, *10*(1), 33–43. https://doi.org/10.1016/j.chom.2011.06.004

Rocha, B. S., Gago, B., Pereira, C., Barbosa, R. M., Bartesaghi, S., Lundberg, J. O., Radi, R., & Laranjinha, J. (2011). Dietary nitrite in nitric oxide biology: a redox interplay with implications for pathophysiology and therapeutics. *Current Drug Targets*, *12*(9), 1351–1363. https://doi.org/10.2174/138945011796150334

Rocha, B. S., Lundberg, J. O., Radi, R., & Laranjinha, J. (2016). Role of nitrite, urate and pepsin in the gastroprotective effects of saliva. *Redox Biology*, *8*, 407–414. https://doi.org/10.1016/j.redox.2016.04.002

Roetzer, A., Gabaldón, T., & Schüller, C. (2011). From *Saccharomyces cerevisiae* to *Candida glabratain* a few easy steps: important adaptations for an opportunistic pathogen. *FEMS*

Microbiology Letters, *314*(1), 1–9. https://doi.org/10.1111/j.1574-6968.2010.02102.x

Romagnoli, G., Luttik, M. A. H., Kötter, P., Pronk, J. T., & Daran, J.-M. (2012). Substrate specificity of thiamine pyrophosphate-dependent 2-oxo-acid decarboxylases in *Saccharomyces cerevisiae*. *Applied and Environmental Microbiology*, *78*(21), 7538 LP – 7548. https://doi.org/10.1128/AEM.01675-12

Sabetkar, M., Low, S. Y., Bradley, N. J., Jacobs, M., Naseem, K. M., & Richard Bruckdorfer, K. (2008). The nitration of platelet vasodilator stimulated phosphoprotein following exposure to low concentrations of hydrogen peroxide. *Platelets*, *19*(4), 282–292. https://doi.org/10.1080/09537100801915142

Sahoo, R., Bhattacharjee, A., Majumdar, U., Ray, S. S., Dutta, T., & Ghosh, S. (2009). A novel role of catalase in detoxification of peroxynitrite in *S. cerevisiae*. *Biochemical and Biophysical Research Communications*, *385*(4), 507–511. https://doi.org/10.1016/ j.bbrc.2009.05.062

Sasano, Y., Haitani, Y., Hashida, K., Ohtsu, I., Shima, J., & Takagi, H. (2012). Enhancement of the proline and nitric oxide synthetic pathway improves fermentation ability under multiple baking-associated stress conditions in industrial baker's yeast. *Microbial Cell Factories*, *11*, 40. https://doi.org/10.1186/1475-2859-11-40

Schuman, E. M., & Madison, D. V. (1991). A requirement for the intercellular messenger nitric oxide in long-term potentiation. *Science*, *254*(5037), 1503 LP – 1506. https://doi.org/10.1126/science.1720572

Seifikalhor, M., Aliniaeifard, S., Bernard, F., Seif, M., Latifi, M., Hassani, B., Didaran, F., Bosacchi, M., Rezadoost, H., & Li, T. (2020). γ-Aminobutyric acid confers cadmium tolerance in maize plants by concerted regulation of polyamine metabolism and antioxidant defense systems. *Scientific Reports*, *10*(1), 3356. https://doi.org/10. 1038/s41598-020-59592-1

Sengupta, S., Deb, M., Nath, R., Prasad Saha, S., & Bhattacharjee, A. (2020). Optimization of ethanol production using nitrosative stress exposed *S.cerevisiae*. *Cell Biochemistry and Biophysics*, *78*(1), 101–110. https://doi.org/10.1007/s12013-019-00897-y

Sergienko, E. A., & Jordan, F. (2002). New model for activation of yeast pyruvate decarboxylase by substrate consistent with the alternating sites mechanism: demonstration

of the existence of two active forms of the enzyme. *Biochemistry*, *41*(12), 3952–3967. https://doi.org/10.1021/bi011860a

Shelp, B. J., Mullen, R. T., & Waller, J. C. (2012). Compartmentation of GABA metabolism raises intriguing questions. *Trends in Plant Science*, *17*(2), 57–59. https://doi.org /10.1016/j.tplants.2011.12.006

Signorelli, S., Dans, P. D., Coitiño, E. L., Borsani, O., & Monza, J. (2015). Connecting proline and γ-aminobutyric acid in stressed plants through non-enzymatic reactions. *PLoS One*, *10*(3), e0115349. https://doi.org/10.1371/journal.pone.0115349

Smith, S. M., Benjamin, N., Drlscoll, F. O., Dougall, H., Duncan, C., Smith, L., & Golden, M. (1994). Stomach NO synthesis. *Nature*, *368*(April), 1994. https://doi.org/10.1038 /368502a0

Söderling, A.-S., Hultman, L., Delbro, D., Højrup, P., & Caidahl, K. (2007). Reduction of the nitro group during sample preparation may cause underestimation of the nitration level in 3-nitrotyrosine immunoblotting. *Journal of Chromatography B*, *851*(1–2), 277–286. https://doi.org/10.1016/j.jchromb.2007.02.036

Souza, J. M., Daikhin, E., Yudkoff, M., Raman, C. S., & Ischiropoulos, H. (1999). Factors determining the selectivity of protein tyrosine nitration. *Archives of Biochemistry and Biophysics*, *371*(2), 169–178. https://doi.org/10.1006/abbi.1999.1480

Spiegelhalder, B., Eisenbrand, G., & Preussmann, R. (1976). Influence of dietary nitrate on nitrite content of human saliva: Possible relevance to in vivo formation of *N*-nitroso compounds. *Food and Cosmetics Toxicology*, *14*(6), 545–548. https://doi.org/10.1016/S0015-6264(76)80005-3

Spinka, M., Seiferheld, S., Zimmermann, P., Bergner, E., Blume, A.-K., Schierhorn, A., Reichenbach, T., Pertermann, R., Ehrt, C., & König, S. (2017). Significance of individual residues at the regulatory site of yeast pyruvate decarboxylase for allosteric substrate activation. *Biochemistry*, *56*(9), 1285–1298. https://doi.org/10.1021/acs.biochem. 6b01158

Tang, M., Li, Z., Luo, L., Cheng, B., Zhang, Y., Zeng, W., & Peng, Y. (2020). Nitric oxide signal, nitrogen metabolism, and water balance affected by γ-aminobutyric acid (GABA) in relation to enhanced tolerance to water stress in creeping bentgrass. *International*

Journal of Molecular Sciences, *21*(20), 1–17. https://doi.org/10.3390/ijms21207460

Tripodi, F., Nicastro, R., Reghellin, V., & Coccetti, P. (2015). Post-translational modifications on yeast carbon metabolism: Regulatory mechanisms beyond transcriptional control. *Biochimica et Biophysica Acta (BBA) - General Subjects*, *1850*(4), 620–627. https://doi.org/https://doi.org/10.1016/j.bbagen.2014.12.010

van den Berg, M. A., de Jong-Gubbels, P., & Steensma, H. Y. (1998). Transient mRNA responses in chemostat cultures as a method of defining putative regulatory elements: application to genes involved in *Saccharomyces cerevisiae* acetyl-coenzyme A metabolism. *Yeast (Chichester, England)*, *14*(12), 1089–1104. https://doi.org/10.1002/(SICI)1097-0061(19980915)14:12<1089::AID-YEA312>3.0.CO;2-K

Vemuri, G. N., Eiteman, M. A., McEwen, J. E., Olsson, L., & Nielsen, J. (2007). Increasing NADH oxidation reduces overflow metabolism in *Saccharomyces cerevisiae*. *Proceedings of the National Academy of Sciences*, *104*(7), 2402 LP – 2407. https://doi.org/10.1073/pnas.0607469104

Verduyn, C., Zomerdijk, T. P. L., van Dijken, J. P., & Scheffers, W. A. (1984). Continuous measurement of ethanol production by aerobic yeast suspensions with an enzyme electrode. *Applied Microbiology and Biotechnology*, *19*(3), 181–185. https://doi.org/10.1007/BF00256451

Vissers, S., Aandre, B., Muyldermans, F., & Grenson, M. (1989). Positive and negative regulatory elements control the expression of the *UGA4* gene coding for the inducible 4-aminobutyric-acid-specific permease in *Saccharomyces cerevisiae*. *European Journal of Biochemistry*, *181*(2), 357–361. https://doi.org/10.1111/j.1432-1033.1989.tb14732.x

Wu, Q., Su, N., Huang, X., Cui, J., Shabala, L., Zhou, M., Yu, M., & Shabala, S. (2021). Hypoxia-induced increase in GABA content is essential for restoration of membrane potential and preventing ROS-induced disturbance to ion homeostasis. *Plant Communications*, *2*(3), 100188. https://doi.org/10.1016/j.xplc.2021.100188

Yoshikawa, Y., Nasuno, R., Kawahara, N., Nishimura, A., Watanabe, D., & Takagi, H. (2016). Regulatory mechanism of the flavoprotein Tah18-dependent nitric oxide synthesis and cell death in yeast. *Nitric Oxide : Biology and Chemistry*, *57*, 85–91. https://doi.org/10.1016/j.niox.2016.04.003

Ždralević, M., Guaragnella, N., Antonacci, L., Marra, E., & Giannattasio, S. (2012). Yeast as a tool to study signaling pathways in mitochondrial stress response and cytoprotection. *The Scientific World Journal*, *2012*, 912147. https://doi.org/10.1100/2012/912147

Zhao, X. J., Raitt, D., V Burke, P., Clewell, A. S., Kwast, K. E., & Poyton, R. O. (1996). Function and expression of flavohemoglobin in *Saccharomyces cerevisiae*. Evidence for a role in the oxidative stress response. *The Journal of Biological Chemistry*, *271*(41), 25131–25138. https://doi.org/10.1074/jbc.271.41.25131

Zhao, Y., He, M., Xi, Q., Ding, J., Hao, B., Keller, N. P., & Zheng, W. (2016). Reversible *S*-nitrosylation limits over synthesis of fungal styrylpyrone upon nitric oxide burst. *Applied Microbiology and Biotechnology*, *100*(9), 4123–4134. https://doi.org/10.1007/s00253-016-7442-7

Zhao, Y., Lim, J., Xu, J., Yu, J. H., & Zheng, W. (2020). Nitric oxide as a developmental and metabolic signal in filamentous fungi. *Molecular Microbiology*, *113*(5), 872–882. https://doi.org/10.1111/mmi.14465

SUPPLEMENTARY INFORMATION

Table S1 List of nitrated protein identified by LC-MS/MS

Protein name	ORF	Function
Ala1	YOR335C	Alanine-tRNA ligase
Dps1	YLL018C	Aspartyl-tRNA synthetase
Fas1	YKL182W	Tetrafunctional fatty acid synthase subunit
Gdh3	YAL062W	NADP(+)-dependent glutamate dehydrogenase
Hsp82	YPL240C	Hsp90 chaperone
Ilv5	YLR355C	Ketol-acid reductoisomerase
Ipp1	YBR011C	Cytoplasmic inorganic pyrophosphatase
Oye2	YHR179W	Conserved NADPH oxidoreductase containing flavin mononucleotide
Pfk1	YGR240C	Alpha subunit of heterooctameric phosphofructokinase
Pma2	YPL036W	Plasma membrane H+-ATPase
Pst2	YDR032C	FMN-dependent NAD(P)H:quinone oxidoreductase
Rps17a	YML024W	Ribosomal protein 51 (rp51) of the small (40s) subunit
Rps19a	YOL121C	Protein component of the small (40S) ribosomal subunit
Scp160	YJL080C	Essential RNA-binding G protein effector of mating response pathway
Shm2	YLR058C	Cytosolic serine hydroxymethyltransferase
Stm1	YLR150W	Protein required for optimal translation under nutrient stress
Ssa1	YAL005C	ATPase involved in protein folding and NLS-directed nuclear transport; member of HSP70 family
Ssa2	YLL024C	HSP70 family ATP-binding protein; involved in protein folding, vacuolar import of proteins
Tef2	YBR118W	Translational elongation factor EF-1 alpha
Ura2	YJL130C	Bifunctional carbamoylphosphate synthetase/aspartate transcarbamylase
Yef3	YLR249W	Translation elongation factor 3

Table S2-1 Details of LC/MS/MS fragmentation of QVNVNTVFGLPGDFNLSLLDKIYEV EGMR

#1	b^{+}	b^{2+}	b^{3+}	Seq.	y^{+}	y^{2+}	y^{3+}	#2
1	129.06586	65.03657	43.69347	Q				29
2	228.13428	114.57078	76.71628	V	3155.62766	1578.31747	1052.54740	28
3	342.17721	171.59224	114.73059	N	3056.55924	1528.78326	1019.52460	27
4	441.24563	221.12645	147.75339	V	2942.51631	1471.76179	981.51029	26
5	555.28856	278.14792	185.76770	N	2843.44789	1422.22758	948.48748	25
6	656.33624	328.67176	219.45026	T	2729.40496	1365.20612	910.47317	24
7	755.40466	378.20597	252.47307	V	2628.35728	1314.68228	876.79061	23
8	902.47308	451.74018	301.49588	F	2529.28886	1265.14807	843.76780	22
9	959.49455	480.25091	320.50303	G	2382.22044	1191.61386	794.74500	21
10	1072.57862	536.79295	358.19772	L	2325.19897	1163.10312	775.73784	20
11	1169.63139	585.31933	390.54865	P	2212.11490	1106.56109	738.04315	19
12	1226.65286	613.83007	409.55580	G	2115.06213	1058.03470	705.69223	18
13	1341.67981	671.34354	447.89812	D	2058.04066	1029.52397	686.68507	17
14	1488.74823	744.87775	496.92093	F	1943.01371	972.01049	648.34275	16
15	1602.79116	801.89922	534.93524	N	1795.94529	898.47628	599.31995	15
16	1715.87523	858.44125	572.62993	L	1681.90236	841.45482	561.30564	14
17	1802.90726	901.95727	601.64060	S	1568.81829	784.91278	523.61095	13
18	1915.99133	958.49930	639.33529	L	1481.78626	741.39677	494.60027	12
19	2029.07540	1015.04134	677.02998	L	1368.70219	684.85473	456.90558	11
20	2144.10235	1072.55481	715.37230	D	1255.61812	628.31270	419.21089	10
21	2272.19732	1136.60230	758.07062	K	1140.59117	570.79922	380.86857	9
22	2385.28139	1193.14433	795.76531	I	1012.49620	506.75174	338.17025	8
23	2563.35561	1282.18144	855.12339	Y-Amino	899.41213	450.20970	300.47556	7
24	2692.39821	1346.70274	898.13759	E	721.33791	361.17259	241.11749	6
25	2791.46663	1396.23695	931.16039	V	592.29531	296.65129	198.10329	5
26	2920.50923	1460.75825	974.17459	E	493.22689	247.11708	165.08048	4
27	2977.53070	1489.26899	993.18175	G	364.18429	182.59578	122.06628	3
28	3108.57120	1554.78924	1036.86192	M	307.16282	154.08505	103.05912	2
29				R-L-Arg(Guanido-13C)	176.12232	88.56480	59.37896	1

Table S2-2 Details of LC/MS/MS fragmentation of TTY157VTQRPVYLGLPANLVDL NVPAK

#1	b^{+}	b^{2+}	b^{3+}	Seq.	y^{+}	y^{2+}	y^{3+}	#2
1	144.06552	72.53640	48.69336	T-Acetyl				25
2	245.11320	123.06024	82.37592	T	2661.51066	1331.25897	887.84174	24
3	423.18742	212.09735	141.73399	Y-Amino	2560.46298	1280.73513	854.15918	23
4	522.25584	261.63156	174.75680	V	2382.38876	1191.69802	794.80111	22
5	623.30352	312.15540	208.43936	T	2283.32034	1142.16381	761.77830	21
6	751.36210	376.18469	251.12555	Q	2182.27266	1091.63997	728.09574	20
7	908.46658	454.73693	303.49371	R-L-Arg(Guanido-13C)	2054.21408	1027.61068	685.40955	19
8	1005.51935	503.26331	335.84463	P	1897.10961	949.05844	633.04139	18
9	1104.58777	552.79752	368.86744	V	1800.05684	900.53206	600.69046	17
10	1267.65109	634.32918	423.22188	Y	1700.98842	850.99785	567.66766	16
11	1380.73516	690.87122	460.91657	L	1537.92510	769.46619	513.31322	15
12	1437.75663	719.38195	479.92373	G	1424.84103	712.92415	475.61853	14
13	1550.84070	775.92399	517.61842	L	1367.81956	684.41342	456.61137	13
14	1647.89347	824.45037	549.96934	P	1254.73549	627.87138	418.91668	12
15	1718.93059	859.96893	573.64838	A	1157.68272	579.34500	386.56576	11
16	1832.97352	916.99040	611.66269	N	1086.64560	543.82644	362.88672	10
17	1946.05759	973.53243	649.35738	L	972.60267	486.80497	324.87241	9
18	2045.12601	1023.06664	682.38019	V	859.51860	430.26294	287.17772	8
19	2160.15296	1080.58012	720.72250	D	760.45018	380.72873	254.15491	7
20	2273.23703	1137.12215	758.41719	L	645.42323	323.21525	215.81259	6
21	2387.27996	1194.14362	796.43150	N	532.33916	266.67322	178.11790	5
22	2486.34838	1243.67783	829.45431	V	418.29623	209.65175	140.10359	4
23	2583.40115	1292.20421	861.80523	P	319.22781	160.11754	107.08079	3
24	2654.43827	1327.72277	885.48427	A	222.17504	111.59116	74.72986	2
25				K-Label:2H(4)	151.13792	76.07260	51.05082	1

Table S2-3 Details of LC/MS/MS fragmentation of GYKPVAVPAR

#1	b^{+}	b^{2+}	Seq.	y^{+}	y^{2+}	#2
1	100.03931	50.52329	G-Acetyl			10
2	278.11353	139.56040	Y-Amino	1020.63323	510.82025	9
3	410.23361	205.62044	K-Label:2H(4)	842.55901	421.78314	8
4	507.28638	254.14683	P	710.43894	355.72311	7
5	606.35480	303.68104	V	613.38617	307.19672	6
6	677.39192	339.19960	A	514.31775	257.66251	5
7	776.46034	388.73381	V	443.28063	222.14395	4
8	873.51311	437.26019	P	344.21221	172.60974	3
9	944.55023	472.77875	A	247.15944	124.08336	2
10			R-L-Arg(Guanido-13C)	176.12232	88.56480	1